Advancing Transcranial Electrical Stimulation for Personalised Cognitive Enhancement

Jake Toth

26th February 2025
Version: Final copy

Advancing Transcranial Electrical Stimulation for Personalised Cognitive Enhancement

by

Jake Toth

A dissertation submitted to

The University of Sheffield

in partial fulfillment of the requirements for the degree of

Doctor of Philosophy

26th February 2025

Jake Toth

Advancing Transcranial Electrical Stimulation for Personalised Cognitive Enhancement

PhD Dissertation, 26th February 2025

Supervisors: Dr Mahnaz Arvaneh
Dr Méadhbh Brosnan

The University of Sheffield

Department of Automatic Control and Systems Engineering

Amy Johnson Building

Portobello Street

Sheffield, S1 3JD

"Dave suddenly turned to me and said you know, these are the good old days. I don't think I would have been more startled if David had announced he was a Martian. I don't remember what I said, but I do remember what I thought, I don't think so!" ... "But you know what, Dave was right."

Michael Abrash

Acknowledgement

I would like to express my deepest gratitude to my supervisor, Dr. Mahnaz Arvaneh. Her unwavering support and guidance have been instrumental in shaping this thesis and my development as a researcher. Dr. Arvaneh's dedication to her students' academic achievement and well-being goes above and beyond, and I am truly grateful for her mentorship, patience, and encouragement throughout this journey. Her insights have been invaluable in refining my work and pushing me to achieve my full potential.

I would also like to thank Dr. Méadhbh Brosnan for her support and contributions to this research. Her expertise and advice have been greatly appreciated.

Thank you to all the support staff at the University of Sheffield, as well as the Engineering and Physical Sciences Research Council and the University of Sheffield for funding this work.

To my partner Lucy, I cannot express enough thanks for your endless support, understanding, and love throughout this challenging process. Your unwavering belief in me has been a constant source of strength and motivation. I truly could not have done this without you.

Last but certainly not least, thank you to my Cocker Spaniel Luna for protecting me from the postman and pigeons, and for being a source of joy and companionship during long days of writing and research

Declaration

I, Jake Toth, declare that the work presented in this thesis is my own. All material in this thesis which is not of my own work, has been properly accredited and referenced.

Sheffield, 26th February 2025

Jake Toth

Abstract

Transcranial electrical stimulation (tES) demonstrates potential for cognitive enhancement, including improvements in vigilant attention. However, its efficacy across the population is limited by numerous challenges, including inter-individual variability in the electric fields induced by tES and brain-state dependent responses to stimulation.

This thesis first presents a comprehensive literature review critically analysing challenges in non-invasive brain stimulation (NIBS) research, encompassing the principal brain stimulation modalities and sources of variability. Recommendations are presented, including accounting for inter-individual variability, inclusive research practices, improving spatial precision, and the use of multimodal and multi-site stimulation, among others.

Following the literature review, this thesis addresses the challenge of accessible, participant-specific tES dose control through a novel MRI-free approach developed using the largest electric field modelling simulation of its kind. This scalable approach, which utilises readily available demographic and morphological data, significantly reduces peak electric field strength variability across participants compared to fixed-dose stimulation.

Commercial and academic trends within NIBS and tES are analysed to assess the market readiness for the proposed MRI-free tES dosing approach. This includes a systematic search of academic publications across NIBS modalities and of clinical trials utilizing tES. In addition, the current state of the commercial usage of tES and intellectual property challenges are discussed.

This thesis then explores the electrophysiological correlates of vigilant attention during a continuous random-dot motion task, known to measure spatial attention performance. Electroencephalography features associated with arousal, active attentional suppression and off-task thought are identified. Potentially enabling the future development of brain-state dependent stimulation.

Subsequently, a within-subject sham-controlled electroencephalography and transcranial direct current stimulation experiment investigates the effects of transcranial direct current stimulation applied to the right dorsolateral prefrontal cortex on vigilant attention. While no significant effects were observed, the methodological insights of this work are discussed.

Together, the advances presented in this thesis contribute to a multifaceted approach to addressing key challenges in NIBS research. This thesis proposes a scalable approach to personalized tES dosing, insights into the electrophysiological underpinnings of vigilant attention and offers broader NIBS recommendations. Ultimately, these contributions aim to advance translational, accessible, and individualized cognitive enhancement.

List of Figures

List of Tables

Contents

1

Introduction

1.1. Background

Non-invasive brain stimulation (NIBS) is the use of electricity, magnetism, ultrasound and/or light to modulate brain activity without the requirement of surgery or pharmaceuticals. NIBS offers a safe [1–4] approach to modulating brain activity with greater patient acceptability than invasive or pharmaceutical approaches [5].

Transcranial electrical stimulation (tES) is an established NIBS modality that works by applying electrical currents through electrodes placed on the scalp to stimulate the brain, altering neuronal excitability [6]. tES has a wide range of applications including treating depression [7], schizophrenia [8], and medically refractory epilepsy [9].

However, the efficacy of tES-based interventions varies on both an inter-individual and intra-individual basis. Inter-individual variability can be due to many factors, including genetics [10], age [11], sex [12] and the existence of brain lesions [13]. A key area of concern for tES research is the variability in the electric field (E-field) generated in the brain. This E-field can vary between individuals with the same dosage applied by up to 100% [14]. To address this variability, current flow modelling guided by participant-specific magnetic resonance imaging (MRI), is used to approximate participant-specific E-fields and subsequently participant-specific tES dosing [15, 16]. Despite the extensive validation of current flow modelling [17–19], many studies do not take advantage of its capabilities. This may be partly explained by the additional time, cost and complexity associated with collecting MRI data and simulating participant-specific E-fields. This approach conflicts with the cheap and accessible nature of tES [20].

Intra-individual variability to tES, i.e. the variability in efficacy in the same individual over a period of time, can also be explained by many factors, including circadian rhythms [21], caffeine [22] and more broadly the functional state of the brain during stimulation [23, 24]. Brain state-dependent tES has been demonstrated with transcranial alternating current stimulation (tACS) by adjusting the phase and frequency of the stimulation based on EEG data [25]. Initial proof-of-concept studies have also demonstrated the feasibility of closed-loop tDCS with short-duration tDCS based on task timing [26] and the real-time adaptation of current magnitude based on EEG markers [27].

While the applications of tES are broad, vigilant attention (VA) enhancement is particularly pertinent. VA, also known as sustained attention, is the ability to maintain the conscious processing of non-arousing stimuli for prolonged periods [28]. VA performance is also related to abilities in other executive and fluid areas of cognition [29]. A deficit in VA has real-world

implications; for instance, VA performance is reduced in older adults [30] and is associated with an increased risk of falls [31]. Additionally, reduced VA performance has been associated with higher driving speeds in a simulated driving task [32]. tES has shown potential in enhancing VA [33].

A broad set of challenges remain in optimising tES efficacy, including the adoption of personalised tES to reduce inter-individual variability and adapting tES to the functional state of the brain.

1.2. Motivation

tES offers an accessible and safe approach to modulating brain activity. However, tES has limited translational uptake, in part due to inconsistent efficacy between individuals and within individuals over time [34]. This work is motivated to address these barriers by developing accessible participant-specific dose control, thereby accelerating the development and adoption of tES. Additionally, there is an exploration into the potential incorporation of the dynamic functional state of the brain into tDCS-based VA enhancement. Ultimately, the motivation of this work is to advance cognitive enhancement through non-invasive brain stimulation.

1.3. Aims and Objectives

The aim of this work is to explore inter and intra-individual variations in the response to tES to inform strategies that could enable personalised, accessible and effective cognitive enhancement. To fulfil this aim, I propose an investigation into the relationship between head morphology and demographic factors with tES dose as well as electrophysiological and behavioural correlates with VA.

The aforementioned aim will be addressed through the satisfaction of the following objectives:

1) Develop an accessible approach to participant-specific tES dose optimisation to reduce inter-individual E-field variability. The following tasks are necessary to achieve this objective.

    - Investigate the correlations between head morphology and demographic factors and the strength of the E-field induced by tES.

- Develop a modelling approach to predict participant-specific dosing and robustly evaluate its performance on out-of-sample participants.
- Evaluate the market readiness to adopt this personalised dose estimation approach.

2) Investigate electrophysiological and behavioural correlates with tDCS efficacy for VA. The following tasks are necessary to achieve this objective.

- Investigate electrophysiological biomarkers associated with deficits in VA in humans.
- Investigate associations between electrophysiological and behavioural markers and the application of tDCS. Testing for any associations with these markers and tES outcomes.
- Investigate the relationship between the predicted E-field strength (using algorithms from Objective 1) and outcome measures for VA.

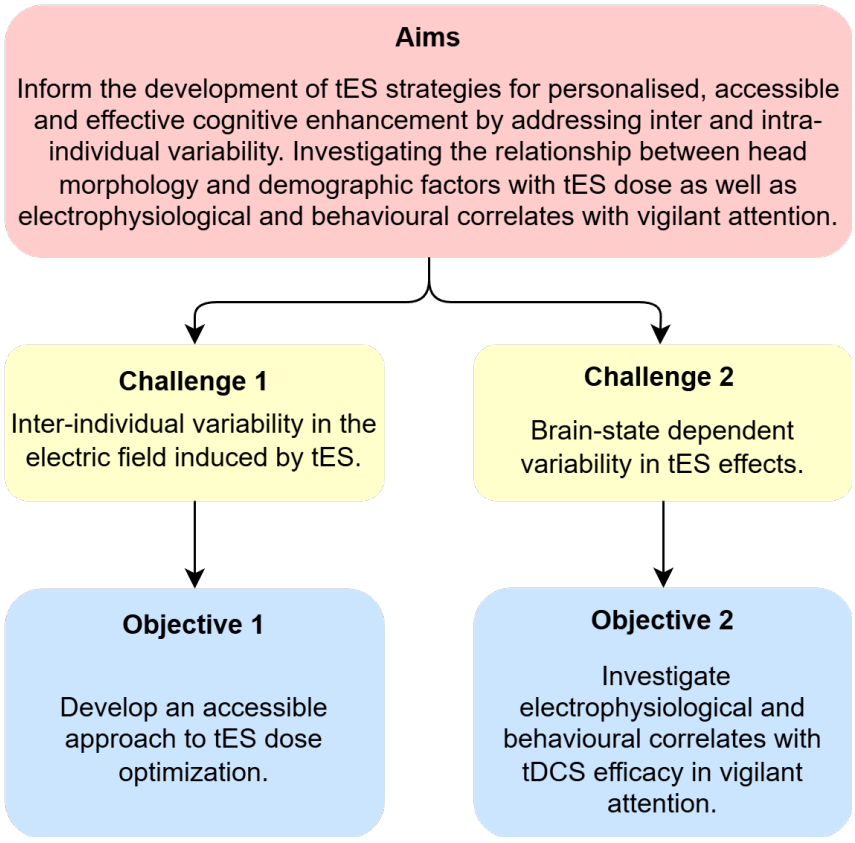

Figure 1.1.: Schematic representation of the thesis aim, challenges, and objectives to advance personalised tES strategies for cognitive enhancement.

1.4. Thesis Overview

The following thesis overview describes the layout of this work and how each chapter relates to the previously listed objectives.

- Chapter 2: This chapter provides a broad perspective on the obstacles and opportunities of NIBS research. In doing so, it provides a foundation for addressing the aims and objectives of this thesis. In this chapter, the four main NIBS modalities and their mechanisms are discussed. Thereafter, the challenges facing NIBS research are critically examined. This includes an overview of the sources of variability in NIBS, including head and brain morphology, neuron type and orientation, exogenous stimuli, endogenous activity and stimulation parameters. Finally, future research directions are considered, including closed-loop NIBS, inclusive research practices, approaches to spatial precision, multimodality and addressing the sample size problem. To conclude, this chapter discusses the implications of this work on NIBS research.

- Chapter 3: To address objective 1, in this chapter, an MRI-free transcranial electrical stimulation dose standardisation algorithm is proposed. To achieve this, 10 tES montages are simulated utilizing MRI scans from 418 participants. Subsequently, a series of correlational analyses confirm that age, head circumference, cephalic index and body mass index are inversely correlated with the simulated peak electric field strength. These measures, along with the participant's gender, are then used in regression models to estimate participant-specific tES dosages without their respective MRI scans. These models significantly reduce the peak electric field strength variation in all conventional and one of four HD montages. In addition, these models explain 43% of the peak E-field strength variation in conventional montages and 21% in HD montages on unseen individuals. Further, the use of linear and non-linear regression models incorporating inter-electrode distance are explored to personalize tES dosing in novel montages. These models, tested against unseen montages and individuals, explain 36% and 13% of peak E-field strength variations in conventional and HD montages, respectively. To conclude this chapter, the impact of this work on tES research and future research directions is discussed.

- Chapter 4: This chapter reviews the literature pertaining to the fulfilment of objectives 1 and 2. To achieve this, the literature on VA is first discussed. This includes the theoretical frameworks that attempt to explain its mechanisms, relevant neuromarkers and approaches to experimental design and the measurement of VA.

Subsequently, previous attempts to enhance VA using tES are considered. Thereafter, this chapter explores approaches to personalize tES and provide 'closed-loop' stimulation that responds to existing brain activity. Finally, this chapter concludes with a discussion of the current state and gaps within the literature regarding tES for VA enhancement.

- Chapter 5: This chapter addresses objective 2 by exploring electrophysiological correlates with VA in a continuous random-dot motion task. In this chapter, frequency domain features associated with VA performance were analysed. This analysis confirms established EEG markers, including frequency bands associated with low arousal, active attentional suppression and off-task thoughts found to be significantly correlated with reaction times. Time domain (event-related potential) features were not visible, which is inferred to be potentially due to ongoing motor processes.

- Chapter 6: This chapter addresses objective 2 by investigating the effects of tDCS on VA. Twenty-nine healthy adults participated in a within-participants, sham-controlled study in which they received sham, 1mA and 2mA of anodal tDCS to the right dorsolateral prefrontal cortex during a continuous random-dot motion task. Resting-state EEG, ADHD questionnaire scores, and other participant-specific predictors were collected to examine potential predictors of tDCS efficacy. Electric field simulations were also performed to compare the montage used with previous work. Contrary to expectations, no significant effects of stimulation on behavioural measures were observed. The chapter discusses potential methodological limitations and provides recommendations for future tDCS studies on VA.

- Chapter 7: This chapter addresses objective 1 by evaluating the potential impact and adoption of the accessible dose standardisation software developed in Chapter 3. A thorough evaluation of the trends in non-invasive brain stimulation publications is performed to achieve this. In addition, conditions that tES clinical trials target are assessed. After that, a list of companies and competitors is compiled, and a series of conversations with businesses is discussed. Finally, intellectual property challenges are examined. The chapter concludes by assessing the commercial viability of this work.

- Chapter 8: Finally, Chapter 8 concludes this thesis. The key achievements and the fulfilment of the research objectives are discussed. Thereafter, future directions in which this research can be taken and improved upon are considered.

1.5. Key Contributions

The key contributions of this work are as follows:

a) The implementation of an accessible tES dosing algorithm that uses accessible morphological and demographic information to estimate participant-specific tES dosing. This contribution is described in Chapter 3.

b) The development and implementation of an experiment on human participants applying EEG-tDCS during a VA task with a series of measures including behavioural, morphological, electrophysiological and demographic. This contribution is described in Chapter 6.

c) An analysis of the field of tES examining commercial, academic and clinical trends. This contribution is described in Chapter 7.

d) The contribution of the paper "Obstacles and Opportunities in Non-Invasive Brain Stimulation" which provides a broad survey of the literature defining key recommendations for the field of non-invasive brain stimulation. This contribution is described in Chapter 2.

e) The contribution of the conference paper "Electrophysiological Correlates of Response Time in a Vigilant Attention Task", which reaffirms previous works on electrophysiological associations with VA. This contribution is described in Chapter 5.

1.6. Works Published During This PhD

1. A journal article was published in Frontiers in Human Neuroscience broadly discussing non-invasive brain stimulation research. This work is discussed in Chapter 2.

   J. Toth, D. Kurtin, M. Brosnan, M. Arvaneh. Opportunities and Obstacles in Non-Invasive Brain Stimulation, *Frontiers in Human Neuroscience*, 2024.

2. At the time of writing, a journal article discussing our approach to predicting the peak electric field induced by tES without participant-specific MRI scans has been submitted for publication. This work is discussed in Chapter 3.

J.Toth, R. King, B. Ivanov, M. Brosnan, M. Arvaneh. Dose Standardization for Transcranial Electrical Stimulation: An Accessible Approach, under review for publication in the *Journal of Neural Engineering*.

3. A conference paper was presented at the IEE EMBC 2022 conference. This work investigated electrophysiological correlates of response time in a random-dot motion task using two electroencephalography channels. This work is discussed in Chapter 5.

   J. Toth, R. Patel, M. Arvaneh. Electrophysiological Correlates of Response Time in a Vigilant Attention Task. In *2022 44th Annual International Conferences of the IEEE Engineering in Medicine & Biology Society (EMBC) Conference*, Glasgow, UK, July 2022.

2

Literature Review: Non-Invasive Brain Stimulation

2.1. Introduction

The contents of this chapter have been published in the journal "Frontiers in Human Neuroscience" [35].

In order to address the aims and objectives of this thesis, I first explored the field of non-invasive brain stimulation (NIBS) more broadly. In this chapter, the predominant NIBS modalities and their mechanisms are discussed. The opportunities within this field are explored, including the sources of variation that impact NIBS efficacy. In this chapter, areas of opportunity in NIBS, such as inclusivity and closed-loop stimulation, are discussed. Finally, recommendations to guide the future of NIBS research are proposed.

The human brain, comprising approximately 80 billion neurons and a similar number of glial cells [36], is a highly complex organ. The brain consumes approximately 20% of the body's metabolic budget while constituting only 2% of its mass [37]. The outsized cardiovascular intake of the brain sustains its many parallel processes, estimated at $(0.18\text{-}6.4) \times 10^{14}$ traversed edges per second [38]. Neuromodulatory interventions aim to deliver targeted perturbations of these neural processes, identifying the optimal targets and methods poses a significant challenge. Additionally, neuromodulation must take into account the cerebrospinal fluid, meninges, skull and scalp in which the brain is ensconced. Yet the ability to modulate brain activity without surgery, both in the cortex and in deep brain structures, has been demonstrated through a broad spectrum of approaches [39].

NIBS is a promising approach for improving brain health and quality of life. Moreover, when appropriately configured it presents minimal risks and costs when compared to invasive brain stimulation [1–4]. Greater patient acceptability facilitates the translation of NIBS to a broader range of applications. For instance, patients with moderate Parkinson's disease consider invasive deep-brain stimulation to be a last resort [40]. In a survey of the general public, ultrasound and magnetic stimulation were preferred over pharmaceuticals and implants as an intervention for mental health [5].

Applications of NIBS include personalised, intermittent theta-burst transcranial magnetic stimulation (TMS), which has been approved by the Federal Drug Administration [41] and boasts a 79% remission rate for patients with treatment-resistant depression [42]. Transcranial electrical stimulation (tES) is being trialled by the National Health Service in the United Kingdom for the treatment of depression [43]. The treatment of drug addiction has promise in preliminary trials using low-intensity focused ultrasound stimulation (LIFUS) [44]. NIBS has also been used for the reduction of chronic pain [45] and the enhancement of attention [33]

and memory [46] in the ageing brain.

NIBS shows promise as a therapeutic intervention for various neurological and psychiatric conditions for both its wide-ranging neuromodulatory capabilities and the accessibility of large-scale manufacturing. The manufacturing of NIBS devices relies largely on the existing electronics manufacturing industry. As a result, it has the potential to scale quickly. This could potentially facilitate adoption curves akin to those seen for blood oxygen sensors or consumer electronics products within the respective patient groups. At this scale and speed, NIBS could have a substantial translational impact. However, the realisation of NIBS's potential is contingent upon surmounting several significant barriers. In this chapter, the different approaches to NIBS and their mechanisms of action describe major challenges facing the field and explore opportunities to overcome them.

2.2. Modalities and Mechanisms of Non-Invasive Brain Stimulation

The four primary approaches to non-invasive brain stimulation are transcranial electrical stimulation (tES), transcranial magnetic stimulation (TMS), transcranial photobiomodulation (tPBM) and transcranial ultrasound stimulation (TUS). Figure 2.1 provides an overview of their respective characteristics.

Transcranial electrical stimulation (tES) passes a current (typically 1-4mA) through active and return electrodes [47]. Stimulation is typically delivered via two electrodes, although more electrodes can enhance stimulation focality [48]. Transcranial direct current stimulation (tDCS), a type of tES, modulates neuronal excitability without reaching the threshold necessary to trigger neuronal depolarizations [49]. This alteration of membrane potentials has been shown to occur through several mechanisms, including decreased γ-aminobutyric acid (GABA) concentrations [50] and increased glutamate and glutamine concentrations [51] with effects modulated by sodium channels [52–54].

tES also comes in other forms, such as Transcranial Alternating Current Stimulation (tACS), which utilises sinusoidal currents thought to entrain brain oscillations [55, 56]. Additionally, Transcranial Random Noise Stimulation (tRNS) is the random sampling of currents from a bell-shaped curve [57]. The mechanisms for tRNS are unclear, but they may involve stochastic resonance [58]. In contrast to tDCS, aftereffects of tRNS are not NDMA receptor-dependent and can be suppressed by benzodiazepines, suggesting an alternative mechanism [59].

	Transcranial Electrical Stimulation (tES)	Transcranial Magnetic Stimulation (TMS)	Transcranial Photobiomodulation (tPBM)	Transcranial Ultrasound Stimulation (TUS)
Modalities	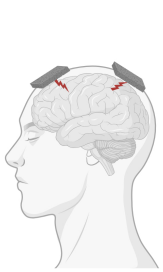	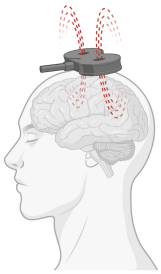	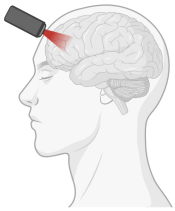	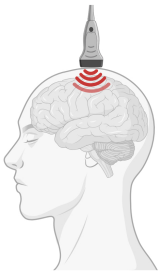
Approaches	• Transcranial direct current stimulation (tDCS) • Transcranial alternating current stimulation (tACS) • Transcranial random noise stimulation (tRNS) • Temporal interference (TI)	• Single-pulse TMS • Repetitive TMS (rTMS) • Theta-burst TMS • Low-intensity repetitive TMS (LI-rTMS) • Deep TMS (dTMS) • Repetitive magnetic temporal interference (rTMI) • Multi-locus TMS (mTMS)	• Continuous wave • Pulsed wave • Intranasal • Oral	• Focused ultrasound stimulation (fUS) • Low intensity focused ultrasound stimulation (LIFUS) • Transcranial pulse stimulation (TPS)
Primary Mechanisms	• Modulating resting membrane potentials • Neurotransmitter modulation • Entraining oscillations (tACS)	• Synaptic plasticity • Long-term potentiation (LTP) (rTMS) • Long-term depression (LTD) (rTMS)	• Increased mitochondrial activity • Modulation of reactive oxygen species • Anti-inflammatory • Pro-neurogenic	• Acoustic cavitation • Mechanical deformation • Thermal
Advantages	• Portable • Inexpensive • Can stimulate deep brain targets (TI)	• Suprathreshold • Not affected by intervening tissue • Can stimulate deep brain targets (rTMI, dTMS)	• Can increase blood-brain barrier permeability • Can be used to activate photoactive drugs • Can be used in Optogenetics	• High spatial resolution • Can stimulate deep-brain targets (fUS) • Capable of tissue ablation and blood brain barrier opening
Limitations	• Can have low spatial resolution (tDCS, tACS, tRNS) • Subthreshold • Requires low impedance with the scalp	• Can have high power requirements • Can be bulky and expensive	• Impeded by hair • Limited depth capabilities	• Limited understanding of mechanisms • Impeded by the skull

Figure 2.1.: Characteristics of the four non-invasive brain stimulation modalities: transcranial electrical stimulation (tES), transcranial magnetic stimulation (TMS), transcranial photobiomodulation (tPBM), and transcranial ultrasound stimulation (TUS). This figure outlines common subtypes, primary mechanisms, advantages, and limitations for each modality. Created with BioRender.com.

Temporal Interference (TI) stimulation employs the convergence of two or more high-frequency (kHz) currents to create a low-frequency envelope that selectively modulates brain activity. Importantly, the high-frequency carrier currents, though present, do not impact neuronal activity due to the low-pass filtering effect of neuronal membranes [60]. This generates a focused electric field (E-field) that oscillates at the difference in frequency of these high-frequency waves [61]. Notably, recent human studies have successfully demonstrated TI for the targeted modulation of the hippocampus [62].

Transcranial magnetic stimulation (TMS) uses electromagnets to induce currents within the brain, producing supra-threshold E-fields on the order of hundreds of V/m [63] compared to less than 1V/m with tES [14]. Approaches to TMS include single-pulse TMS for the exploration of brain function and repetitive TMS (rTMS) used to induce effects lasting longer than the stimulation period [64]. TMS can induce long-term potentiation (LTP) through the unblocking of post-synaptic NDMA receptors blocked by magnesium ions, resulting in an influx of calcium ions in post-synaptic neurons [65]. Additionally, long-term depression (LTD) can be induced through the slow flow of calcium ions from lower-frequency stimulation [66]. TMS can also alter gene expression and enzyme production along with a multitude of other effects [66]. Notably, rTMS effects are frequency-dependent, with inhibition below 1Hz and facilitation above 5Hz, although this generalisation is disputed [67].

The application of TMS involves diverse pulse patterns tailored to specific purposes. One notable example is theta-burst TMS, showing promise in treating major depressive disorder. This method employs short bursts of 50Hz stimulation to mimic the effects of LTP and LTD, thought to induce synaptic plasticity while offering shorter, lower-intensity procedures than traditional rTMS [68]. Low-Intensity Repetitive TMS (LI-rTMS) uses an order of magnitude weaker magnetic field strengths (1-150mT) and remains subthreshold, unlike typical TMS that can evoke motor potentials [69, 70]. Furthermore, deep brain regions can be stimulated with deep TMS (dTMS) using a specialised coil known as the Hesed coil [71]. Additionally, repetitive magnetic temporal interference (rTMI), which utilizes the electrotemporal interference of high-frequency TMS holds promise for selectively modulating deep-brain targets [72]. Finally, multi-locus TMS (mTMS) is an approach that uses an array of electronically controlled coils, allowing for the shifting and re-orienting of the induced E-field [73].

Transcranial Photobiomodulation (tPBM) commonly employs near-infrared light (600nm-1100nm) to modulate brain activity [74]. Light that reaches the brain is absorbed by chromophores, particularly Cytochrome c oxidase, increasing mitochondrial activity and Adenosine triphosphate production. This also modulates reactive oxygen species and the release of calcium ions, activating transcription factors for long-term cellular effects [75]. Resultant bio-

logical responses include improved oxidative metabolism and increased blood flow [75]. tPBM is also thought to have anti-inflammatory and pro-neurogenic effects [76]. However, the absorption of light by hair limits tPBM applications outside of the forehead region, intranasally or through the oral cavity [74, 77]. While tPBM traditionally uses a continuous wave, recent work explores pulsed wave tPBM, allowing for short, high-power pulses [78].

Thus far, conclusive evidence regarding the efficacy of tPBM for depression and dementia is yet to emerge [79, 80]. However, there are encouraging results regarding the effects of tPBM on cognitive abilities and brain function during ageing [81]. Aside from modulating neural activity directly, a picosecond 532nm pulse has been observed as temporarily improving blood-brain barrier permeability [82], enhancing the delivery and efficacy of paclitaxel in mice with glioblastoma [83]. Additionally, advances in photopharmacology offer the potential to precisely control pharmaceuticals within the brain using light [84].

Transcranial ultrasound stimulation (TUS) uses high-frequency sound waves for non-invasive neural modulation. It is employed in various applications, including the increase of blood-brain barrier permeability via cavitation [85] and tissue ablation through heating [86]. Alternatively, low-intensity ultrasound has been demonstrated to modulate brain activity. Examples include the attenuation of thermal pain sensitivity [87] and sensory-evoked brain oscillations [88]. Focused ultrasound stimulation (fUS) uses out-of-phase high-frequency waves to stimulate deep brain regions with sub-centimetre precision [89]. Low-intensity focused ultrasound (LIFUS) is the application of ultrasound stimulation at low intensities to modulate neuronal activity without causing tissue damage. Thermal effects are thought to be negligible from LIFUS as tissue temperatures rise by less than 0.1°C. Non-thermal effects from LIFUS include acoustic cavitation, which involves pressure-induced oscillations of gas-filled microbubbles and influencing neuron excitability via membrane deformation. Additionally, LIFUS can alter ion channel permeability and membrane characteristics through mechanical energy, impacting ion flux and neuronal membrane discharge from mechanosensitive ion channels. These complex interactions are thought to contribute to the neuromodulatory effects of LIFUS [90]. Transcranial pulsed stimulation (TPS) employs short pulses of ultrasound lasting $3\mu s$. These short pulses mitigate brain heating and preliminary evidence suggests cognitive benefits in Alzheimer's patients [91].

2.3. Obstacles to Non-Invasive Brain Stimulation Research

The brain can be considered a dynamical, emergent complex system [92]. Put simply, ongoing brain function is a result of the interplay between exogenous stimuli/perturbations and endogenous processes and goals. The brain presents both stochastic and deterministic characteristics, underpinning the difficulty in developing a mechanistic understanding of brain function and behaviour. While the causal perturbations of NIBS facilitate the characterisation of neural mechanisms, the complex, individual nature of brain structure and function makes the optimisation of NIBS challenging. These sources of variation are illustrated in Figure 2.2.

2.3.1 Inter-Individual Morphological Variability

One source of complexity is the inter-individual variation in head and brain morphology. For instance, skull thickness [93] and cortical thickness, volume, and surface area are negatively correlated with age [94]. In adults, ventricles within the brain become larger with age and both white and grey matter volumes are reduced [95]. These inter-individual and intra-individual variations are particularly consequential in tES. For example, current flow modelling has demonstrated that identical tES parameters result in an over 100% difference in the intensity of the E-field generated in the motor cortex [14]. There is also the potential for unintentional stimulation of off-target regions, especially when individualised modelling is not performed [96].

2.3.2 Dose-Response Relationships

The correlation between the applied stimulation dose and the resulting response remains unclear. In tPBM, a biphasic dose-response curve is suggested [97]. Conversely, a positive relationship between the dose of TUS applied to the lateral geniculate nucleus and the subsequent suppression of visually evoked potentials has been observed [98]. Regarding tDCS, a simple linear dose-response relationship may be an oversimplification [99]. Dose-response relationships across NIBS remain unclear, likely due to a complex interplay of factors, including the functional state of the brain during stimulation.

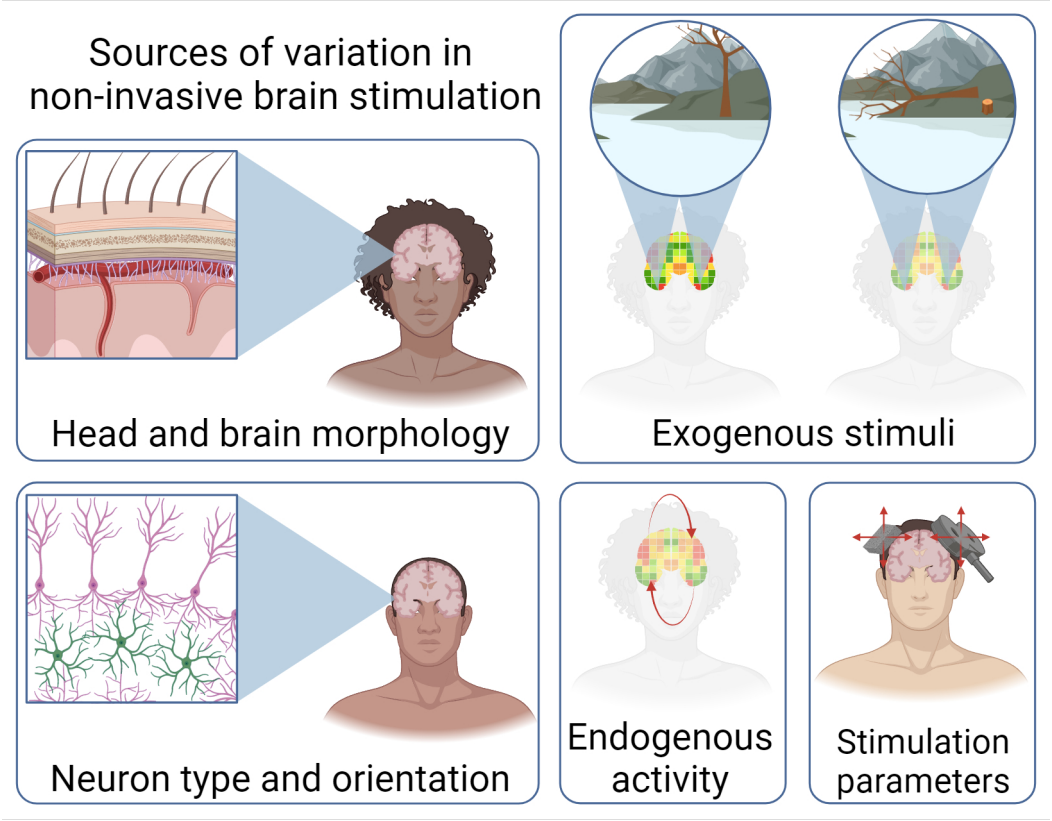

Figure 2.2.: Illustration of the sources of variation that influence the efficacy of non-invasive brain stimulation. Variations in head and brain morphology, exogenous stimuli, neuron type and orientation, as well as activity and stimulation parameters. Created with BioRender.com.

2.3.3 Functional Brain State Dependency

The functional state of the brain during stimulation is an important area of consideration when optimising NIBS [23]. For instance, responses to tES are associated with pre-existing concentrations of the neurotransmitters GABA and glutamate [24]. However, the specific nature of the brain-state dependent dose-response relationship in tES remains inadequately understood [20]. Similarly, tFUS differentially affects active and resting neurons [100]. The use of electroencephalography (EEG) for measuring TMS evoked potentials has proven effective in optimising stimulation orientation in the left pre-supplementary motor area [101]. Additionally, it enables real-time adjustment of stimulation protocols to control the efficacy of plasticity induction in the motor cortex [102]. As with NIBS more broadly, applying these state-dependent techniques beyond the motor system is an additional challenge.

2.3.4 Neuron Type and Orientation

The type and orientation of neurons being stimulated is another complicating factor in elucidating dose-response relationships. For instance, when tFUS is applied, neurons exhibit varying responses to different pulse frequencies, influenced by their distinct action potential waveforms and genotypes [103]. An important factor of the efficacy of tES is the orientation of neurons relative to the E-field generated. Additionally, neurons with highly-branched axons are less sensitive to the relative direction of the E-field [104]. Interestingly, stimulation itself can also change structural components of the brain. For instance, subthreshold rTMS alters the dendritic spine structure in pyramidal neurons in mice [105], and static magnetic stimulation through the use of a permanent magnet has been shown to decrease the length of the axon initial segment in cell cultures [106]. In the development of stimulation configurations, modelling current flow allows for a comprehensive understanding of the interplay between stimulation montage, E-field, and neural orientation [20]. Further developments in multi-scale modelling may elucidate these relationships.

2.3.5 Multi-Locus Stimulation

It is common practice in NIBS to focus on stimulating a single brain region, even though many targeted behaviours involve a distributed network of activity. For instance, in depressed populations, the prefrontal cortex is often targeted, but depression symptoms are linked to activity changes in various brain regions, including the thalamus and hippocampus, among others [107]. Consequently, achieving optimal stimulation parameters may necessitate simultaneous stimulation of multiple targets. Although progress has been made in this direction [108, 109], it remains a relatively unexplored area.

2.3.6 Other Factors

There are a multitude of other factors that may impact the efficacy of NIBS, from circadian rhythms [21] to caffeine [22] and broader genetic predispositions [10]. Brain temperature variations linked to age, sex, and menstrual cycle [110] may also impact NIBS. As with all experimental studies, excluding common disorders like dyslexia or ADHD limits the generalizability of findings from healthy controls, given that 15-20% of the population is neurodivergent [111]. Further, underdiagnosis in certain groups, such as females with ADHD [112], may result in the inadvertent inclusion of undiagnosed neurodivergent individuals. Overly broad exclusion

criteria can introduce population bias; insufficient accommodations for individuals who wear head coverings or exhibit sensory processing sensitivity may hinder diverse participation. Many studies, excluding those focusing on disorders prevalent in older adults, predominantly involve young participants and are conducted in a limited number of countries [113–115].

2.4. Areas of Opportunity and Future Research Directions

2.4.1 Closed-Loop Non-Invasive Brain Stimulation

The effects of NIBS are state-dependent, making adaptive stimulation attuned to brain dynamics crucial for maximizing the potential of NIBS [116]. In a closed-loop NIBS system, brain activity is continuously monitored and compared to a desired state, and stimulation parameters are adjusted in real-time to optimise the therapeutic effects. To facilitate a greater understanding of the mechanisms and predictors of NIBS efficacy, multi-scale models will be informed by multi-scale imaging from synapse to lobe [117]. Ultimately, state-dependent neuromodulation could be delivered in more wearable form. EEG captures ongoing brain states non-invasively and has enabled tACS delivered to match the phase and frequency of slow-wave oscillations to enhance long-term generalised memory consolidation post-sleep [25]. Additionally, high-definition diffuse optical tomography provides high spatial resolution capture of hemodynamics in the cortex [118] and Optically Pumped Magnetometers - Magnetoencephalography (OPM-MEG) enables high spatial and temporal resolutions and sensitivity [119]. Optimising stimulation parameters based on real-time brain state is both necessary and attainable.

2.4.2 Spatial Precision in Non-Invasive Brain Stimulation

A central challenge in NIBS research is ensuring consistent stimulation of the intended target. Stimulation parameters are chosen to stimulate a target region, in practice the position and intensity of stimulation in the brain varies between individuals and sessions. Precise sensor and stimulator positioning is crucial for accuracy [120, 121]. Achieving such precision involves structural imaging, simulation, and neuronavigation, a resource-intensive process. More scalable approaches are needed, potentially combining participant-specific MRI approximated with generative modelling [122] and utilising smartphone-based 3D head scanning [123]. Additionally, techniques such as electrical impedance tomography and pulse-echo ultrasound

can estimate the electrical and acoustic properties of the head, respectively [124, 125]. Notably, advances in low-field MRI may offer more accessible structural imaging with 64mT mobile scans approaching the quality of 3T scans [126]. Statistical techniques that account for inter-individual variability, such as mixed-model analyses or cluster analysis, may also be used as opposed to the standard population-based approaches [21].

2.4.3 Inclusivity

One source of bias in NIBS research is rooted in the challenges associated with gaining access to the scalp, especially when dealing with long, thick, and/or curly hair [127]. There is a recognised bias in neuroscience concerning race and sex [128]. Addressing these biases could involve implementing inclusive training and recruitment procedures. Technological solutions, such as 3D-printed electrodes designed for various hair types, may also contribute to mitigating these challenges [129]. Additionally, offering additional remuneration for participants with hair that requires more time for preparation and washing is a consideration. To foster more representative research samples, further open-sourcing of datasets containing demographic information is recommended for the benefit of future researchers.

2.4.4 Multimodal Non-Invasive Brain Stimulation

The efficacy of NIBS could potentially be enhanced by combining stimulation modalities, as each approach offers unique benefits and mechanisms of action. For instance, priming with tDCS before applying TMS may produce more robust effects [130]. Similarly, concerning closed-loop NIBS, multi-modal approaches for reading brain activity can be more effective at classifying brain states as has been demonstrated by the combination of EEG and functional Near Infrared Spectroscopy to improve seizure detection accuracy [131]. Multi-modality may potentially extend to non-invasive optogenetics, with recent work showing the delivery of viral vectors facilitated by FUS to increase blood-brain barrier permeability, followed by channel activation using light in mice [132]. As such, it may be pertinent for further advancement of multi-modal sensing and stimulation.

2.4.5 Statistical Power in Non-Invasive Brain Stimulation Research

Finally, statistical power emerges as a noteworthy concern in NIBS research. The average sample size in studies involving tDCS and TMS is 22, leading to a situation where NIBS studies

may miss 50% of true positive results [133]. While practical constraints often limit the sample size of initial studies, enhancing statistical power through adequately powered studies is crucial. In instances where inter-individual variability is not accounted for through brain imaging and simulation, broader utilisation of 'N-of-1' trials with a single individual with openly available data might be a pertinent approach for NIBS research as it is with personalised medicine more broadly [134]. The aggregation of such studies has the potential to offer valuable insights beyond the conventional population-based approach, as the inter-individual source of variability is not a concern. This could also allow for greater use of longitudinal study designs that investigate the long-term effects of multi-session stimulation.

2.5. Conclusions

In this chapter, the multifaceted landscape of NIBS has been explored, including the four main modalities: tES, TMS, tPBM and TUS. Each modality possesses unique attributes, mechanisms and challenges, contributing differently to the field of neurostimulation. Yet all must deal with the inherent complexities and challenges associated with individual morphological and physiological variations, as well as the dynamic nature of the brain and the subsequent state-dependent nature of stimulation.

Looking forward, this chapter highlights several avenues for advancing NIBS. The development of closed-loop systems that integrate real-time brain state monitoring with stimulation holds the promise of enhancing efficacy. Overcoming the challenge of consistently stimulating the intended brain regions across individuals necessitates innovative approaches, potentially leveraging advances in imaging technologies and computational modelling. Addressing biases in NIBS research and its applications, including those related to race, sex, and neurodiversity, is critical for ensuring the broad applicability and effectiveness of these technologies. Furthermore, exploring the synergistic potential of multi-modal NIBS approaches may improve outcomes. Finally, tackling the issue of underpowered studies through adequately sized trials, personalisation and appropriate statistical methods. Implementing these recommendations could help propel NIBS towards achieving its full therapeutic potential across diverse populations.

3

An Accessible Approach to Transcranial Electrical Stimulation Dose Standardisation

3.1. Introduction

The contents of this chapter has been submitted to the "Journal of Neural Engineering"
In this chapter, an accessible approach to dose standardisation in tES is introduced to satisfy objective 1. As described in Chapter 2 tES is a non-invasive brain stimulation method that influences brain activity primarily by modulating neuronal membrane potentials [135]. This is achieved by applying a weak electrical current (typically 1-4 mA) through one or more electrodes placed on the scalp. The potential applications of tES are broad, ranging from treating depression [136] and long COVID [137] to mild cognitive impairment [138].

However, the efficacy of tES has been hampered by the variability of its effects across individuals [139]. A potential source of this variability lies in the heterogeneity of the E-field generated within the brain, even with identical stimulation parameters [140]. For instance, the strength of the E-field generated in the motor cortex can vary by up to 100% between individuals given a fixed stimulation dose [14]. Increasing evidence suggests that E-field strength may be directly linked to behavioural changes (e.g., [141] [142]), highlighting the importance of addressing this inter-individual variability to improve tES outcomes [20] [143].

Individualised E-field simulations, which use participant-specific structural MRI scans and finite element methods, offer a promising solution for estimating individualised tES dosing. This approach has been validated through intracranial recordings [17], cerebral blood flow measurements [19], and associations with neurotransmitter changes [144]. However, the requirement for MRI scans and specialised expertise presents a significant barrier to widespread adoption, undermining the cost-effectiveness and accessibility of tES [20].

Inter-individual E-field variability can arise due to variations in anatomic factors, including bone density [145], CSF thickness [140], and head circumference [146]. E-fields have also been found to vary with demographic factors such as sex [12], age [11], and the inter-electrode distance [147]. This work tests the hypothesis that integrating demographic and anatomical parameters, such as head circumference and inter-electrode distance, into E-field dose optimisation models will significantly reduce inter-individual variability in peak E-field strength, providing a scalable alternative to MRI-based approaches. (See [146] for a previous demonstration of the feasibility of such an approach using head circumference in a small sample of 47 participants).

This approach is expected to provide a scalable alternative to MRI-based dosing, enabling accurate participant-specific dose estimation using readily available demographic and morphological data These include, age, gender, head circumference, cephalic index (skull width

to length ratio), body mass index, and inter-electrode distance. Here, a series of robust multiple linear regression models were trained on a large E-field dataset of 418 adults to estimate participant-specific dosing across 10 commonly used tES montages. The models were trained using independent variables that are straightforward to obtain in most laboratory and clinical environments, with a notable exclusion of costly neuroimaging metrics.

More specifically, first, independent associations between these variables and MRI-obtained peak E-field strengths were tested across the 10 montages using Spearman's rank-order partial correlations. Montage-specific robust multiple linear regression models were then trained for each montage using 5-fold cross-validation to estimate the required dose for unseen participants. The estimated peak E-fields from the proposed MRI-free models were compared to those obtained using MRI-informed E-field simulations, using normalised root-mean-squared error and adjusted R^2.

To demonstrate the scalability of this approach to novel montages, montage-agnostic dose estimation models are proposed. This was achieved using two types of regression models: one incorporating inter-electrode distance as a linear term and another including inter-electrode distance as both linear and quadratic terms. The proposed montage-agnostic models were evaluated on previously unseen montages and unseen participants.

In summary, this chapter presents a simple, scalable approach toward standardising tES dosages without participant-specific MRI scans. It also introduces a method to generalize individualised dose estimation to novel, unseen montages.

3.2. Materials and Methods

To develop models that can estimate individualised tES dosages without relying on individual MRI scans, E-fields were simulated using MRI scans from a large population. This approach was designed to test the hypothesis that integrating demographic and anatomical parameters into dose optimisation models can reduce inter-individual peak E-field strength variability. The relationship between peak E-field strengths obtained from these MRI scans and easily accessible features such as age, gender, and head circumference was investigated. Using this information, models were developed to estimate individualised tES dosages by predicting peak E-field strengths solely based on these MRI-free, easily accessible features. The details of this approach are described below.

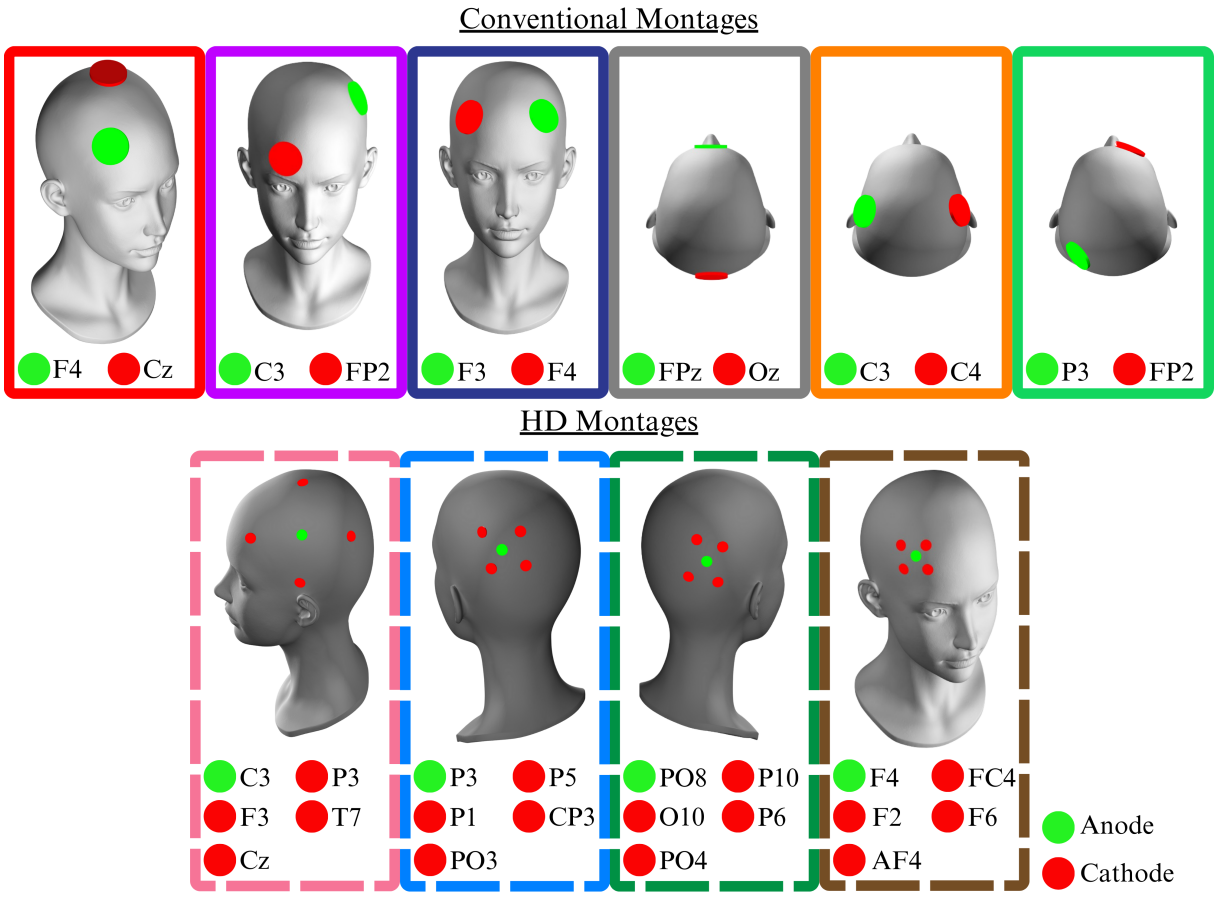

Figure 3.1.: Illustration of the electrode positions of all 10 montages simulated in this work. In the six conventional montages on the first row, anodes (green) supplied 1mA of current, and the cathodes (red) were set to -1mA. The four high-definition (HD) montages on the second row each had one anode (green), which supplied 1mA, and the four cathodes (red) were set to -0.25mA.

3.2.1 Dataset

MRI scans from the CamCAN repository (available at http://www.mrc-cbu.cam.ac.uk/datasets/camcan/) [148, 149] were used in this analysis. The MRI scans from all 653 participants were segmented and manually inspected for imperfections such as scalp contact with the CSF and incomplete eye segmentation. 200 participants were removed due to low-quality segmentation maps, 254 were manually adjusted to correct for minor errors. Of the remaining 453 participants, 35 were excluded due to the Jacobian determinant lying outside of the default range of between 0.01-100 [150] during the non-linear transformation to MNI152 space using the FNIRT function [151]. More information on this registration procedure can be found in Section 3.2.4. After artefact rejection, the final dataset comprised 418 participants, 202 were male, and 216 participants were female, with a mean±SD age of 52.5 ±18.2.

3.2.2 Montage Selection

Electrode positions were selected on the basis of their positional variation on the head and their use in previous works. Conventional montages were stimulated with an anode set to 1mA and a cathode set to -1mA. Conventional montage positions are fronto-central (anode: F4, cathode: Cz) [33], centro-frontal (anode: C3, cathode: FP2) [152], cross-hemisphere frontal (anode: F3, cathode: F4) [153, 154], parietal-frontal (anode: P3, cathode: FP2) [155], cross-hemisphere central (anode: C3, cathode: C4) [156] and midline fronto-occipital (anode: FPz, cathode: Oz) [157].

HD montages included one central anode set to 1mA surrounded by four return electrodes set to -0.25mA. The HD montages were positioned as follows: frontal (anode: F4, cathodes: F2, AF4, F6, FC4) [158], central (anode: C3, cathodes: P3, Cz, T7, F3) [159], parietal (anode: P3, cathodes: P1, CP3, P5, PO3) [160] and parietal-occipital (anode: PO8, cathodes: P6, PO4, P10, O10) [161]. All montages are visualised in Figure 3.1.

3.2.3 Electric Field Simulations

E-field simulations were performed using ROAST version 3.0, an open-source, automated, E-field simulation pipeline [15] in MATLAB (2021a).

As part of the ROAST pipeline, all structural MRI scans were segmented using SPM12 [162],

after which isotropic electrical conductivities were assigned to both head and brain tissue and the electrodes. The default conductivity values (white matter 0.126 S/m, grey matter 0.276 S/m, bone 0.01 S/m, skin 0.465 S/m, air 2.5e-14 S/m, gel 0.3 S/m, electrode 5.9e7 S/m) were applied. The conductivity value of 0.85 S/m was used for CSF to account for the meninges [18].

Electrodes were placed, and meshes were generated using the MATLAB toolbox iso2mesh [163]. Finally, the finite element methods solver, getDP [164], was used to solve the underlying Laplacian equation [165]. Conventional montages used electrodes with 28mm radii, while high-definition montages used electrodes with 10mm radii. Both types of electrodes were 1mm thick. Both T1 and T2 weighted scans were used for E-field simulation to produce more accurate meshing than just T1 weighted scans alone [166]. In this work, the strength of the E-field was considered, and the E-field direction was discarded.

3.2.4 Electric Field Registration to MNI152 Space

E-field results were transformed to the MNI152 6th generation reference space [167]. These transformations used FSL version 6.0 (http://fsl.fmrib.ox.ac.uk/fsl/) [168]. Linear transformations (FLIRT) [169], followed by non-linear transformations (FNIRT) [151], were applied to the T1 MRI scans. This transformation was subsequently applied to E-field voxels corresponding to the grey matter in the segmentation maps used in the E-field simulation pipeline. This pipeline is illustrated in Figure 3.2.

Finally, the peak E-field strength was extracted. This was defined as the average of the 95th percentile of the E-field strength within grey matter voxels. To ensure data quality, extreme outliers were removed from the dataset. Outliers were defined as peak E-field strength values that fell outside three times the interquartile range (IQR) for each montage. These extreme outliers may have been caused by the non-deterministic nature of mesh generation, which can cause local defects. Of the 4,180 E-fields generated across all 10 montages, 19 were rejected, resulting in the final dataset of 4,161 E-fields.

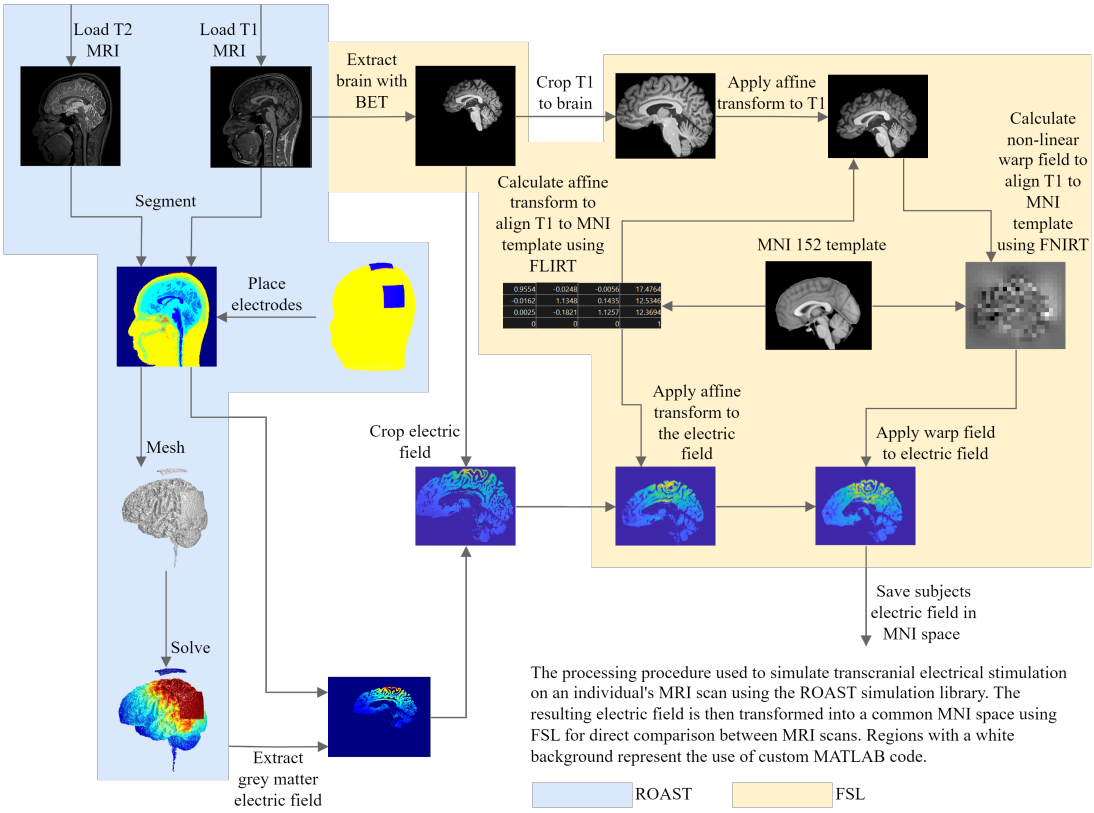

Figure 3.2.: Illustration of the pipeline used in this work to simulate the electric field generated in the grey matter and its transformation to a common MNI152 space. The background colours indicate the software used for each step: blue for ROAST, yellow for FSL, and white for MATLAB.

3.2.5 Feature Extraction

In addition to age and gender, the proposed tES dosage estimation models used anatomical features such as head circumference, cephalic index, BMI, and inter-electrode distance. The CamCAN repository provided information on age, gender, height, and weight, which were used to calculate BMI. In 54 out of 418 participants, BMI was not calculable due to missing data. For these cases, the missing BMI values were imputed using the median BMI of the dataset (24.0543). As head circumferences and cephalic indexes were not included, these values were estimated using MRI scans.

Head circumference was measured by placing 60 points around the transverse plane slice of the MNI152 template; a similar approach was used by Antonenko et al. [146]. The inverse of the participant-specific affine linear transform was then applied to these points, and the sum of the Euclidean distance between the points in native space was used to estimate the head circumference. The measured head circumferences were compared to those predicted by Bushby et al.'s models [170] to validate this approach. This model predicts mean head

circumferences of 577mm for males and 553mm for females based on height. This is within 6mm of the proposed approach for males (mean±SD, 583mm±14.5mm) and within 1mm for females (mean±SD, 552mm±13.5mm).

Head length and width were measured on the same transverse plane slice of the MNI152 template used for head circumference calculation. The length was measured as the distance between the most distal points of the forehead and the back of the head (mean±SD, 190mm±9.0mm). The width was measured as the maximum distance between the most lateral points of the head along the axis perpendicular to the length axis (mean±SD, 158mm±6.7mm). These measurements were transformed from MNI152 space to native space using the inverse of the linear affine transformation, as with the head circumference calculation. The cephalic index (mean±SD, 83.1±4.09) is the ratio of the head width to length, calculated as the head width divided by the length and multiplied by 100.

Inter-electrode distances were extracted from native space where montages are in a common Right, Anterior, Superior (RAS) orientation. The inter-electrode distance was calculated as the Euclidian distance between the midpoints of the electrode meshes of the stimulation and return electrodes. In conventional montages, the inter-electrode distance was measured between the single return and stimulation electrodes. For HD montages, the inter-electrode distance was the average distance between the stimulation electrode and the four return electrodes.

Finally, data standardisation was applied across all data types with appropriate techniques depending on their approximate distributions. Min-max scaling was applied to the uniformly distributed age, and z-score standardisation was applied to the normally distributed head circumference, cephalic index, and peak E-field strength. Median interquartile range standardisation was applied to the skewed BMI distribution, and gender values were set to 0 (male) or 1 (female).

3.2.6 Developing MRI-free Models for the Estimation of Peak Electric Field Strength

Montage-Specific Peak Electric Field Strength Estimation

To train the MRI-free models for estimating peak E-field strength, the testing and training datasets were compiled using MRI-based simulations as detailed in Sections 3.2.3 and 3.2.4. The relationship between the features extracted in Section 3.2.5 and the peak E-field strengths

were analysed using pairwise correlation analyses. Pearson's linear correlation was applied to compare peak E-field strengths against head circumferences and cephalic indices, as these variables were normally distributed. For the non-normally distributed variables, age and BMI, Spearman's Rho correlation was used. Additionally, two-sample t-tests were performed to compare the peak E-field strengths between genders. To understand the independent correlations of each variable, Spearman's rank-order partial correlations were conducted. Bonferroni correction was applied to all tests to adjust for multiple comparisons.

Following the correlational analyses a series of robust multiple linear regression models were trained using an iteratively re-weighted least squares approach with the bi-square weight function. These models were designed to predict peak E-field strength values specific to each montage. The mathematical representation of these montage-specific models is shown in equation 3.1. The predicted montage-specific (MS) peak E-field strength is defined as E_{MS}. β weights are present for each predictor, including age (x_{age}), gender (x_{gender}), head circumference (x_{HC}), cephalic index (x_{CI}), and BMI (x_{BMI}) as well as the intercept (β_{MS_0}).

To assess the accuracy of predicted peak E-field strengths (E_{MS}) compared to MRI-obtained peak E-field strengths when 1mA of stimulation was applied, 5-fold cross-validation was employed. The model's performance on each test set was evaluated using adjusted R^2 and normalised root-mean-square error (NRMSE).

$$\begin{aligned} E_{\text{MS}} = &\beta_{\text{MS}_1} x_{\text{age}} + \beta_{\text{MS}_2} x_{\text{HC}} + \beta_{\text{MS}_3} x_{\text{CI}} + \\ &\beta_{\text{MS}_4} x_{\text{BMI}} + \beta_{\text{MS}_5} x_{\text{gender}} + \beta_{\text{MS}_0}. \end{aligned} \tag{3.1}$$

Montage-Agnostic Peak Electric Field Estimation

Montage-agnostic models were designed to generalize to unseen electrode configurations, unlike montage-specific models, which are limited to the particular montage on which they were trained. To achieve this, two different sets of montage-agnostic regression models were trained, one for HD montages and one for conventional montages.

First, robust multiple linear regression models were developed to predict the peak E-field strength (E_{LMA}). These models included the inter-electrode distance term (x_{ED}) to account for differences in peak E-field strength between montages, as shown in Equation 3.2. In this case, the generated E-field is based on 1mA of stimulation. To ensure independent training and test data, a leave-one-out approach was applied across the montages, and 5-fold cross-validation was used across participants.

$$E_{\text{LMA}} = \beta_{\text{LMA}_1} x_{\text{age}} + \beta_{\text{LMA}_2} x_{\text{HC}} + \beta_{\text{LMA}_3} x_{\text{CI}} + \beta_{\text{LMA}_4} x_{\text{BMI}} + \beta_{\text{LMA}_5} x_{\text{gender}} + \beta_{\text{LMA}_6} x_{\text{ED}} + \beta_{\text{LMA}_0}. \tag{3.2}$$

Secondly, non-linear regression models were trained, one for HD montages and one for conventional montages to predict the peak E-field strength (E_{NMA}) in a montage-agnostic manner. These models included a quadratic term for electrode distance (x_{ED}^2), as shown in Equation 3.3, to capture the non-linear relationship between electrode distance and E-field strength [171].

$$E_{\text{NMA}} = \beta_{\text{NMA}_1} x_{\text{age}} + \beta_{\text{NMA}_2} x_{\text{HC}} + \beta_{\text{NMA}_3} x_{\text{CI}} + \beta_{\text{NMA}_4} x_{\text{BMI}} + \beta_{\text{NMA}_5} x_{\text{gender}} + \beta_{\text{NMA}_6} x_{\text{ED}} + \beta_{\text{NMA}_7} x_{\text{ED}}^2 + \beta_{\text{NMA}_0}. \tag{3.3}$$

The same montage-wise leave one out and participant-wise 5-fold cross-validation approach as in the linear montage agnostic models were applied. As in the montage-specific models, model performance was evaluated on the respective test sets using adjusted R^2 and NRMSE.

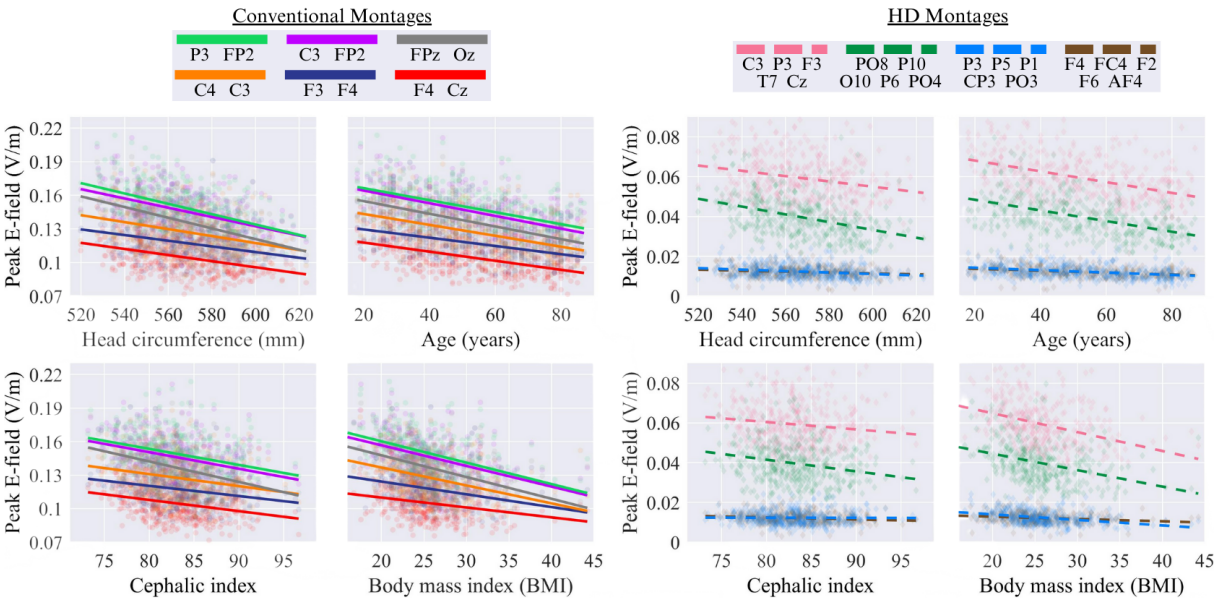

Figure 3.3.: Overview of the relationships between peak E-field strengths and demographic and morphological information for conventional montages to the left and HD montages to the right. A negative correlation is observed between head circumference, age, cephalic index, and body mass index (BMI).

Individualised tES Dose Estimation

Given the direct relationship between applied current and resulting E-field strength, the participant-specific current dosage, $I_{\text{individualised}}$, can be calculated using Equation 3.4. The target peak E-field strength, E_{target}, can be set to any desired value depending on the specific requirements of a study or application. Traditionally, a current I_{applied} was administered in MRI-informed participant-specific simulations to achieve a generated peak E-field strength, $E_{\text{generated}}$. The values of $E_{\text{generated}}$, I_{applied}, and E_{target} were then used to determine the participant-specific current dosage, $I_{\text{individualised}}$.

$$I_{\text{individualised}} = \frac{I_{\text{applied}}}{E_{\text{generated}}} \times E_{\text{target}}. \tag{3.4}$$

The proposed MRI-free models predict $E_{\text{predicted}}$ when 1 mA is applied (i.e., I_{applied}). Please note, in the results section, for illustration purposes, I set the target peak E-field strength as 0.1V/m. Levene's tests with Bonferroni correction were applied to compare the variance of the resulting E-field distributions between standardised and fixed dosing.

3.3. Results

3.3.1 Peak E-field Strength Variation with Age, Gender, and Head Morphology

To ensure the artefact rejection and outlier removal processes did not introduce selection bias, the demographics of the original dataset (n=653) with the reduced dataset post-processing (n=418) were compared. A Chi-squared test for the participants' gender, the pairwise Kolmogorov-Smirnov test for age, and the Mann-Whitney U test for BMI distribution, excluding participants whose BMI was not calculable from the original dataset. These tests indicated no statistically significant differences ($p > .05$).

Pearson's linear correlation between head circumference and MRI-derived peak E-field strength confirmed significant negative correlations across all montages ($p < .01$). Additionally, Spearman's Rho correlation analysis indicated significant negative correlations between age and peak E-field strength ($p < .001$) and BMI and peak E-field strength ($p < .05$). The cephalic index was negatively correlated with peak E-field strength in all conventional montages ($p < .001$), but it was only significantly correlated in the HD montage with the anode at

PO8. Additionally, independent t-tests revealed significant peak E-field differences between genders in 5 out of the 10 montages. A detailed table of results can be found in Appendix A.

Thereafter, Spearman's rank order partial correlations between each variable and the peak E-field strength were performed, controlling for all other variables as shown in Figure 3.4. Age is the most prominent factor ($p < .001$) across all montages), followed by head circumference ($p < .001$) across all conventional montages). Finally, a weak correlation between the cephalic index and peak E-field strength, particularly in anterior-posterior montages, is observed.

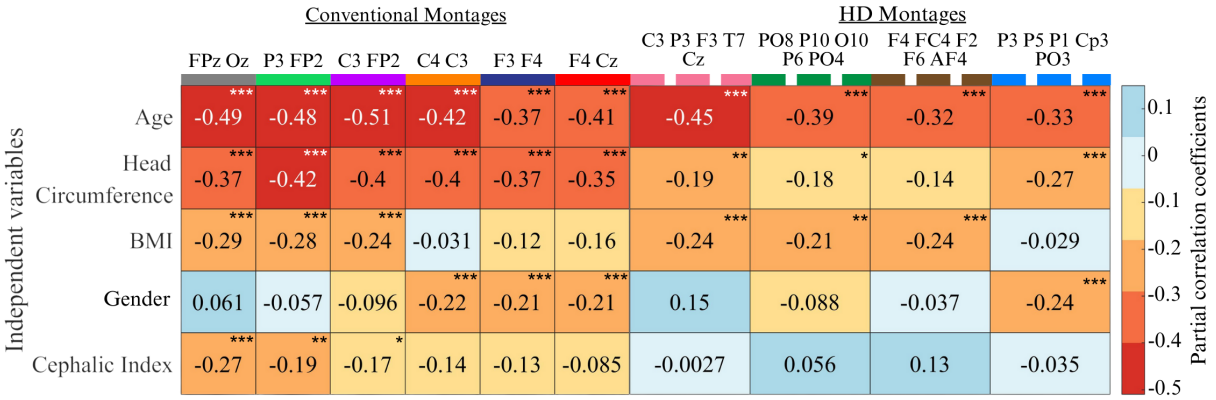

Figure 3.4.: Spearman's rank order partial correlations values between each independent variable and the peak E-field strength, controlling for the influence of all other independent variables. Conventional montages are on the left, and HD montages are on the right. (*** denotes $p < .001$), ** denotes $p < .01$), and * denotes $p < .05$))

3.3.2 Montage-Specific Dose Standardisation

Figure 3.5 compares the distributions of peak E-field strengths induced by a 1mA fixed-dose, scaled to have a mean of 0.1V/m, with those induced by individualised dosages determined by the proposed models. Notably, for all conventional montages, significant reductions in peak E-field variability ($p < .01$) were observed when applying individualised dosages. In HD montages, while individualised dosages generally reduced peak E-field strength variability, only one montage (anode at PO8) showed a significant reduction ($p < .001$).

We compared the peak E-field strengths predicted by the proposed models against values obtained directly from the MRI scans across 10 montages and 5-fold test sets. Figure 3.7 illustrates the proportion of variance in the peak E-field strength explained by these models, measured by the adjusted R^2 on test sets. Models trained on conventional montages had a mean adjusted R^2 of 0.43, and those trained on HD montages had a mean adjusted R^2 of

0.21, as shown in Figure 3.7. Anterior-posterior conventional montages (anode: FPZ, cathode: Oz), (anode: P3, cathode: FP2), (anode: C3, cathode: FP2) had the highest performance, likely related to the significant partial correlations with the cephalic index. HD montages performed comparatively worse, particularly those with close inter-electrode distances (anode: P3) and (anode: F4).

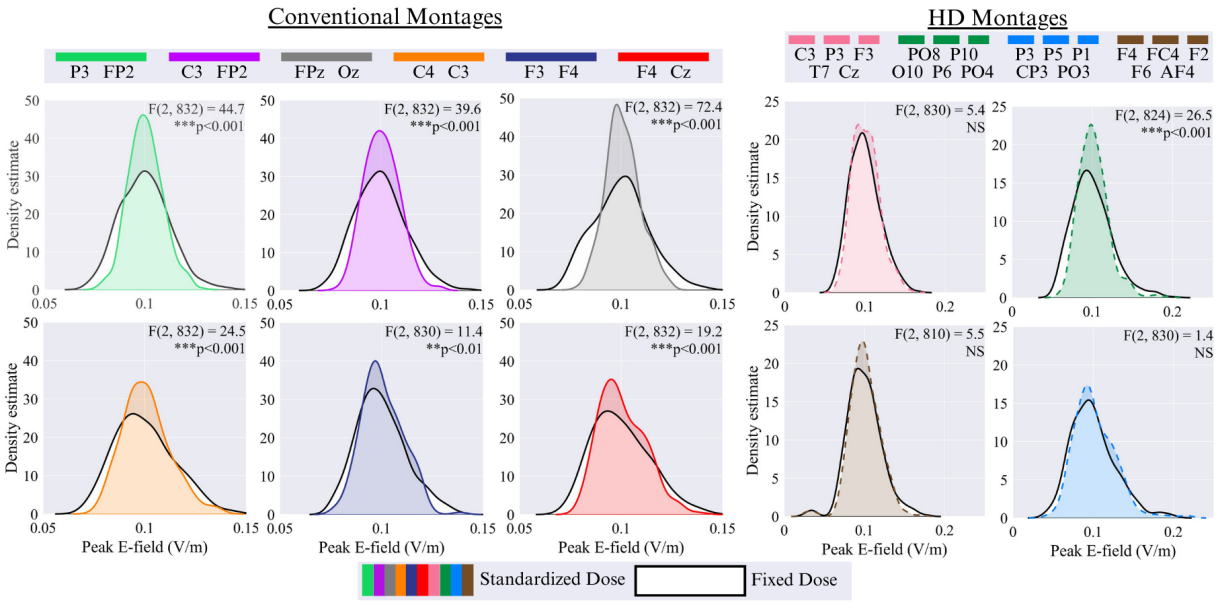

Figure 3.5.: This figure compares the variability in peak E-field strengths between a fixed dose and the proposed individualised dosage across the population. Peak E-field strength distributions induced by individualised doses are depicted in colour, while those induced by fixed doses are shown in black and white. Each plot includes Levene's test for variance to assess the significance of personalization on E-field variability. NS denotes not significant.

3.3.3 Montage-Agnostic Dose Standardisation

In montage-agnostic models, inter-electrode distance was included as an additional input alongside the features used in montage-specific models. The relationship between inter-electrode distance and the peak E-field is shown in Figure 3.6.

To develop montage-agnostic models, in the first instance, robust multiple linear regression was used. These models accounted for 35% of the peak E-field strength variability in conventional montages and 13% of the peak E-field strength variability in HD montages. Subsequently, in an attempt to account for the non-linear relationship between inter-electrode distance and peak E-field strength, a quadratic term was integrated. These models performed comparably to the linear models, explaining 36% and 11% of the variance in conventional and HD montages, respectively. Results tables for all models can be found in the Appendix

A.

The performance of the linear and non-linear models in terms of the adjusted R^2 as well as NRMSE is shown in Figure 3.7. Overall, montage-specific models explained more of the E-field variability than montage-agnostic models. Furthermore, the introduction of the quadratic term did not yield an appreciable improvement in performance.

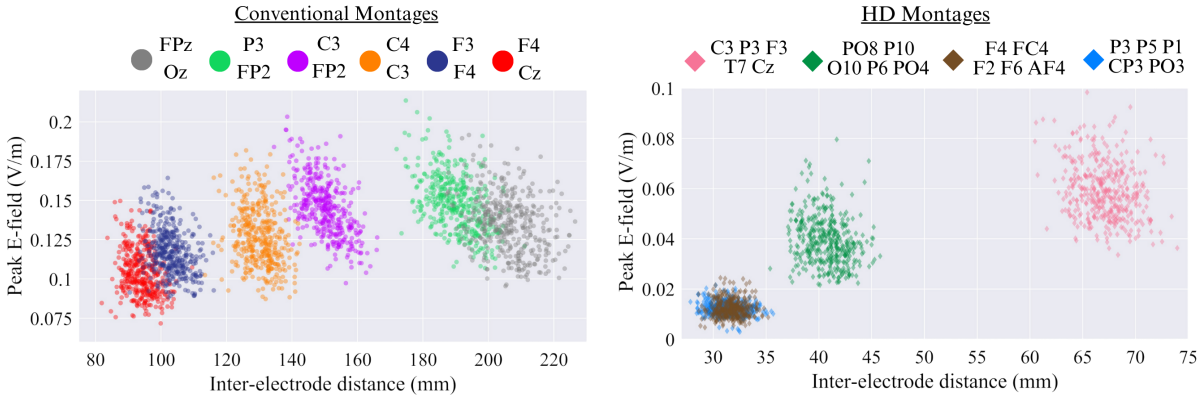

Figure 3.6.: Scatter plot of the peak E-field and electrode distance for each participant. Conventional montages are displayed on the left, and HD montages are displayed on the right.

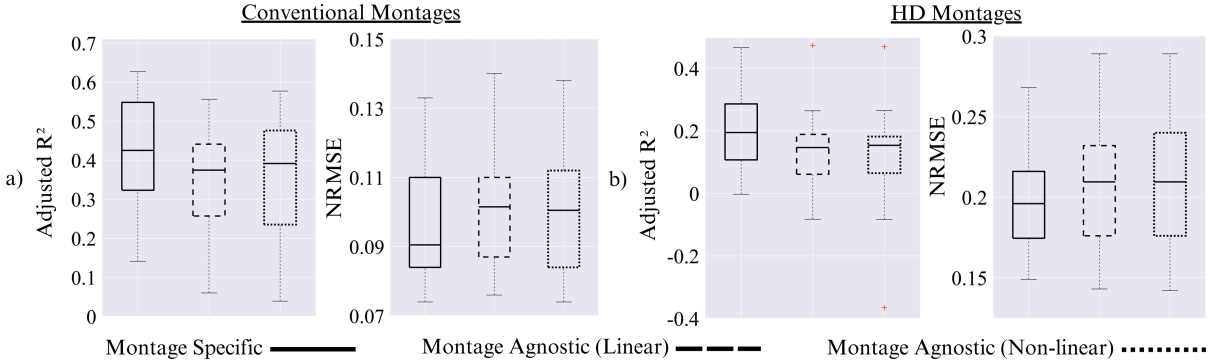

Figure 3.7.: Model performance in terms of the adjusted R^2 (left) and NRMSE (right) between the MRI-informed E-fields and the E-field predicted by our model across all test sets. a) Conventional montages. b) HD montages. Performance for montage-specific, linear montage-agnostic, and non-linear montage-agnostic models are shown. Box plot whiskers represent extreme values, the upper and lower bounds of the boxes indicate the 75th and 25th percentiles and the horizontal line within the boxes displays the median value. Outliers are shown as crosses.

3.4. Discussion

In this chapter, it was hypothesised that integrating demographic and anatomical parameters, such as head circumference and inter-electrode distance, into E-field dose optimisation models will significantly reduce inter-individual variability in peak E-field strength, providing a scalable alternative to MRI-based approaches. This was achieved this by incorporating a wide array of predictors, including age, gender, head circumference, cephalic index, BMI, and inter-electrode distance, to estimate peak E-field strength using robust multiple linear regression models. These models were developed and validated using the largest dataset of its kind, comprising n=4,161 total simulations across 10 montages. Crucially, these models were validated against unseen test data.

Spearman's partial regression analysis indicates that age is the strongest predictor of E-field variability, followed by head circumference. Interestingly, gender alone often showed a statistically significant influence on E-field strength. While peak E-field strength appeared higher in females than males, consistent with previous findings [172], interpreting gender-related results requires caution due to assumed uniform resistivity across the skull. Local variations in skull resistivity may impact results across the genders [145]. Additionally, multicollinearity exists between variables such as gender and head circumference. Notably, a correlation between BMI and peak E-field strength was observed, contrary to previous findings [173]. Unlike [173], we did not segment fat tissue, potentially leading to additional fat being interpreted as skin, which is more conductive.

Montage-specific models for HD montages do not appear to perform as well as those for conventional montages. However, caution should be exercised when making such direct comparisons. The average of the 95th percentile of the E-field magnitude within grey matter values was used as the measure of the peak E-field strength, which is consistent in volume regardless of the montage used. As a result, the measure of peak E-field strength did not account for the additional focality of HD montages, potentially making direct comparisons between the two montage types misleading. A threshold or region of interest-based approach may be more appropriate when comparing montages with differing focalities. However, previous works utilizing head circumference and a region of interest-based approach found models trained on focal montages performed better than those trained on conventional montages [146]. In addition, HD montages have previously been reported to induce more variable E-fields compared to conventional montages [174].

Montage-specific models outperformed montage-agnostic models in explaining the peak E-field strength variability. I explored both linear and non-linear models when incorporating

inter-electrode distance. The non-linear relationship between inter-electrode distance and peak E-field strength observed in this work has been noted in previous work [171]. However, a notable difference in performance between the linear and non-linear montage-agnostic models was not observed, likely due to the small number of unique montages. For instance, in the case of HD montages, only three montages were used for training. Thus, further research incorporating more montages could potentially improve the models. Additionally, factors such as electrode size and shape must also be considered to ensure montage-agnostic dose estimation is universally applicable to novel montages.

Future work could improve model performance and applicability by addressing simulation inaccuracies, moving beyond peak E-field strength to more complex E-field measures, and incorporating additional participant-specific measures. Since all E-fields were registered to the MNI152 space, future work could also investigate E-field positions and directions.

This work used the standard ROAST E-field simulation pipeline. However, it should be noted that E-field values are sensitive to the simulation approach used [175]. More complex E-field simulations that incorporate multi-layer skull models [176], fat tissue segmentation [173], or anisotropic tissue conductivity may improve accuracy. However, there may be diminishing returns when creating increasingly complex simulations, particularly when looking at macro-level features [177]. Additionally, the participant's posture in the MRI scanner also impacts the E-fields generated [178].

Alternative measurement techniques to estimate participant-specific head and brain characteristics without MRI scans could improve accuracy. Suitable techniques may include electrical impedance tomography [179] and resting-state electroencephalography [180]. In future works, additional participant-specific information such as ethnicity or genetic data may also improve model performance. Finally, generative modelling of structural MRI scans conditioned on participant-specific information [181] could also be used to improve E-field estimations.

3.5. Conclusions

Achieving consistent E-fields across participants through individualised dosing presents a fundamental challenge for tES research. Although participant-specific MRI scans and E-field simulations provide a precise solution, their high cost and limited accessibility hinder widespread use. This chapter addressed these constraints by developing robust multiple regression models that could accurately predict peak E-field strength using easily accessible demographic data, head morphology, and inter-electrode parameters. These results largely support the hypothesis that using demographic and anatomical parameters in E-field dose optimisation models significantly reduce inter-individual variability in peak E-field strength. Future experimental validation will be crucial to understanding the impact of the proposed approach to individualised dosing on tES efficacy and treatment outcomes, paving the way for more effective and accessible tES protocols.

4

Literature Review: Cognitive Enhancement and Transcranial Electrical Stimulation

4.1. Introduction

Chapter 2 introduced non-invasive brain stimulation (NIBS), encompassing a wide range of modalities and topics. This chapter focuses on the aspects of NIBS that align closely with the aims and objectives of this work, in particular, the literature on transcranial electrical stimulation (tES) for cognitive enhancement. Vigilant attention (VA) is further reviewed as an example of cognitive enhancement, including, an exploration of theoretical frameworks and approaches to measuring VA. Real-time biomarkers of VA and the use of tES for VA enhancement are also explored. Furthermore, potential strategies for reducing brain-state dependent variations by adjusting stimulation parameters in response to these markers are reviewed. This knowledge subsequently informs work addressing objective 2 in Chapters 5 and 6. To address objective 1, this chapter then examines the application of tES for VA enhancement and discusses the impact of inter-individual variation in tES efficacy. This includes an assessment of the state of electric field (E-field) simulations and dose estimations research, which informs subsequent work performed in Chapter 3.

4.2. Transcranial Electrical Stimulation for Cognitive Enhancement

As discussed in Chapter 2 tES is the application of small currents (1-4mA) to the scalp to modulate brain activity. tES is typically applied in one of four patterns of stimulation, as shown in Figure 4.1. Further information on the mechanisms of action of these stimulation patterns can be found in section 2.2. tES has been applied for the enhancement of a range of cognitive functions, including memory, attention, creativity and language [182]. Enhancing these processes has the potential to impact society by improving quality of life with age, boosting productivity, and aiding recovery from neurological conditions such as stroke. However, advancements in this field remain nascent, with limited translation beyond academic research.

The categories of cognition that will be covered in this section broadly reflect those discussed by P. Harvey. Namely, perception and sensation, motor skills, attention and concentration, memory, executive functioning, processing speed and language and verbal skills [183].

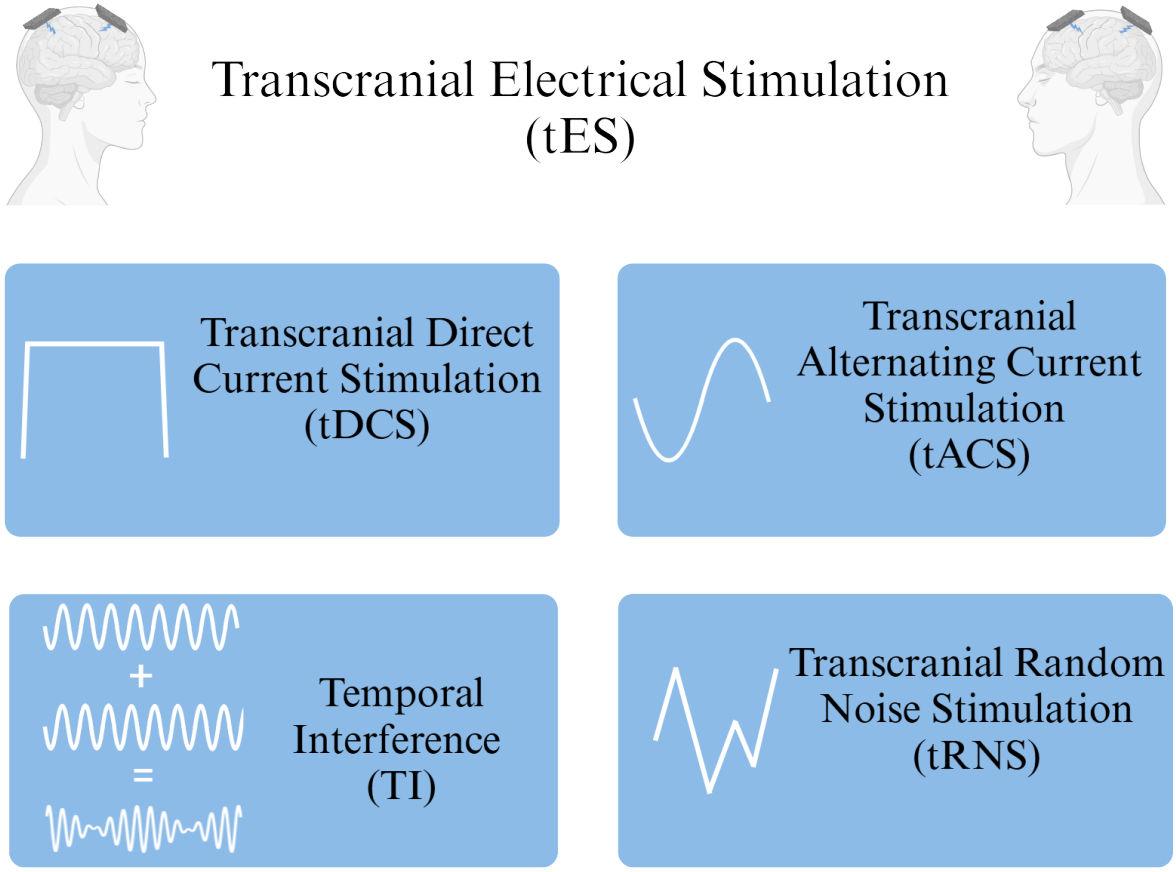

Figure 4.1.: An illustration of the main transcranial electrical stimulation (tES) patterns, including transcranial direct current stimulation (tDCS), transcranial alternating current stimulation (tACS), temporal interference (TI) and transcranial random noise stimulation (tRNS). Created with Biorender.com.

Perception and Sensation

The ability to sense stimuli (sensation) and process and integrate this information (perception) is another key area of cognition. One form of perception is object perception. This is the transformation of the raw visual information corresponding to an object into information that can be interpreted within an individual's perceptual framework. A systematic review and meta-analysis of the effects of tDCS on object perception in healthy adults by Lavezzi et al. concluded that tDCS enhances accuracy scores by an average of 8.8% when stimulating frontal sites but not occipital or parietal sites. However, the effect sizes at non-frontal sites may be explained by fewer studies included in these groups (6 studies in the frontal subgroup, 4 in the occipital subgroup and 2 in the parietal subgroup). There were also comparatively few cathodal tDCS studies included in this review (3 out of 18) [184]. There has also been significant work on pain perception, with a recent meta-analysis in tDCS for pain in healthy participants concluding that there is very limited evidence of anodal tDCS over the primary sensory cortex and primary motor cortex increasing pain perception thresholds and reducing evoked pain intensity respectively. Gurdiel-Álvarez et al. also found low-level evidence of anodal tDCS of the DLPFC reducing cold pain thresholds [185].

Motor Skills

In a systematic review and meta-analysis of the effects of tDCS on upper-limb motor performance by Patel et al., performance was found to improve in healthy adults. These effects were significant across reaction times, execution time and increased force. However, significant heterogeneity was observed across the literature [186]. Kang et al. analysed research focusing on longer-term changes in motor learning in post-stroke patients. In this work, they found significant positive effects of tDCS to motor learning, with robust long-term improvements across different protocols and recovery stages [187]. tACS applied to healthy individuals was also found significant improvements in motor learning. However, motor performance was not observed to improve. Notably, only gamma (>30Hz) frequency stimulation improved performance [188]. Finally, in a randomised, sham-controlled, double blind study, Vassiliadis et al. applied TI to reinforcement motor learning in humans through the targetting of the striatum. This work demonstrated that 80Hz striatal stimulation disrupts reinforcement-related motor learning [189].

Attention and Concentration

Evidence suggests tES can enhance attention and concentration, although these findings remain mixed. For instance, Brosnan et al. applied anodal tDCS to the right pre-frontal cortex (PFC) and observed improvements in sustained attention in both older adults with a cognitive deficit and a cognitively healthy adults [33]. Similarly, Weiss et al. demonstrated that cathodal tDCS over the posterior parietal cortex reduced response times in a high attentional load flanker task, suggesting that downregulating activity in specific areas can sometimes benefit attention [190]. Harty et al. also found that tRNS over the right DLPFC or right inferior parietal regions significantly improved reaction time variability when administered at 1mA [191]. However, other attempts, such as applying tES to the orbitofrontal cortex, did not significantly improve attention [192], highlighting the complexities and potential for variability across stimulation parameters and brain regions. A meta-analysis including the use of tDCS for attention/vigilance in patients with various brain disorders found that tDCS was superior to sham stimulation over 29 studies [193].

Memory

At the outset of this thesis the ability for tES to selectively stimulate deep brain targets in humans had not been demonstrated. However, as mentioned in Chapter 2, TI stimulation has since been demonstrated to change the blood oxygenation level-dependent (BOLD) signal and behaviour in the form of enhanced episodic memory [62]. Memory related networks also reside in cortical regions and as such are accessible by methods such as tDCS and tACS. A review of the effects of tDCS and tACS on working memory (WM) found that there was no reliable effect from single session tDCS studies on WM and moderate effects of multi-session tDCS and single session tACS [194]. Indeed, a review of HD-tDCS for WM concluded that HD-tDCS may potentially increase WM performance, but heterogeneity in both experimental design and outcomes across participants has been observed. This work, consistent with a common theme in tES research, highlights the importance of individualised montages and within-participant designs to mitigate inter-individual heterogeneity [195].

Executive Functioning

Executive functioning is the control of other cognitive abilities for their efficient utilizations to solve problems and plan for the future [183]. In a review of 63 studies, pre-frontal excitatory (anodal) NIBS showed a small positive effect on performance in both the stop signal and

Go/No-Go tasks, where these tasks cover the inhibition aspect of executive function. In addition, inhibitory (cathodal) stimulation was shown to have a small negative effect on Flanker task performance which also measures inhibition. Working memory and flexibility tasks were not impacted by NIBS, and planning tasks were inconclusive. It should be noted, however, that the studies included in this analysis were across both tES and TMS and included a broad set of parameters [196]. Recent work by Lu et al. explored the effects of tDCS and tACS on executive functions, specifically targeting the right inferior frontal gyrus (IFG) in 229 healthy participants. As in previous work, their study demonstrated that tDCS improved inhibition as evidenced in responses to the colour-word stroop task. In addition, cognitive flexibility was shown to improve through reduction in the shift cost during the shifting number task. However, both cognitive flexibility and WM were not improved by tDCS. Interestingly, these benefits were accompanied by a reduction in resting-state functional connectivity in the right IFG and frontal pole region, suggesting enhanced neural efficiency during stimulation. The lack of efficacy, particularly in the WM experiment, may have been due to ceiling effects caused by the high cognitive level of participants and the relatively low task difficulty level. This underscores the need for carefully tailored task designs to capture nuanced cognitive benefits in healthy populations [197].

Processing Speed

Findings on the effects of tDCS on processing speed are inconsistent and require further investigation. In a meta-analysis analysing 24 studies targeting processing speed in participants with brain disorders including depression, schizophrenia and stroke, tDCS did not have a significant effect [193]. A subsequent meta-analysis looking at individuals with ADHD specifically found limited effects on processing speed improvements with studies primarily targeting the left DLPFC [198].

Language and Verbal Skills

In a meta-analysis conducted by Price et al. significant and reliable effects of single-session anodal tDCS on language measures, such as verbal fluency, when applied to the left PFC were observed [199]. Furthermore, Monti et al. reviewed studies on tDCS and language, highlighting its potential to modulate linguistic abilities in healthy individuals and improve performance in patients with aphasia. Overall, they show that tDCS was able to improve language performance in both groups. They recommend a systematic approach to assessing the clinical features of patients as well as the need to optimise stimulation parameters [200].

Conclusions

The application of tES has been explored across various cognitive domains, including perception, motor skills, language, and executive functions, yet results remain inconsistent. Attention emerges as a particularly promising target given its broad relevance to other cognitive processes and the positive findings reported in various tES protocols. While not necessarily the definitive domain for cognitive enhancement, preliminary evidence suggests that the application of tDCS to attention. Informed by these findings, the following section narrows the focus to VA.

4.3. Vigilant Attention

VA is the ability to maintain conscious processing of non-arousing stimuli over prolonged periods [28]. One of the first systematic experiments related to VA in modern times was conducted in 1948, inspired by the need to understand how radar operators could maintain accurate vigilance for detecting anomalies. In a laboratory environment, the Mackworth clock task involved a participant watching a clock hand moving for up to two hours, at inconsistent intervals the clock hand would move twice the normal distance which the participants were instructed to note down. Over the length of a session, participants increasingly missed the larger clock hand movements due to a vigilance decrement [201].

However, the consequences of a deficit in VA go far beyond this simple task. This includes broad impacts on cognitive performance, including WM, long-term memory and fluid intelligence [29] and an increased risk of falls in older adults [31]. Additionally, a VA deficit has been associated with higher driving speeds in a simulated driving task [32].

4.3.1 Theoretical Frameworks of Vigilant Attention

Several theoretical frameworks have been proposed to explain the behavioural and neurological observations. These frameworks attempt to explain the cognitive processes underlying VA and the factors that influence attentional performance over time. The following section outlines some of the key theoretical perspectives on VA, their core propositions, and the associated brain regions and networks.

Name	Description	Ref
Arousal	Controls the amount of available resources. Hypoarousal, associated with mind wandering (MW). Hyperarousal is associated with distraction.	[202]
Opportunity cost	Task performance declines due to the brain's continuous evaluation of current versus alternative uses of limited cognitive resources.	[203]
Executive failure	Failure in executive control to maintain task-focused attention causes MW.	[204, 205]
Decoupling hypothesis	MW causes attention to be decoupled from task-related thoughts competing for executive resources.	[206]
Meta-awareness	The awareness (or lack of awareness) of one's own MW controls the length of MW episodes. An absence in the ability to notice MW is a lack of meta-awareness.	[207]
Information processing	VA performance is driven by the neural representation and communication of task-relevant stimuli.	[208]
Cognitive flexibility	MW involves flexible switching between task-related and task-unrelated mental sets, regulated by executive control processes.	[209]

Table 4.1.: A brief overview of some of the main theoretical frameworks of VA. Including their names, brief descriptions, associated brain regions and key references (VA = Vigilant attention, MW = Mind wandering).

Arousal is a key component of VA that is modulated by tonic norepinephrine levels in the locus coeruleus, which influences the fronto-parietal network among other neural systems. The fronto-parietal network regulates the processing of task-relevant information and the suppression of irrelevant stimuli. Consequently, the locus coeruleus-norepinephrine system and fronto-parietal network play critical roles in VA, with optimal performance occurring at moderate arousal levels. Hypoarousal (low arousal) is associated with mind wandering (MW), which is the unintended internal generation of task-unrelated thoughts and diminished

alertness. Intermediate levels facilitate focused attention, and hyperarousal (high arousal) is linked to stress and distractibility [202].

The opportunity cost model proposed by Kurzban et al. posits that the calculated opportunity cost of continuing with on-task thoughts is a considerable contributor to attention and task performance. That is, given the limited capacity of executive function, the benefits of maintaining on-task thoughts are in constant conflict with the opportunity costs of off-task thoughts. Thus, a decrement in attention can be thought of as the benefits of staying on-task being outweighed by the costs. The neural mechanism of this model is thought to manifest as a ventromedial prefrontal-ventral striatal network for cost and benefit encoding. To satisfy the model, the authors describe the requirement for limited executive function, fulfilled by the lateral prefrontal executive network. Finally, the model requires the calculated cost to be fed back and modulate the lateral prefrontal executive network. This can be explained by the anterior cingulate cortex or prefrontal cortical dopamine levels [203].

The information processing perspective suggests that maintaining optimal attention requires information from the stimuli to be represented and communicated optimally within the brain [208]. This theory is extended by the efficiency model, which posits that optimal attention occurs when minimal resources are used for processing task-related stimuli [210]. The information processing perspective is supported by optimal attentional states being associated with enhanced fidelity or reliability of visual representations and improved communication between visual and attentional control brain regions [208].

The executive failure hypothesis posits that MW represents a failure to maintain executive control over task-relevant processing. According to this view, suppression of task-unrelated thoughts requires executive resources. MW episodes occur when these control processes are inadequate to prevent the intrusion of task-unrelated thoughts [204, 205].

The decoupling hypothesis posits that MW is due to attention being coupled to task-unrelated thoughts, 'decoupling' resources from the task at hand [206]. As both task-related and task-unrelated thoughts rely on many of the same cognitive mechanisms, MW directly competes for executive resources. This was hypothesised to manifest in the brain as a reduction in the signal-to-noise ratio of the sensory stream [211]. There is supporting evidence for this theory in terms of both pupillary diameter analysis [211], and that off-task thoughts reduce sensory processing capabilities [212].

An alternative explanation of MW is cognitive flexibility. This describes MW as the inhibition of the task-related mental set and the activation of task-unrelated thoughts in WM. Wong et al. suggest that the lower rates of MW in older adults may be explained by declines in cognitive

flexibility, making it more difficult to switch between task-related and task-unrelated thoughts. This perspective also offers an alternative interpretation for some neurophysiological findings associated with MW, such as reduced P300 event-related potential amplitudes, which has also been observed in task-switching paradigms [209].

This non-exhaustive list of theories behind VA and MW represents a distinct but not incompatible set of theories. Ultimately, VA may be best explained by combining these theories. A set of integrated theories of VA are described hereafter.

The resource-control model attempts to reconcile the control model and information theory perspectives. In the resource-control model, MW is the default state of the brain. This is controlled by the default mode network. Maintaining attention takes executive control, which the frontal-parietal and dorsal attention networks may be responsible for [216].

The optimal state of VA, as defined by Esterman et al., combines arousal, the opportunity-cost model and the resource-control theory. The authors posit that, at an optimal attentional

Name	Description	Ref
Resource control	MW is the default brain state. This is associated with default mode network activity. The maintenance of attention requires executive control, which may be modulated by fronto-parietal and dorsal attention activity.	[213]
Process occurrence framework	Distinguishes between the initiation of MW (which can be explained by theories such as executive failure) and its continuation (explained by the decoupling hypothesis). Meta-awareness plays a role in regulating MW episodes.	[214]
Resource availability	Integrates arousal, executive control and information processing. Distraction and MW occur when the primary task does not fully engage cognitive resources, allowing task-unrelated thoughts or stimuli to capture unused resources.	[215]
Esterman's integrated framework	Combines arousal, the opportunity cost model and resource control theory. Arousal controls attentional resource availability, motivation is required, and executive control is required to maintain attention, satisfying the opportunity cost model and resource control theory.	[210]

Table 4.2.: A brief overview of some of the main integrated theories of VA. Including their names, a brief description, associated brain regions and key references.

state, arousal is sufficient to produce maximal attentional resource availability. At the same time, motivation to the task at hand is maintained to satisfy the opportunity cost model. Executive control is also actively used to maintain attention, reducing instances of MW as is prescribed by the resource control theory [210].

Smallwood & Schooler propose the process-occurrence framework, which distinguishes between two aspects of MW: its occurrence and its continuity [214]. The framework considers various explanations for the occurrence of MW, including the executive failure hypothesis, [204], while the process of maintaining internal thoughts is explained by theories such as the decoupling hypothesis and meta-awareness [206].

The resource availability model asserts that, at a given moment in time, cognitive resources are used for a single purpose. As a result, MW and distraction can occur simultaneously, assuming they are using separate resources. For example, Taatgen et al. demonstrated that the more complex a mental arithmetic/memory/visual attention task was, the more distracted participants were by a flanking (irrelevant) video. This was explained by the added complexity of the mental arithmetic/memory/visual attention task, resulting in prolonged task-related thinking, thus resulting in low resource utilisation of the not task-unrelated visual system, making them vulnerable to a visual distraction [215].

There are many theories of VA and the causes of MW and distraction. However, there is not yet a consensus on a holistic framework for VA that is consistent with all behavioural and neuroscientific evidence. Indeed, multiple theories have been used to explain the same phenomenon. For instance, resource-control theory, decoupling hypothesis, and cognitive flexibility perspective draw on similar neuroimaging evidence, particularly the anti-correlation between the default mode network and task-positive networks. However, each theory interprets this evidence differently. This underscores the complexity of VA and MW phenomena, demonstrating how the same neuromarkers can support multiple theoretical perspectives. Such convergence of evidence, viewed through different theoretical lenses, highlights the need for a holistic, integrated framework for understanding VA.

The aforementioned theoretical frameworks attempt to collate a range of neuroimaging and experimental data to provide a grounded and cohesive account for the process of MW and VA. However, the heterogeneous nature of VA theories, and indeed the distributed nature of VA within the brain, makes leveraging this information to inform tES protocols for VA enhancement challenging. For instance, the optimal approach may be a multi-site solution that could emerge over time, following successive studies independently testing the effects of each target site. Indeed, the optimal solution may also require stimulation that adapts

to a participant's brain activity at a given moment in time. A literature survey regarding neuromarkers associated with VA is described in Section 4.3.2. Additionally, previous attempts to stimulate the brain with tES and the associated outcomes are evaluated in Section 4.4.

4.3.2 Neuromarkers of Vigilant Attention

This section provides an overview of the neuromarkers associated with VA obtained from a variety of brain imaging modalities. This is in an effort to further understand the mechanisms of VA, and subsequently design stimulation protocols from an informed perspective.

Functional Magnetic Resonance Imaging and Positron Emission Tomography

Langner et al. performed a meta-analysis of the neural mechanisms of VA and compared neuromarkers across 67 experiments using functional magnetic resonance imaging (fMRI) and positron emission tomography (PET). Significant convergence in 14 distinct clusters in mainly right lateralised regions, including the mid-lateral prefrontal cortex, was identified. The probability of convergence on right lateralised regions was also associated with greater time on task, strengthening the likely role of the right hemisphere on VA [217].

Rosenberg et al. investigated the role of resting-state connectivity in VA task performance. Resting-state connectivity is the measure of how spatially distinct brain regions interact with each other while the participant is at rest. The authors found that resting-state connectivity from fMRI predicts performance in VA tasks [218]; this work also provided further evidence that networks associated with attention are complex, with connections between the motor cortex, occipital lobes and cerebellum being primary predictors of task performance in a VA task. Participants with better attentional performance also appear to have stronger connections between the subcortical cerebellum and the medial frontal lobe, motor cortex visual 1 and visual association networks.

Electroencephalography

Electroencephalography (EEG) is the use of electrodes on the scalp to measure electrical activity propagating from the brain. The electrical activity measured largely comprises the summation of many postsynaptic potentials [219]. EEG data can be evaluated in terms of time domain and frequency domain components. In the case of frequency domain components,

these are often separated into specific frequency bands. For instance, a global reduction in the alpha (8-13Hz) band EEG in resting-state eyes-open EEG is associated with an increase in arousal [220]. Event-related potentials (ERPs) are commonly used for time domain components of EEG. ERPs are voltage fluctuations that are time-locked with a particular stimulus, which can be endogenous or exogenous [221].

The ratio of the theta (4-8Hz) and beta (13-30Hz) bands on a central EEG electrode (Cz) location is reduced in individuals with VA deficits due to Attention Deficit Hyperactivity Disorder (ADHD) compared to participants without ADHD (n=1,770) [222]. Notably, baseline frontal and central theta:beta ratios have also been found to be a predictor of transcranial random noise stimulation (tRNS) stimulation efficacy in a VA task [191]. While the precise mechanisms underlying the theta:beta ratio remain unclear, its significance extends beyond VA. It has been proposed as a potential indicator of cognitive processing capacity [223]. Furthermore, in the context of executive function, the frontal theta:beta ratio has been found to correlate with executive attentional control. Specifically, higher ratios are associated with decreased attentional control in healthy adults [224].

In addition to the resting-state theta:beta ratio O'Connell et al. were able to predict lapses in attention up to 20 seconds before a behavioural response indicated this was the case. Increased posterior alpha (8-14Hz) activity was observed preceding a missed target [225]. Martel et al. further validated this phenomenon with increased alpha activity observed in the 10 seconds before a missed target in a modified Mackworth clock task [226].

Posterior alpha activity has been stipulated as a measure of arousal levels [227]. Total change in alpha across the posterior region is hemisphere-specific and corresponds to a stimulus being ignored, indicating an active, sustained visuospatial attentional suppression mechanism [228].

Regarding time domain features, the frontal ERP, P300, has also been shown to decrease in magnitude and precede lapses in attention in VA tasks by approximately 4 seconds. This frontal ERP was present in six channels surrounding Fz. A reduction in the magnitude of the P300 is associated with attentional lapses, as it reflects disengagement from task-related monitoring and attentional mechanisms [225]. Two subcomponents of the P300, P3a and P3b occur in frontal and parietal regions respectively and are associated with the engagement of attention and the processing of novel stimuli (P3a), and the updating of working memory in response to task-relevant events (P3b). The P300 engages a distributed network, including the dorsolateral prefrontal cortex, as demonstrated through intracranial electrode and lesion studies [229].

Another ERP related to motor preparation, named the lateralised readiness potential, has been observed during a random-dot motion task. This fronto-central marker is measured by subtracting ipsilateral and contralateral ERPs and appears as a negative voltage approximately 320ms before a response peaking at the time of response. In addition, another ERP termed centro-parietal positivity, peaks at 170ms before a response is measured in the centroparietal region in the form of a positive voltage. This marker increases with evidence accumulation, and the amplitude at the time a reaction occurs is negatively correlated with the reaction time to the stimuli [228].

4.3.3 Experiment Design for Vigilant Attention

Tasks such as the finger tapping task, random sequence generation task, or the combined finger tapping random sequence generation task have been used in VA experiments. The finger-tapping task requires a participant to tap a button, often in time with an audible cue. When a lapse in attention occurs, variability in finger-tapping timing increases. In the random sequence generation, task participants are asked to press two buttons in a random order. The generation of random sequences requires the recruitment of executive resources. When a lapse in attention occurs, measures of approximate entropy typically decrease, reflecting less random and more predictable sequences. Boayue et al. combined these tasks, asking the participants to randomly press two buttons in time with an audible cue presented every 750ms that lasted for 75ms. Thereby allowing for the simultaneous measurements of executive control through the randomness of the sequences generated by participants, behavioural variability through timing deviations in finger-tapping and mind wandering through self-reported thought probes [230].

Several tasks designed for VA experiments require the participant to respond and/or not respond to a given stimulus. The rate at which a participant hits or misses the target is known as the miss/hit rate. This miss/rate and the time taken for the participant to react (reaction time) are measures of attention. When lapses in attention occur, the miss rate and reaction time are expected to increase. As previously mentioned, a classical experiment for VA is the Mackworth clock task, in which the Royal Air Force measured VA with a ticking clock. This clock would unpredictably move the hand twice as far as normal, which the participants were instructed to note down [201]. Modified computerised versions of this experiment have since been designed, such as the modified Mackworth clock task proposed by Martel et al. [226]. In this experiment, 42 white circles are arranged in a circle on a display, much like the hours on a clock face. The colour of a circle changes to green in a clockwise sequence around the circle, much like the second hand on a ticking clock. Participants are instructed to gaze at

the fixation cross positioned in the centre of the display. In 10% of the instances in which the green dot moves around the circle, it moves twice as far, missing one position. Participants are instructed to press a button as fast as they can when they notice this double motion. Neural habituation of visual stimuli was also considered by slowly changing the colour of the fixation cross and asking participants to perform microsaccades between 'ticks'. EEG measures of increased alpha activity and attenuation of the P300 preceding a missed double movement have been observed during this task [226].

Other commonly used tasks include the continuous performance task and the psychomotor vigilance task. The continuous performance task requires participants to respond to flashing letter stimuli and press a key when a specific letter is shown [192]. The psychomotor vigilance task presents the participant with a blank screen, followed by a timer counting up. The participant is tasked with pressing a button as soon as the timer appears, with the displayed number counting up then pausing when the button is pressed and the displayed number representing their reaction times [231].

The random dot motion task requires participants to observe dots moving in random directions on a display. At specified intervals, the dots move coherently together in a specified direction; the level of coherence (percentage of dots that move together rather than randomly) can also be adjusted by the experimenter. The participant focuses on the centre of this display and is asked to press a button in response to coherent motion. This experiment has been used with corresponding EEG measures such as parietal alpha, which precede lapses in attention with measures such as reaction time and miss rate measured in relation to the coherence of dot movement [232].

In sum, these experiments represent a broad spectrum of approaches to measure VA. Regarding their application to the simultaneous EEG/tES experiment defined in objective 2 in Chapter 1, there are two considerations. Firstly, real-time task performance measures are desirable to enable closed-loop tES. In this case, the finger tapping and random number generation tasks may not be the optimal experiments. This is due to the derivation of task performance originating from the estimation of randomness within the sequences generated by participants or the variability in finger tap timing. Both of which are challenging in real-time. Secondly, a precedent for real-time EEG measures associated with them is preferred. To that end, the continuous performance task and the psychomotor vigilance tasks do not have a large corpus of real-time EEG measures predicting lapses in attention associated with them. The random-dot motion task meets the criteria for use in closed-loop experiments due to the aforementioned established measures of attention lapses from EEG [232], as well as the continuous performance measures of the hit/miss rate and reaction times.

4.3.4 Qualitative Measures of Vigilant Attention

In addition to quantitative measures, such as reaction time or miss rate, qualitative measures can provide insights into VA. Several questionnaires could be used to help determine baseline VA performance.

Brosnan et al. stimulated the right prefrontal cortex (PFC) for VA enhancement. In this work, the Montreal Cognitive Assessment was used to determine if aged participants had a cognitive deficit [33]. While a general cognitive assessment score may correlate with attentional performance, it is not solely focused on attention. The Epworth sleepiness scale could also be used to determine if participants are often 'sleepy' [233], which is likely to impact their VA due to their low arousal state. However, this, once again, does not directly measure attention. Finally, the World Health Organisation's Adult ADHD Self-Report Scale (ASRS) v1.1 is a widely used ADHD screener with high test-retest reliability [234]. This test asks questions specifically about attention as it is intended to assist with ADHD diagnosis. While it does not solely measure attention, it could be used as a baseline for qualitative attentional performance.

Thought probes can also be used to assess the participant's attention on-task during the experiment. For instance, Walker et al. utilised thought-probes in a simulated driving experiment to check whether participants were thinking about driving [32]. Thought probes can be considered in addition to questionnaires and task performance measures. They can also help delineate between types of attentional lapses by asking participants whether, during attentional lapses, they were MW or distracted by external stimuli.

4.4. Transcranial Electrical Stimulation for Vigilant Attention Enhancement

As described in Chapter 2 tDCS is the application of a small, constant current, usually less than 4mA, to the scalp of a participant through electrodes. Anodal tDCS is the application of a positive current, which is traditionally considered to increase neuronal excitability, although other factors such as neuron orientation should be considered [20]. In addition to modulating neuronal excitability, there is also evidence that tDCS changes neurotransmitter concentrations [235]. Dopamine is a neurotransmitter associated with cognition and attention [236], and extracellular dopamine has been shown to increase in concentration in the right dorsal striatum as a result of anodal tDCS over the left Dorsolateral Prefrontal Cortex (DLPFC) [237]. Norepinephrine, which influences arousal by modulating frontal-parietal regions [210], does

not appear to increase with frontal brain stimulation [238]. Through these mechanisms and others, tES may have the capacity to modulate VA. Below are a series of experiments where tES was utilised to modulate VA.

Evidence has been accumulating to suggest that dopamine plays a key role in attention performance, with deficits in attention from Parkinson's and ADHD patients associated with deficits in dopamine and dopaminergic medication improving attention [239]. In a study by Fukai et al., participants (n=20) were provided with anodal stimulation over the left DLPFC (F3) and the cathode placed over the right DLPFC (F4). Active or sham stimulation was provided for 26 minutes, after which PET scans for dopamine, MRI scans for locating regions of interest and cognitive tests were performed. Higher accuracy and speed in a reaction time task were associated with a higher dopamine concentration in the right ventral striatum, indicating that improved attentional performance is associated with anodal left DLPFC stimulation and higher dopamine concentrations [240]. This contradicts the work by Fonteneau et al., which found an increase in dopamine in the right dorsal striatum and left putamen under a similar montage (n=32) [237]. This may be explained by differences in stimulation duration and timing.

As previously mentioned, a large network of right lateralised regions is shown to be recruited during VA tasks in fMRI and PET studies. As such, several studies have attempted to improve attentional performance by stimulating various right lateralised regions.

Brosnan et al. applied anodal tDCS to the right PFC over two distinct groups and tasks. The first group (n=26) contained healthy older adults with reduced VA performance based on their score in the Montreal Cognitive Assessment, and stimulation was provided while a Sustained Attention to Response Task (SART) was performed. 1mA anodal right PFC stimulation with the anode placed over F4 and the cathode placed over Cz reduced the number of attentional lapses compared to sham stimulation. The second independent group (n=23) was not preselected based on their score in the Montreal Cognitive Assessment, and a different Continuous Temporal Expectancy Task (CTET) was performed; stimulation once again improved performance. The authors conclude that rPFC excitability changes are process-specific rather than merely task-specific [33].

Harty et al. explored the impacts of transcranial Random Noise Stimulation (tRNS) over the DLPFC (F4) and right inferior parietal lobe (P4) on attention. A reaction time task was performed before, during and after stimulation of 1mA, 2mA or sham (n=72). They found that 1mA tRNS significantly improved individuals' coefficient of variation reaction times and that theta:beta ratios, measured with EEG, were a significant indicator of the tRNS effect.

However, a stimulation intensity of 2mA did not significantly improve reaction times [191].

The previously mentioned examples use anodal tES with the intention of upregulating activity; however, in some instances, one may wish to downregulate activity to enhance performance. Weiss et al. improved response times during a task that elicited high attentional load by providing cathodal stimulation to the Posterior Parietal Cortex (PPC). Participants performed a flanker task. In this case, the cathode was at P4, while the return electrode was placed on the contralateral supraorbital forehead. The task is to search for the target letter in the group, while non-target letters are also shown. A target letter is also shown next to or inside the circle of letters of interest, which the participants are told to ignore. The higher attentional load condition had a larger number of non-target letters visible. Cathodal stimulation over the PPC was only shown to reduce the time taken to find the target letter during this high attentional load scenario. The authors theorise that this is explained by the attentional load paradigm, in which irrelevant stimuli are processed more effectively under low attentional load [190].

Luna et al. proposed an anodal 1.5mA HD-tDCS montage during an attentional networks task in a 4-by-1 configuration, either on the right PPC (anode at P4), right DLPFC (anode at F4) or sham condition (n=92). EEG data was also recorded. Both stimulation montages impacted measures of VA, notably mitigation of phasic alertness (the ability to rapidly change attention due to a brief event) and executive vigilance (the ability to sustain the capacity to perform complex tasks), while only the stimulation of the right prefrontal cortex reduced alpha power measured via the EEG electrodes [241]. This is in contrast to the previously discussed work from Weiss et al. However, the electrode positions and tasks are not directly comparable. Further work is required to determine the role of anodal and cathodal stimulation targeting the PPC in VA.

In addition to the work targeting the right DLPFC and PPC, Ouellet et al. targeted the right orbitofrontal cortex (anode at Fp1, cathode at Fp2) with 1.5mA of stimulation (n=45). In this work, performance on a Continuous Performance Task did not significantly improve [192].

While the activity in the brain associated with VA is largely right lateralised, Boayue et al. note the role of the left DLPFC in executive function. As such, they stimulated the left DLPFC with an HD-tDCS montage around F3 during a finger-tapping random sequence generation task (n=100). MW is associated with less random number generation from participants, as well as a reduced capacity to tap to a metronome beat. Combining these tasks was intended to test MW in the context of both executive control, which is recruited for the random number sequence generation, and behavioural variability associated with the finger-tapping task.

This approach was found to reduce the propensity to mind-wander when compared to the sham stimulation group [230]. This work contradicts previous work in this area as Axelrod et al. applied 1mA of tDCS to the left DLPFC (anode at F3, cathode at the right supraorbital area) and found an increased propensity to mind wander [242]. Boayue et al. simulated both their HD-tDCS and Alexrod et al.'s tDCS protocols and concluded that the discrepancy in results is likely due to the non-HD-tDCS approach inadvertently stimulating non-target brain areas.

Stimulation of the left DLPFC has also been compared to the consumption of caffeine. McIntire et al. analysed participant performance in several tasks, including the Mackworth Clock task, over 30 hours of extended wakefulness under the influence of caffeine, 2mA of anodal left DLPFC stimulation or a sham condition. This study found significant improvements in stimulation efficacy over both the sham group and the group that consumed caffeine [231].

The cerebellum is traditionally associated with motor control [243], however in recent years anatomical and functional evidence has been accumulating that suggests the cerebellum may also significantly contribute to cognition, including attention, WM and learning [244]. Mannarelli et al. explored the impacts of anodal, cathodal and sham tDCS on the left cerebellar cortex for attention (electrodes were placed at 1 cm below and 4 cm lateral to the inion and over the left deltoid muscle) (n=25). The Attention Network Test asked a participant to respond to a row of symbols on a display as quickly as possible, providing the direction of the central arrow. The central arrow can be in between lines or other arrows which are pointing in the same (congruent) or random (incongruent) directions. This study found that cathodal stimulation significantly reduced reaction times for the congruent target. The authors theorise that this is due to reduced efficacy in error processing in the cerebellum [245].

Recent work has attempted to employ closed-loop tDCS to enhance VA. That is, the stimulation dose is adjusted in real-time based on EEG parameters. Despite the study's sample size (n=10), Caravati et al. analysed the affects of their adaptive tDCS protocol applied to frontal (anode Fp2, cathode F3) and/or parietal (anode P3, cathode P4) sites during a variation on the continuous performance task. Reaction times and the inverse efficiency rates (the ratio between reaction time and the accurate answer rate) were significantly improved compared to fixed stimulation. However, the RT variability and accuracy was not improved by closed-loop stimulation compared to fixed stimulation. This proof of concept work indicates that changing the stimulation amplitude based on frontal entropy-based metrics and theta power may enhance the efficacy of tDCS for VA enhancement [27].

4.4.1 Challenges in Transcranial Electrical Stimulation for Vigilant Attention

In each experiment described in section 4.4, the same current intensities were applied across the respective populations. However, 3D finite elements method (FEM) models, informed by structural MRI scans, show clear differences in the E-field generated in the brain between participants with the same stimulation intensity applied at the scalp. In a 4x1 1mA montage, simulated E-field intensities ranged between 0.1546 V/m and 0.2933 V/m between participants due to differences in head and brain morphology. The authors suggest optimising for standardised E-fields in the brain across participants, as opposed to current at the scalp [99]. These results are supported by Laakasi et al. and their modelling study for tDCS inter-participant variability in which they state, "The variations in the E-fields are mainly caused by differences in the individual morphology of the cerebral spinal fluid and brain, and hence, cannot be controlled in experimental studies unless detailed image processing is performed." [140]. An approach that takes into account the differences in the head and brain morphology between participants is required.

The majority of the studies described in Section 4.4 did not adjust stimulation parameters in response to changes in the state of the brain. This standard open-loop approach leads to large variability in outcomes between participants and overtime for the same participant [246]. Arousal levels explain some of the variability in stimulation efficacy [247], and stimulation to the prefrontal cortex modulates executive control [248], which are two traits of VA [210]. Adjusting stimulation intensity and, therefore, linearly increasing E-field intensity in the brain as attention lapses occur is intended to improve efficacy as a result.

As discussed in previous works, tES dosages typically range from 1-2mA. However, 4mA of stimulation has been applied to humans with minimal reported instances of pain or other side effects. An adaptive approach was employed to achieve this. In this approach, the current provided was subject to change relative to the impedance at the electrode site. If during a ramp-up / down period, impedance exceeded 20kΩ or if during the main stimulation period, impedance surpassed a 10kΩ threshold, the current was reduced accordingly. Self-reported pain increased with the addition of a relax button, which participants could press to reduce the current, suggesting this addition may increase rumination on sensation [249].

4.5. Closed-Loop Non-Invasive Brain Stimulation

The state-of-the-art stimulation for VA does not change stimulation intensity over time as the participants' attention wanes. As previously mentioned, the standard open-loop approach is a significant factor behind the heterogeneity in results that is visible in the literature [246]. For instance, levels of arousal arousal explain some of the variability in outcomes for NIBS [247]. Adjusting stimulation intensity, and therefore linearly increasing E-field intensity in the brain as attention lapses occur, is intended to improve efficacy.

There are examples of closed-loop stimulation in the literature, albeit in different contexts. For example, in a closed-loop transcranial Alternating Current Stimulation (tACS) study, participants received stimulation based on their EEG neuromarkers to improve memory consolidation. Participants (n=16) were trained to identify targets in a complex visual scene. They were then tasked with identifying targets after sleeping and receiving closed-loop stimulation or sham stimulation. Slow-wave oscillations (0.5-1.1Hz) during sleep are associated with memory consolidation. Stimulation was applied at the same phase and frequency as slow-wave oscillations measured via EEG. This closed-loop augmentation of slow-wave oscillations was found to improve memory consolidation beyond comparable open-loop significantly tACS [25].

Closed-loop stimulation can also be applied in response to task performance or task difficulty as opposed to neuromarkers. This approach has the benefit of being easier to measure in a controlled experiment but with potentially less generalised performance outside of the laboratory when task performance and difficulty are not controlled. Closed-loop tDCS may require short, well-timed stimulation doses. Javadi et al. applied short-duration 1.5 mA anodal or cathodal tDCS to the left DLPFC before or after participants memorised a word (n=13). Anodal stimulation preceding word memorisation was the most effective at improving performance, while cathodal stimulation significantly reduced performance [26].

4.5.1 Classifying Lapses in Vigilant Attention

In order to perform closed-loop stimulation, lapses in attention must be classified. This can be achieved using task measures, but the physiological classification of attentional lapses for closed-loop stimulation is both task-independent and can be used to separate different types of attention lapses.

Several studies have attempted to classify lapses in attention with varying levels of success.

Zhang et al. evaluated 0.8s segments of EEG data, band-pass filtered the data and extracted delta, theta, alpha, beta and gamma frequency bands using discrete wavelet composition. Approximate entropy, total variation, standard variation, energy and skewness features were then extracted as features for all of these bands and used to train a support vector machine classifier, which achieved 73.59% classification accuracy. This work used a dry, single-electrode EEG headset and did not attempt to classify the P300 ERP [250].

Conversely, Martel et al. classified MW with a classification accuracy of 71.6% using a 64-electrode EEG headset and a range of features, including parietal alpha of the P300 ERP. They iteratively tested a wide range of frequency bands, channel selection and time period combinations. The combinations with the higher classification accuracies corresponded to frontocentral channels, the alpha band (8-14Hz), and the P200 ERP as opposed to the P300 ERP reported in the literature [251].

4.6. Personalised Transcranial Electrical Stimulation

In subthreshold tDCS, the induced E-field strength linearly alters the neuronal membrane voltage [235]. As a result, participant-specific stimulation protocols standardised by E-fields in the brain (as opposed to the dose applied at the scalp) may improve outcomes [252]. Personalising stimulation intensity using motor threshold stimulation has been attempted with some success. Caulfield et al. applied a 200μs pulse of up to 400V and up to 58.0mA to the left motor cortex of participants. The motor threshold is reached when detectable signals are received from the participant's muscles, triggered by the high-intensity stimulation. This tES-based motor threshold approach was able to estimate 45% of the reverse-calculated tDCS dose variance [253]. The more commonly used approach is to purely simulate the E-field in the brain using structural MRI scans for each participant. These scans are then used in a FEM simulation [140].

4.6.1 Simulating Transcranial Electrical Stimulation

Segmentation of MRI scans is the classification of tissue types at each voxel of an MRI scan. Specific models vary in their implementation, but a commonly used software package named Statistical Parametric Mapping (SPM) uses a Gaussian mixture model to classify voxels. These models work by fitting a Gaussian distribution to the intensity of different voxels that are associated with different tissue types. However, these per-voxel probability values may not

accurately represent the real tissue distribution, so a Gaussian low-pass filter is used to smooth the tissue masks. Voxels that are classified differently from their neighbouring voxels are also assigned a tissue class based on their surrounding voxels. The intensity of a given voxel can then be mapped to the probability that voxel belongs to a tissue class [254].

Commonly used segmentation software include SPM, as previously discussed, and FreeSurfer. An in-depth analysis of these approaches by Palumbo et al. demonstrates that both have a high test-retest correlation, although inter-method comparisons showed variations in the overlap of the tissue maps (0.76-0.83 measured by the DICE index) [255]. Additionally, in a comparison by Huang et al. between automatic segmentation and a hand-segmented MRI scan, ROAST (using SPM12 and a custom post-processing script) achieved greater accuracy of the total absolute volume of white matter, grey matter and CSF volumes when compared to various versions of SimNIBS. Surface-based segmentation approaches, such as that used by FreeSurfer and FSL, more accurately capture the structure of cortical folds at a higher computational cost [15].

Once an MRI model is segmented, a volumetric mesh is generated, breaking up the 3D model into discrete tetrahedral blocks. This then informs subsequent finite element modelling steps. There are multiple meshing approaches available that have a relatively inconsequential impact on the end results in regard to the simulated E-field in the brain and CSF, which differ by 0.01V/m 0.1V/m respectively [15].

Finally, FEM analysis is used to numerically solve for the voltage distribution using the open-source software getDP [15]. A comparison of SimNIBS and ROAST found that the E-fields predicted by each approach differ significantly. However, these trends are not systematic, and no individual simulation tool appears to be significantly more accurate [256].

4.6.2 Validation of Simulations for Transcranial Electrical Stimulation

The utility of these models is predicated on the simulated E-fields accurately reflecting the real induced E-fields. There are several areas in which these models oversimplify or ignore aspects of the real world, and this impacts their validity.

For example, the skull bone is often assumed to be a homogeneous conductor in simulation. The conductivity of the homogeneous skull is set to approximately 0.01S/m as the layers of the skull are not easily extractable from MRI scans [254]. In reality, the skull bone is made up of a spongy diploë inner table, which is sandwiched between two layers of dense cortical bone known as the outer table [93]. These layers each have different conductivities

that also vary between participants, with one study putting the top outer table layer as 5.4-7 mS/m, the lower outer table at 2.8-10.2 mS/m and the inner spongy later at 16.2-41.1 mS/m [257]. Crucially, the thickness of each of these layers also varies by age and gender [93]. In a simulation study comparing the use of three layers of skull material and a single layer, it was found that modelling these layers individually is not necessary as long as the value of conductivity chosen is as close to that of the real skull as possible [258]. This participant-specific value for skull conductivity is not evident from MRI scans used for simulation. As a result, the approximated value of 0.01S/m is a cause of uncertainty.

Similarly, the volume between the skull and the brain is typically modelled as homogeneous CSF, which, in reality, half consists of meninges layers that have lower conductivity than CSF [18]. Typically 1.65S/m is used as the conductivity of CSF, by taking into account the meninges layers a more realistic conductivity value is 0.85S/m. This updated value was validated with intracranial recordings provided by Huang et al. [17] and was found to better reflect the real voltages measured [18].

Ultimately, the validity of these models can be defined by their correlations with data recorded in the real world. To this end, Jamil et al. performed tDCS on participants while measuring cerebral blood flow. They then compared this blood flow to the E-field predicted by FEM modelling. The spatial distribution of the measured cerebral blood flow change under the stimulation condition moderately correlated with the modelled E-field strengths [19]. While correlations of blood flow with non-participant-specific models are an indicator, participant-specific models of E-field, validated by comparing with intracranial electrodes, is a more relevant methodology. Huang et al. performed 2mA stimulation on epilepsy patients (n=10) with pre-existing intracranial electrodes and compared the estimated E-field from individualised models with the E-field recorded at each electrode. They found predicted and real E-fields were highly correlated at cortical sites (r=0.86) and deep brain sites (r=0.88) [17, 259].

4.6.3 Factors Influencing Transcranial Electrical Stimulation Induced Electric Fields

In the previous section, the use of, and validity of using, MRI scans to inform E-field modelling was discussed. However, to understand the literature necessary to meet the accessibility requirement of objective 1, other factors beyond expensive MRI images are reviewed below.

Head and brain morphology changes with age. For example, skull thickness is negatively

correlated with age (n=123) [93]. Cortical thickness, volume and surface areas are also all negatively correlated with age [94]. Age also had a significant impact on brain tissue volumes, with older adults having lower grey and white matter volumes and higher ventricular volumes [95]. In a simulation study testing the effects of age on induced E-field strengths, older adults had less intense E-fields induced than younger adults [155].

Antonenko et al. used linear mixed models to find the optimal stimulation intensity for a participant, given their head circumference. They found that head circumference is negatively correlated to E-field strength across six commonly used montages (n=47). Their models accounted for 28% and 24% of peak E-field strength variability for conventional and HD-tDCS montages, respectively [146].

Obesity leads to a layer of subcutaneous fat around the head. This fat has a relativity low conductance 0.025S/m. A simulation study comparing peak E-field intensity over 5 participants of varying body mass index ranging from normal to super obese found no significant impact in E-field intensity [173].

Sex also has a significant impact on head morphology, with females typically having thicker skulls than males on average [93]. On average, women have a higher percentage of white matter and CSF compared to men [260]. These differences in morphology have an impact on the E-field generated in the brain, with males having a greater E-field intensity compared to females, especially in the parietal region where females have denser bone [145].

Finally, there is a non-linear relationship between the distance between electrodes and the strength of the E-field that is induced [171, 261]. As a result, models trained to infer E-field strength that are informed by the inter-electrode distance would likely be able to account for more of the E-field variability.

To date, the correlation between factors such as age, sex and head size have been observed. However, a single model that incorporates many of these measures to produce estimations of E-field measures, such as peak E-field intensity, does not currently exist.

4.7. Conclusions

VA is a key part of cognition. Improving VA performance across the population would have a significant impact on quality of life from older adults [31], to safer driving [32] and other areas of cognition [29]. While there are many brain areas associated with VA [217], the right hemisphere, specifically the right prefrontal cortex, is of significant importance [262].

Stimulation efficacy varies across participants, in part due to the difference in the E-field generated in the brain with the same stimulation montage [140]. Personalising stimulation based on head morphology using simulation has been proposed as a solution to this problem and has proved to be successful [252]. However, this approach requires MRI scans to be taken of each participant, which is expensive and time-consuming. The E-field generated in the brain changes as a function of sex [145], age [155], head circumference [146] and electrode location [261]. Estimating the E-field generated based on these parameters could provide an MRI-free way of keeping consistent E-fields across participants. A new framework is required that provides stimulation that is both personalised for a participant's head and brain morphology and responds to dynamic changes in attention.

5

Electrophysiological Correlates of Response Time in a Vigilant Attention Task

5.1. Introduction

This chapter contributed to material published in the proceedings of the 44th International Conference of the IEEE Engineering in Medicine and Biology Society (EMBC 2022) [263].

This chapter explores electroencephalographic (EEG) correlates with VA in contribution to the satisfaction of objective 2 of this thesis, defined in Chapter 1. As discussed in Chapter 4, VA is the ability to maintain the conscious processing of non-arousing stimuli for prolonged periods [28]. A VA deficit in an individual is linked with a deficit in several other cognitive abilities such as working memory, long-term memory and fluid intelligence [29]. VA performance is reduced in older adults [30] and is associated with an increased risk of falls [31]. A VA deficit has also been associated with higher driving speeds in a simulated driving task [32].

Detecting lapses in VA before it influences behaviour can allow for interventions such as alerting the participant [264] or perhaps non-invasive stimulation which has been used in a closed-loop fashion in other scenarios such as sleep-dependent long term memory generalization [25]. An EEG headcap can be used to predict lapses in attention before it produces behavioural outcomes.

EEG markers of a decrement in VA come in the form of event-related potentials (ERPs) and band power features. ERPs notate EEG voltage fluctuations that are time-locked to stimuli. An ERP, known as the P300, is the cognitive response of the brain to a relevant but infrequent stimulus [229]. The elicitation of the P300 is delayed, reduced in amplitude, and accumulates slower when a VA decrement occurs [225].

In regard to band power features, increased alpha (8-14Hz) activity has been observed preceding a missed target [225]. O'Connell et al. observed this increase in parietal alpha up to 20 seconds before a behavioural response indicated this was the case. Martel et al. further validated this phenomenon with increased alpha activity observed in the 10 seconds before a missed target in a modified Mackworth clock task [226].

Kelly et al. observed a build-up of post-stimulus, pre-response parieto-occipital alpha band activity during a random-dot motion task, described as a supramodal decision signal. Increased reaction times (RTs) from participants were also correlated with increased alpha band amplitude [232]. A reduction in posterior alpha power has been stipulated as a measure of increased arousal levels [227], which are a key component of VA [210]. EEG measures of both hemispheres during an attentional task with bilateral flickering stimuli found that the

total change in alpha across the posterior region is hemisphere specific, demonstrating a retinotopic active sustained visuospatial attentional suppression mechanism [228]. In addition, activity within the high-beta/low-gamma frequency band (25-35Hz) has been found to be one of the most discriminative features between on-task and off-task thought in parieto-occipital channels [251].

This chapter investigates the hypothesis that EEG markers, including pre-stimulus frequency domain features and post-stimulus event-related potentials are significantly correlated with VA performance. VA performance is measured by response times in a random-dot motion (RDM) task with varying levels of difficulty. To test this hypothesis pre-stimulus frequency domain features from 4-40Hz are extracted, and post-stimulus time domain data is analysed. These data are explored in relation to the tasks difficulty and RT.

5.2. Methodology

5.2.1 Participants

30 young adults between the ages of 20-39 years of age participated in this study (12 males, 18 females). Participants had no history of neurological illness or cardiac disease and had normal or corrected to normal vision. All participants provided written informed consent, and this study was approved by the ethical review board of the School of Psychology, Trinity College Dublin in accordance with the Declaration of Helsinki.

5.2.2 EEG Data Acquisition

An ActiveTwo Biosemi system with a sampling rate of 512Hz and 8 electrodes at positions Fz, C3, Cz, C4, P3, Pz and Oz according to the 10-20 standard system [265] was used to acquire the EEG data. The impedance at each electrode was kept below 5kΩ.

5.2.3 Continuous Random-Dot Motion Task

Participants took part in a continuous random-dot motion (RDM) task. In this task, participants are shown dots moving incoherently in random directions on a display. At random time intervals of 3.1, 4.2 or 5.7 seconds a percentage of these dots move either left or right,

coherently together as shown in Figure 5.1. Participants are asked to respond to the coherent motion by pressing a button with their left hand if the dots move left, or to press a button with their right hand if the dots move right. Coherent motion lasted for 1.9 seconds, with coherence levels at either 19% or 25%. The white dots were presented against a grey background on a cathode ray tube monitor, with a refresh rate of 85Hz and a resolution of 1024x768 pixels. 118 dots were displayed in total, each 6x6 pixels in size, the positions of the dots were updated every 47ms. Participants underwent three practice sessions with coherence levels of 80% or 60%, 40% or 30% and finally 25% or 20%. To ensure participants' comprehension of the task, in the practice session they were provided with verbal feedback on hits, misses and false alarms. During the recorded experiment, each participant participated in two sessions of the task, each with 40 trials evenly split between low coherence (LC) and high coherence (HC) stimuli, with the coherence level set to 19% and 25% respectively. Each session lasted approximately 4 minutes.

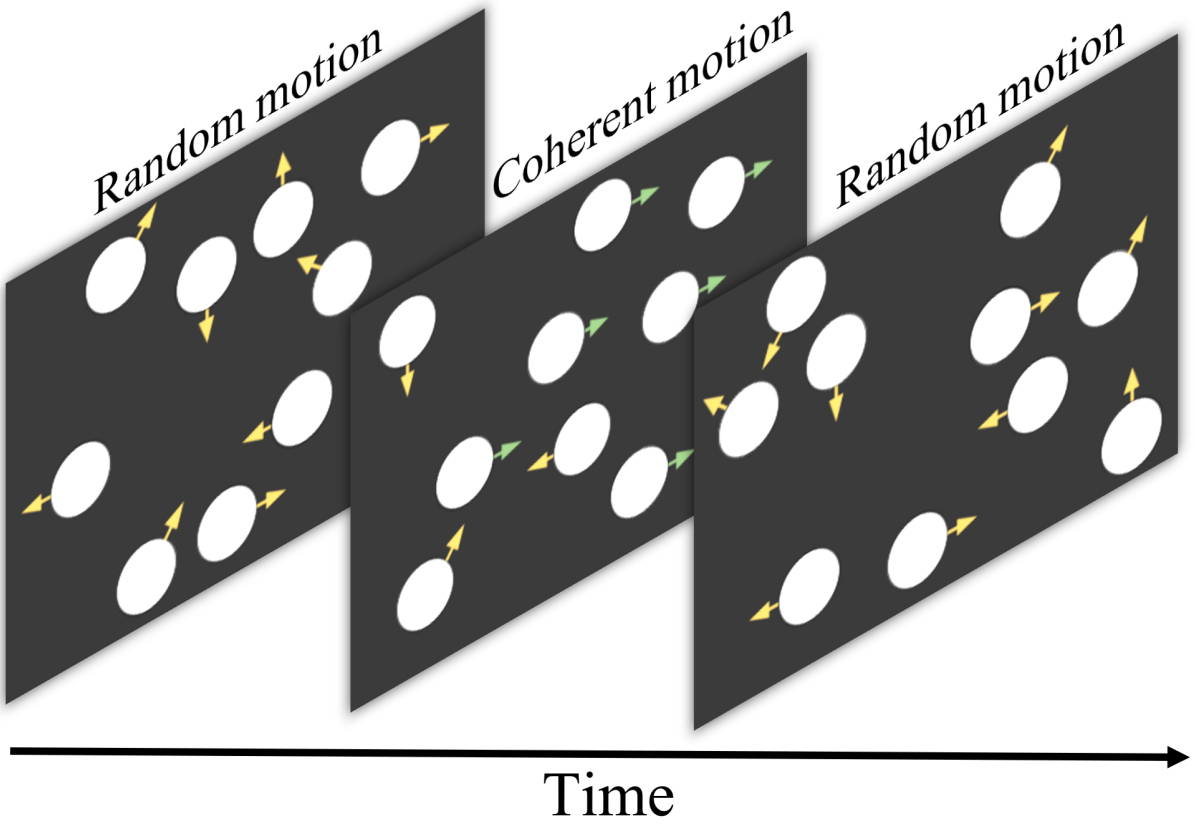

Figure 5.1.: Illustration of the continuous random-dot motion task. Arrows are not visible in the experiment but illustrate the movement direction. Yellow arrows=incoherent motions, green arrows=coherent motions.

5.2.4 Behavioural Analysis

RTs and miss rates (MRs) were analysed to provide an overview of task performance in response to HC or LC stimuli. At the population level, RTs were aggregated across all participants in each condition. Kernel density estimation was used to create smoothed distributions for visualising RTs. For each participant, the RTs were split evenly resulting in the slowest 50% of responses being placed in the slow RT subset and the fastest 50% of responses placed in the fast RT subset. In addition to the plots, the median and inter-quartile ranges for both RTs and MRs are reported. Individual RTs are also illustrated in the form of box and scatter plots for both HC and LC conditions. All analyses, including the generation of kernel density plots, box plots, and the calculation of medians and inter-quartile ranges, were conducted in MATLAB R2023a.

5.2.5 EEG Data Processing

Pre-Processing

Frequency domain trials were extracted from 777ms preceding the presentation of the stimulus, up to its presentation from a parietal electrode (Pz). 777ms was chosen to balance the minimisation of spectral leakage during the fast Fourier transform, the need for sufficient frequency resolution and the appropriate pre-stimulus sample length. Artefact rejection was performed by excluding trials where the difference between the maximum and the minimum amplitude of the frontal electrode Fz was greater than 70μV. Sessions were excluded if greater than 50% of the trials within that session were rejected due to artefacts. The single-channel Pz, used to extract the magnitude of different frequency bands, was referenced to the frontal channel Fz. Trials were split into six subsets, slow RT HC, slow RT LC, fast RT HC, fast RT LC, no response LC and no response HC. 'No response' subsets refer to when a participant did not respond to a given stimulus.

Feature Extraction

Before extracting frequency domain features, a zero-phase, IIR 3rd order Butterworth band-pass filter between 0.1Hz and 45Hz was applied. The magnitudes of the frequency bands were calculated for each trial using the fast Fourier transform. The mean average of nine frequency bands in increments of 4Hz was calculated from 4-40Hz. These 4Hz increments were chosen because they align with commonly referenced frequency bands (i.e. theta (4-8Hz), alpha (8-12Hz), etc). The frequency band less than 4Hz was not considered due to the potential of noise having a large influence on the results.

Before extracting time-domain features, a zero-phase Butterworth band-pass filter between 0.1Hz and 10Hz was applied. Trials were baseline corrected using a period of 200ms before the stimuli were presented. All signal processing was performed using MATLAB r2020b.

Statistical Tests

Once the magnitudes of the 8 frequency band values were calculated non-parametric Wilcoxon rank-sum tests were performed across four conditions (HC slow RT, HC fast RT, LC slow RT and HC fast RT) using all the pooled trials. P-values have been Bonferroni-corrected to reflect multiple comparisons. In addition the difference in medians across is presented to show the directionality of any effects.

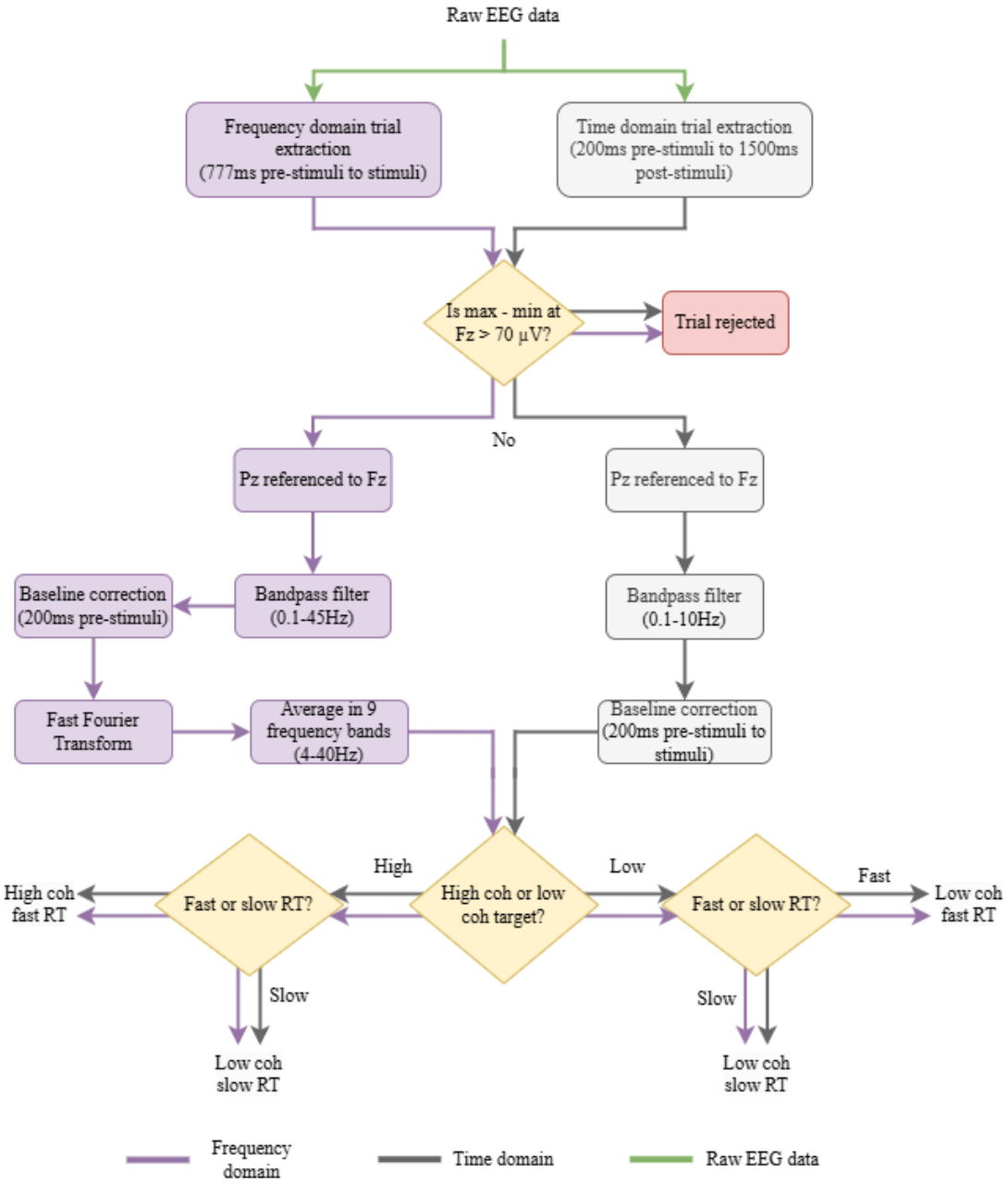

Figure 5.2.: Illustration of the EEG processing procedure used to extract time domain and frequency domain features. RT = reaction time, coh = coherence.

5.3. Results

5.3.1 Behavioural Results

RTs were measured for both LC and HC stimuli. For LC stimuli, the median reaction time was 793 ms (Q1 = 727 ms, Q3 = 948 ms). For HC stimuli, the median was 683 ms (Q1 = 604 ms, Q3 = 830 ms). The distributions of RTs across the population are illustrated in Figure 5.3 a). For each of the stimuli conditions RTs were split into 'slow' and 'fast', which corresponds to the largest and smallest 50% respectively. The median RT for HC stimuli was 541ms and 846ms for fast and slow response times respectively. The median RT for LC stimuli was 648ms and 1082ms for fast and slow response times respectively. Median RTs are also illustrated in Figure 5.3 b). Miss rates for low-coherence stimuli had a median of 9.46% (Q1 = 3.73%, Q3 = 21.3%), while high-coherence miss rates had a median of 6.49% (Q1 = 2.50%, Q3 = 21.9%).

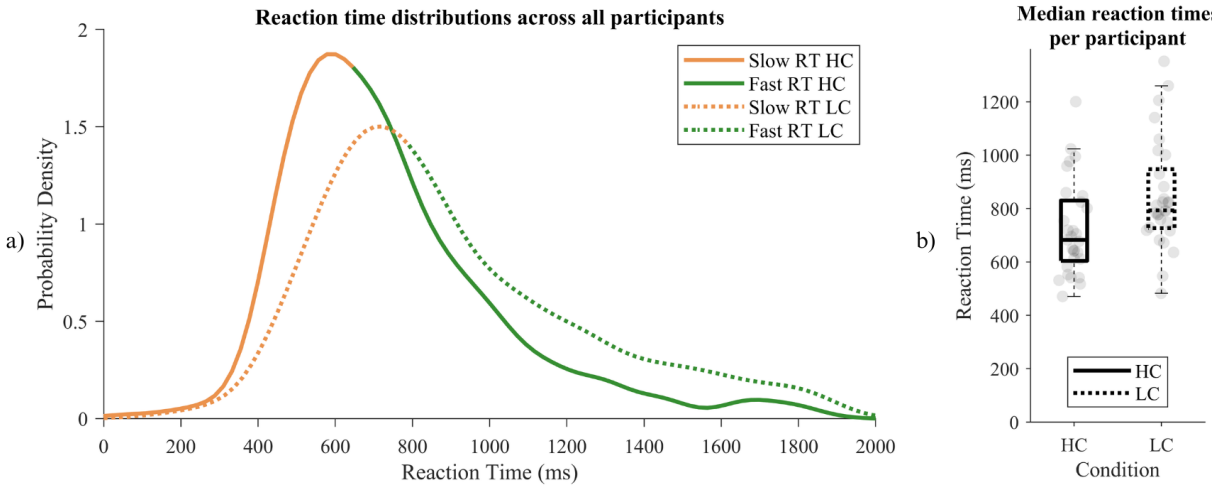

Figure 5.3.: Reaction times (RTs) for high coherence (HC) and low coherence (LC) stimuli. (a) Probability density of RTs across participants: solid lines represent HC (orange=slow RT, green=fast RT), and dotted lines represent LC. (b) Box plots of median RTs per participant: solid boxes indicate HC, and dotted boxes indicate LC. Whiskers show extreme values, boxes span the 25th to 75th percentiles, and the horizontal line represents the median.

5.3.2 Frequency Domain EEG

Frequency domain graphs were produced for LC stimuli (see Figure 5.4) and HC stimuli (see Figure 5.5). These figures illustrate the difference in the magnitude of the pre-processed EEG signal at Pz across different frequencies, for fast RT, slow RT and no response at a given stimuli coherence level, with shaded regions for standard error. A peak is visible around 21Hz. As the white dots presented to the participant in the experiment moved every 47ms the peak around 21Hz is likely to be a steady-state evoked potential in response to this motion.

After artefact rejection, a low number of trials for the 'no response' condition were available for both the LC and HC stimuli (i.e. N=164 and N=77 for low and HC conditions, respectively). This is in part due to the low miss rate of the participants and also the artefact rejection rate (i.e. 28.5% of 'no response' trials) potentially due to eye movements and other muscular movements. As a result, the 'no response' condition was not included in the statistical analysis, however, these results were included in Figures 5.4, 5.5 and 5.6 for completeness and comparisons.

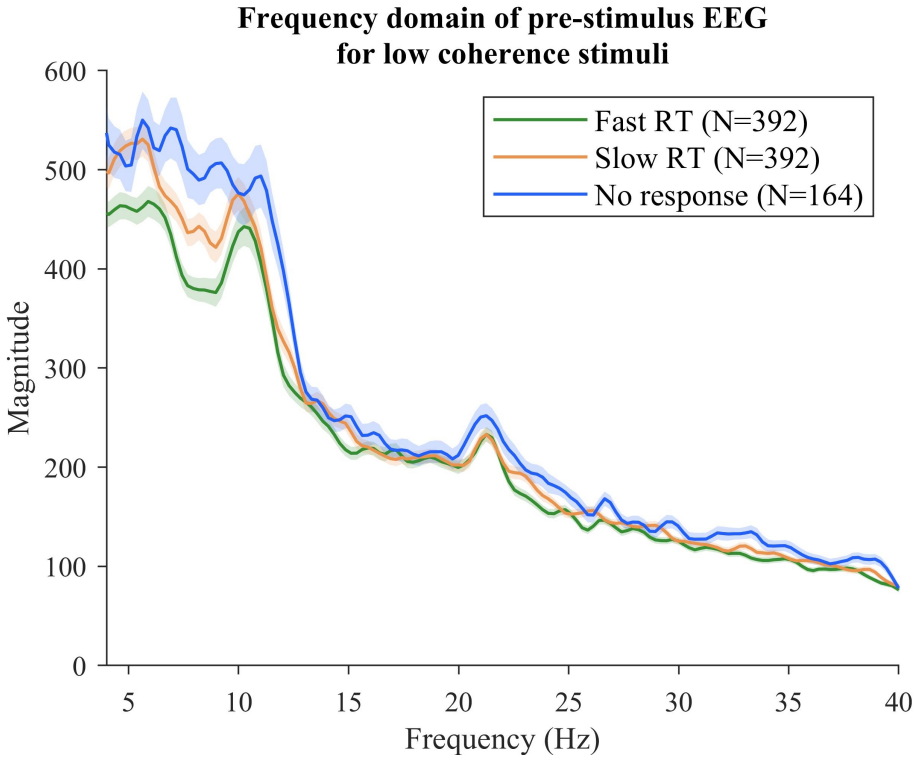

Figure 5.4.: Pre-stimulus frequency domain response from the posterior electrode Pz for fast RT, slow RT and no reaction to low coherence stimuli. (RT=reaction time, N=number of trials)

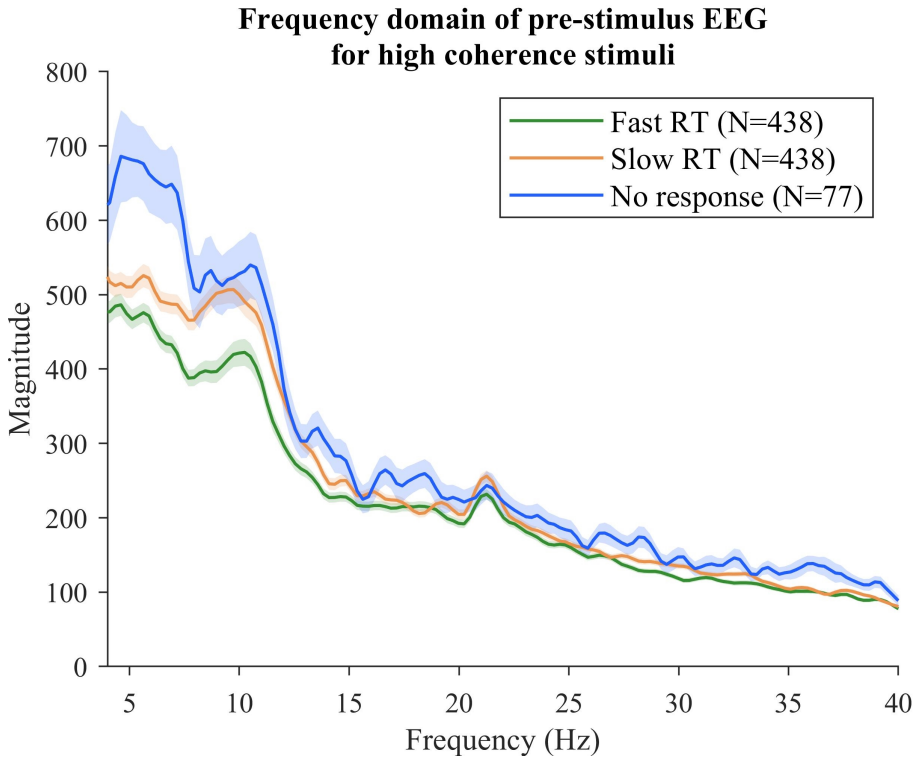

Figure 5.5.: Pre-stimulus frequency domain response from the posterior electrode Pz for fast RT, slow RT and no reaction to high coherence stimuli. (RT=reaction time, N=number of trials)

As can be seen in Table 5.1, there is a statistical significance between magnitudes of different frequency bands. For HC stimuli, significant differences are observed in the theta (4-8 Hz), alpha (8-12 Hz), low-beta (12-16 Hz), and high-beta/low-gamma (28-32 Hz) bands. For LC stimuli, significant differences are found in the theta (4-8 Hz) and alpha (8-12 Hz) bands.

The alpha component (8-12Hz) was significantly higher with slower responses compared to faster responses in both HC and LC stimuli. Increased alpha power is associated with an active visuospatial attention suppression mechanism and may play a crucial role in distractor suppression during tasks requiring sustained visuospatial attention [228]. Increased alpha power is also associated with a greater propensity to miss targets in a continuous temporal expectancy task [225]. In addition, Martel et al. have demonstrated that alpha activity is a prominent marker of deliberate off-task states, suggesting that increased posterior alpha reflects internally directed attention and a top-down inhibition of irrelevant sensory input [251]. Barry et al., also observed a reduction in global alpha power being associated with a higher arousal state [227], indicating that participants may have been in a state of lower arousal when they reacted slowly to stimuli.

In addition, Martel et al. found that oscillations in the 25-35Hz range were one of the most discriminative features between on-task and off-task thought in parieto-occipital channels,

which is within the range of the high-beta/low-gamma 28-32Hz significant region observed in this work for HC stimuli [251]. A significant difference was not observed for LC stimuli in this frequency band. Significant differences were also observed in the theta band (4-8Hz) and the low-beta band (12-16Hz).

Comparing the impact of coherence level during solely fast or solely slow RTs provides no significant results across all frequency bands. As the time period measured here is from 777ms pre-stimulus up to the stimuli being shown, and the order of coherence level is randomised, this is to be expected. The previous stimuli may have an impact on arousal levels, or other measures of attention but future stimuli has no impact, as a result these analyses serve as a quasi-control set.

Frequency bands (Hz)	**High coh** Fast vs Slow RT		**Low coh** Fast vs Slow RT		**Fast RT** High coh vs Low		**Slow RT** High coh vs Slow	
	Δ	p-value	Δ	p-value	Δ	p-value	Δ	p-value
4–8	-45.3	$**p < 0.01$	-33.5	$*p < 0.05$	9.0	$p > 0.1$	19.4	$p > 0.1$
8–12	-72.7	$**p < 0.01$	-49.4	$**p < 0.01$	8.5	$p > 0.1$	20.8	$p > 0.1$
12–16	-27.3	$**p < 0.01$	-21.6	$p > 0.1$	0.5	$p > 0.1$	6.1	$p > 0.1$
16–20	-11.7	$p > 0.1$	0.6	$p > 0.1$	-7.0	$p > 0.1$	5.2	$p > 0.1$
20–24	-16.2	$p > 0.1$	-2.9	$p > 0.1$	4.8	$p > 0.1$	18.1	$p > 0.1$
24–28	-6.8	$p > 0.1$	-8.6	$p > 0.1$	3.6	$p > 0.1$	1.7	$p > 0.1$
28–32	-7.4	$*p < 0.05$	-1.4	$p > 0.1$	-3.6	$p > 0.1$	2.4	$p > 0.1$
32–36	-7.1	$p = 0.095$	-8.5	$p > 0.1$	1.4	$p > 0.1$	0.0	$p > 0.1$
36–40	-1.3	$p > 0.1$	-2.6	$p > 0.1$	1.9	$p > 0.1$	0.6	$p > 0.1$

Table 5.1.: Significance (Bonferroni-corrected) and direction (Δ=median difference) across 9 frequency bands using Wilcoxon rank-sum tests. (RT=reaction time, coh=coherence)

5.3.3 Time Domain EEG

A large peak is present post stimuli, with this peak appearing later in the slow RT response, compared to the fast RT response as shown in Figure 5.6. These large peaks may be motor movement processes, such as activity in the motor cortex and/or electromyographic interference.

The P300 peak is typically between 280-400ms after a stimulus is presented [225], whereas the peaks in this case are between 541 and 1082ms post-stimuli. Delayed post-stimuli peaks are similar to the median RT data for the respective conditions. The fast RTs are 541ms for HC stimuli and 648ms for LC stimuli, compared to 614ms and 652ms for their respective time domain EEG peaks. The slow RTs are further from their respective EEG peaks, with median RTs of 846ms for HC stimuli and 1082ms for LC stimuli compared to 696ms and 725ms for their respective EEG peaks.

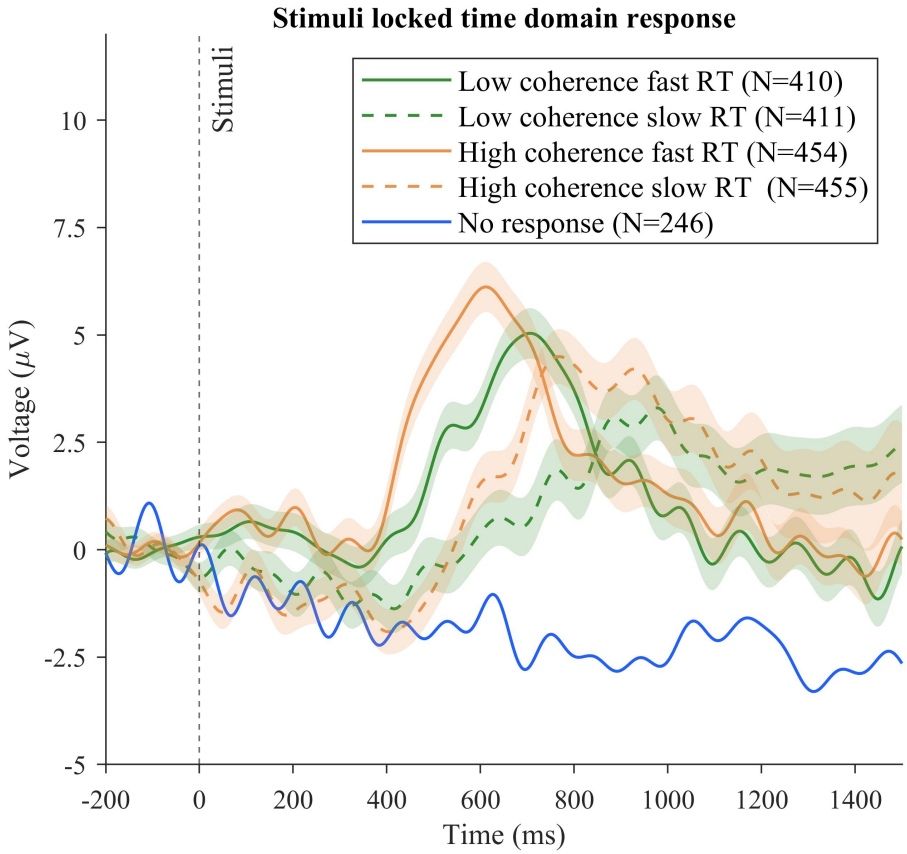

Figure 5.6.: Stimuli locked grand average. (RT=reaction time, N=number of trials)

5.4. Discussion

The work presented in this chapter tested the hypothesis that time and frequency domain EEG markers are significantly correlated with VA performance. Frequency domain markers were indeed significantly correlated with fast and slow RTs in response to HC and LC stimuli. The frequency domain markers found in this work have previously been reported in the literature, such as higher alpha (8-12Hz) components correlating with slower responses. This is consistent with work on distractor suppression [228], the missing of targets in a continuous temporal expectancy task [225] and deliberate off-task thoughts [251]. In addition, a global increase in alpha power may indicate a lower state of arousal [227]. The significant difference in the high-beta/low-gamma frequency band (28-32Hz) seen in the HC data is consistent with analysis by Martel et al. that found 25-35Hz was a highly discriminate feature between on-task and off-task thought [251]. The lack of a significant effect in the LC data may indicate that off-task thought results in missing the target rather than slower RTs with LC stimuli.

The significant results in the theta band (4-8Hz) which was found for both LC and HC stimuli and the low-beta band (12-16Hz) is less well understood and warrants further investigation. While the mechanism behind this theta activity is unclear, the activity in the low-beta band may in fact be explained by high-alpha activity. In the works previously referenced that found significant effects in the alpha band they defined this band as 8-14Hz [251], 8-13Hz [227], 8-15Hz [228] and 8-14Hz [225] respectively. As a result, the significant result in what is defined as the 'low-beta' band in this work may in fact be due to 'high-alpha' band activity.

The frequency domain analysis analysed frequency bands from 4-40Hz in steps of 4Hz. This frequency band iteration scheme was chosen due to its use in previous work analysing EEG data [266], and because many of the resultant bands fit within commonly referenced frequency bands. Although these can vary in the literature as previously discussed. The choice of these frequency bands was not optimised, a finer division of frequency bands may help further elucidate frequency responses associated with RTs under different task conditions.

The behavioural results were largely as expected, with participants responding faster to HC stimuli (median RT 683ms) compared to LC stimuli (median RT 793ms). Participants also missed more LC stimuli 9.46%) compared to HC stimuli (6.49%). This indicates that participants comprehended the task well.

Contrary to the hypothesis, time domain EEG results did not correlate with VA performance. This may be due to the large peaks that were presented with similar characteristics to the

reaction time data. As a result, these peaks may be explained by motor responses rather than the P300 ERP that was expected. Notably, RTs in the fast groups were closer to their respective EEG peaks in time than the slower response groups. This may be due to the long-tailed nature of RTs, where the slower responses are more spread out as is demonstrated in Figure 5.3, the time domain EEG peaks are also more spread out in the slow conditions in Figure 5.6.

Future work could focus on separating the motor responses seen the time domain data to the P300 ERP. This may be achieved through a different approach to signal processing, such as through the use of independent components analysis.

5.5. Conclusions

Electrophysiological correlates of vigilant attention in a continuous random-dot motion task were found to be significantly correlated with performance in a VA task. Frequency bands associated with low arousal [227], active attentional suppression [228] and off-task thought [226] were found to be significantly correlated with fast and slow RTs, regardless of the coherence level. The frequency domain features recognised in this work could be used in future work to actively provide intervention in the event of a deficit in vigilant attention. However, time domain EEG features did not correlate with VA performance, contrary to the hypothesis for this chapter. This may be explained by EEG data associated with the motor response of individuals.

6

Vigilant Attention Enhancement with Non-Invasive Brain Stimulation, an Exploratory Study

6.1. Introduction

Vigilant attention (VA), also known as sustained attention, is the ability to self-sustain the conscious processing of non-arousing stimuli, which would otherwise lead to habituation and distraction to other stimuli [28]. A deficit in VA has wide-ranging consequences as VA is also related to abilities in other areas of cognition, such as executive and fluid abilities [29]. Additionally, a deficit in VA has real-world implications. For instance, it is associated with an increased risk of falls [31]. However, VA is a complex, multifaceted cognitive process characterised by its distributed nature [217].

Transcranial direct current stimulation (tDCS) is a non-invasive technique that applies a low-intensity electrical current (typically 1–4 mA) to the scalp through electrodes. Several research groups have attempted to enhance VA using transcranial electrical stimulation [33, 191, 192]. Anodal tDCS is typically associated with increased neuronal excitability, although other factors such as neuron orientation should be considered [20]. tDCS also works through modulating neurotransmitter concentrations [235].

tDCS has been applied to VA through the stimulation of the right dorsolateral prefrontal cortex (rDLPFC) which controls VA by modulating attentional resources. Stimulating the rDLPFC with anodal tDCS has been shown to improve VA performance, potentially by modulating top–down attentional networks mitigating the executive vigilance decrement [33, 241]. However, the optimal parameters for tDCS for VA and the factors influencing individual responses remain unclear.

This builds upon the existing literature by comparing different stimulation intensities and by exploring the factors contributing to response variability. A part of the complexity associated with VA is the variability in task performance and the predictors of this variability which this work aims to explore. Arousal, a key component of attentional control [202] can be used as a predictor of VA performance. The resting-state alpha component of electroencephalography (EEG) signals has been identified as a marker of arousal in individuals with attention-deficit hyperactivity disorder (ADHD) [220]. The theta:beta ratio has also been identified as a potential marker of cognitive processing capacity [223] and higher ratios have been associated with decreased attentional control [224]. In addition to electrophysiological markers of attention, self-reported markers such as the widely used screening questionnaire for ADHD, the ADHD Self-Report Scale (ADHD ASRS) [234], may also be used to measure attentional performance. In this work, these measures will be used to look for correlates with VA performance.

Factors associated with the efficacy of tDCS for VA are also of interest. This could facilitate future work in which for responders and non-responders could be identified. One contributory factor to efficacy variability of this may be the magnitude of the electric field (E-field) induced in the brain of participants, which can vary by up to 100% between individuals with identical current applied to the scalp [14]. However, the relationship between the E-field magnitude and outcomes in unclear [99]. For example, recent work by Laakso et al. found that personalised dosing through E-field modelling did not enhance TMS induced MEPs [267]. However, in a closed-loop VA tDCS study, the optimum tDCS magnitude varied across participants [27], although it is unclear how much of this variability can be explained by peak E-field magnitudes. Using the algorithm developed in Chapter 3, this work aims to test if the estimated peak E-field magnitude correlates with stimulation efficacy.

Age may also be a factor in predicting the efficacy of tDCS, with a variety of factors potentially influencing stimulation effects, including macroscopic brain atrophy and a loss of synaptic spines [268]. In addition to potentially using EEG markers to predict task performance, they may also be used to predict tDCS responses. For instance, resting-state theta:beta ratios have been demonstrated to moderate the effects of 1mA tRNS in VA [191]. Arousal levels explain some of the variability in tDCS efficacy when applied to the left DLPFC [247]. One measure of arousal is EEG alpha power as previously described. In previous work targeting the rDLPFC tDCS did not reduce alpha power [241].

This chapter addresses objective 2 from Chapter 1 by exploring the application of tDCS to the rDLPFC. A within-participant sham-controlled experiment was conducted, with participants undergoing sham, 1mA, or 2mA stimulation during a VA task.

In this work it is hypothesised that participants reaction times (RTs) and miss rates (MRs) will increase over the duration of the random-dot motion task. Additionally, it is hypothesised that 1mA stimulation will enhance task performance. However, the effects of 2mA stimulation are uncertain. The performance changes will be observable both between the sham and stimulation sessions and over the duration of the task. The predicted peak E-field magnitude for each participant is also hypothesised to correlate with changes in task performance.

Furthermore, it is further hypothesised that the magnitude of these performance changes will be inversely correlated with the participants age, ADHD ASRS inattentive scores and eyes-open frontal theta:beta ratios. Both eyes-closed and eyes-open resting-state alpha power are also expected to be negatively correlated with task performance, but any changes in outcomes due to tDCS are not expected to change resting-state alpha power.

6.2. Methodology

6.2.1 Participants

Twenty-nine healthy adults were recruited to participate in this study. Two participants were excluded due to a technical fault resulting in the loss of data in their final session. In addition, eight participants were removed due to poor task performance explained in Section 6.2.5. As a result, data from nineteen healthy adults were used in subsequent analyses (nine female, nine male, one undisclosed, with a mean±SD age (of 27.4 ± 10.6 years) and a mean ±SD head circumference of (55.3 ± 1.63cm). All participants had normal or corrected-to-normal vision and had no history of epilepsy, stroke, heart attack, psychiatric illness, migraines, seizures, head injury or any medical diagnosis of psychological or neurological disorders. Additionally, all participants were not pregnant and did not report damaged skin on the scalp. All participants provided written, informed consent before taking part in the experiment. All procedures were performed in line with the Declaration of Helsinki and were approved by the University of Sheffield Ethics Committee in the Automatic Control and Systems Engineering Department. All participants received a £40 Amazon voucher at the end of the experiment.

6.2.2 Experimental Setup

EEG/tDCS Setup

Resting-state EEG data were acquired preceding each session using the Starstim 8 (Neuroelectrics) headset. Electrodes were secured in place with a neoprene cap, 6 EEG channels using Ag/AgCl sintered electrodes with a 1.75 cm^2 circular contact area and electrolytic EEG gel were used. Five channels were used to record EEG data, positioned in accordance with the international 10-20 EEG system at the following locations (Fz, Pz, P3, P4 and Oz) as illustrated in Figure 6.1. The reference electrodes were placed on the mastoid bone with pre-gelled single-use electrodes. Data was recorded with a 500Hz sample rate on a Windows 11 desktop PC using the Neuroelectrics Instrument Controller (NIC) software. The StarStim 8 headset was connected to the desktop PC using a USB cable. During the collection of resting-state EEG data, participants were asked to avoid motor movement. During the eyes-open resting-state EEG data collection, participants were asked to stare at a white fixation cross on the screen in front of them, and during eyes-closed resting-state EEG data collection, participants were asked to keep their eyes closed until they were told to open them. Both eyes-open and

eyes-closed resting-state data were recorded for a period of 3.5 minutes.

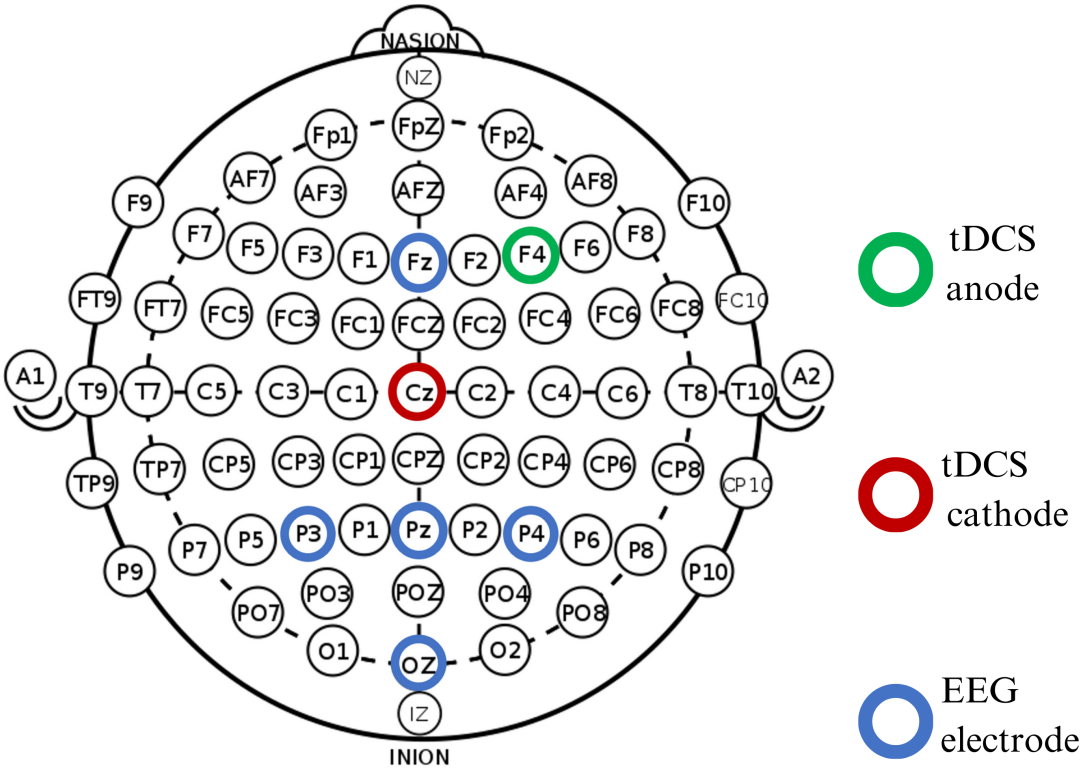

Figure 6.1.: An illustration of the EEG and tDCS electrode positions according to the international 10-20 system. (EEG=electroencephalography, tDCS=transcranial direct current stimulation)

In addition, tDCS electrodes were placed on the scalp with the cathode at Cz and the anode at F4. Neuroelectrics Sponstim sponge electrodes with a 28mm radius were soaked in saline solution before placement on the scalp. Before stimulation, impedance levels were confirmed as being below 10kΩ. At the beginning and end of each block, stimulation was ramped up and ramped down over a 20-second period to reduce participant discomfort.

As illustrated in Figure 6.2, participants attended three sessions. In all three sessions, resting-state EEG was followed by a sham stimulation block. Each block consisted of 6 minutes and 20 seconds of the continuous random-dot motion task. 30-second breaks were provided between blocks. Sham stimulation was generated by a 20-second ramp up to 1mA, followed by an immediate ramp down to 0mA over 30 seconds. The subsequent four blocks contained either sham, 1mA or 2mA of stimulation. Participants attended all three sessions in a randomised order, with at least a 7-day washout period between each session.

Figure 6.2.: A diagram of the experimental protocol timeline. All sessions started with collecting resting-state EEG data, followed by one block of sham stimulation during the continuous random-dot motion task. This was followed by four stimulation blocks lasting 6 minutes and 20 seconds each. Between each block, participants had 30 seconds of rest. Participants underwent sham, 1mA or 2mA of stimulation in sessions A, B and C, respectively. Session orders were randomised for each participant. (EEG=electroencephalography, tDCS=transcranial direct current stimulation)

Continuous Random-Dot Motion Task

Participants took part in the continuous random-dot motion task, as described in Chapter 5 Section 5.2.3, and illustrated in Figure 5.1. However, the parameters used were modified compared to those used in Chapter 5. Dots moved in random directions, and then at random time intervals of 3.2, 4.2 or 5.7 seconds, a percentage of these dots moved coherently left or right. Participants were asked to respond to coherent motion with a right or left mouse click that corresponded to the motion of the coherent dots. Coherent dot motion occurred for 1.9 seconds. In this experiment, there were two coherence modes: low coherence (LC) and high coherence (HC). LC corresponds to 25% of dots moving coherently, and HC corresponds to 50% of dots moving coherently. An LCD monitor with a resolution of 2,000 x 1,025 and a refresh rate of 60Hz was used. The region of the display containing the dots fits within 5 degrees of the participants field of view. This was calibrated at the beginning of each session by measuring the distance between the participants eyes and the display.

Finally, before the first session, descriptions of the experiment were provided in both the information sheet and verbally. Participants also took part in a practice session involving the continuous random-dot motion task with coherence levels of 100%, 80%, 60%, 50% and 25%. As in the real experiment, participants were asked to click the mouse button in the direction of the dot motion. Participants were only able to proceed with the experiment when they could consistently click the appropriate mouse button.

Questionnaire

All participants completed the Adult Attention Deficit Hyperactivity Disorder Self-Report Scale (ADHD ASRS) v1.1, a questionnaire comprising eighteen questions such as "How often do you make careless mistakes when you have to work on a boring or difficult project ?". Each question was asked in the context of the last six months. Answer choices and their corresponding numerical value are as follows: never (0), rarely (1), sometimes (2), often (3), and very often (4). The first nine questions correspond to inattention symptoms [269]. The sum total of the participants scores in these nine questions was used in subsequent analyses.

6.2.3 EEG Analysis

Eyes-open and eyes-closed resting-state EEG was collected at the beginning of each session for 3.5 minutes each. A 40Hz lowpass zero-phase Butterworth filter was applied to remove high-frequency noise, followed by a 1.5Hz highpass zero-phase Butterworth filter to remove low-frequency drift. The initial 10 seconds of each resting-state EEG recording were discarded to mitigate potential artefacts arising from participant movement. Filtered data were split into two-second epochs. A threshold-based artefact rejection procedure was used to remove epochs with a peak-to-peak amplitude of greater than $\pm 70 \mu V$ at the frontal channel Fz. Four participants were removed at this stage, two due to over 70% of their data being rejected in at least one block and two due to missing or corrupted data. This resulted in 23 participants being used in subsequent EEG analyses.

To extract the relevant frequency domain features, the power spectral density was calculated for each epoch using Welch's method, with a 50% Hamming window. Subsequently, the absolute power for the alpha (8-13Hz), beta (14-30Hz) and theta (4-7.5Hz) frequency bands, as well as the full spectrum (1.5-30Hz), were extracted. The theta:beta ratio was calculated as the theta power divided by the beta power in the Fz channel, as this provides a similar theta:beta ratio to that obtained from central cites [191]. This data was extracted for the

eyes-open condition.

The relative alpha power was calculated as the alpha power divided by the full spectrum power. Alpha power was extracted from parietal and occipital electrodes (Pz, P3, P4 and Oz) for the eyes-open and eyes-closed condition. The eyes-closed resting-state alpha activity was computed to serve as a baseline arousal level, while the eyes-open resting-state alpha activity was used as an activated arousal level [220]. Finally, the average values for both the alpha power and theta:beta ratio were obtained across all non-rejected epochs.

6.2.4 Peak E-field Strength Estimation

As described in Chapter 3, the strength of the E-field generated with identical montage parameters is heterogeneous across individuals. As such, accounting for the real dose, as opposed to the current applied at the scalp, is pertinent. As a result, the montage-specific robust multiple-linear regression model for the electrode positions F4, Cz described in Chapter 3 was used to estimate the peak E-field strength of each participant (calculated at the average of the 95th percentile). This regression model was informed by each participants age, gender and head circumference. Head circumference was measured manually using measuring tape. Body mass index and cephalic index, both parameters in the regression model, were not measured. To account for this, participants' body mass index was assumed to be the median of the CamCAN dataset population (24.1), and the cephalic index (83.1) was assumed to be the mean of the CamCAN population. One participant did not disclose their gender. As a result, the average value between males and females was used in the regression model.

6.2.5 Measures of Task Performance

RTs and MRs were recorded. As dots moved coherently for 1.9 seconds, a reaction was recorded when a click was registered within 1.9 seconds of the initiation of dot movement. A 'miss' was recorded if no click was registered during this period. The MR was calculated as the percentage of the total number of stimuli presented that did not receive a response for the participant. Participants were excluded from this analysis if their MR during HC stimuli was more than 10% in any of their sessions (n=19). This was to ensure only participants who understood the task and generated sufficient RT samples were included in subsequent analyses.

To account for the positively skewed nature of RTs, an exponential Gaussian (ex-Gaussian)

distribution was fit to the RT data. The ex-Gaussian distribution is the convolution of a Gaussian and exponential distribution. This approach allows for the decomposition of the RT distribution into the Gaussian mean (μ), Gaussian standard deviation (σ) and exponential long-tail component (τ). Yamashita et al. demonstrated that these parameters can provide insights into different aspects of cognitive performance during VA tasks [270].

6.2.6 Statistical Analyses

Effects of Stimulation on Task Performance

Throughout the following analyses, Maulchys tests for sphericity and Shapiro-Wilk tests for normality were performed using IBM SPSS 29.0. Friedman and Spearman's tests were performed using MATLAB r2023a. Bonferroni-corrections were applied to account for multiple comparisons.

To test the effects of stimulation on task performance, the following procedures were implemented. The MRs and RTs were recorded separately for HC and LC stimuli. In the first instance, the first sham block at the beginning of each session was discarded. The remaining blocks, which included either entirely sham, 1mA or 2mA of stimulation were subsequently compared. The data were separated into four groups: HC RT, HC MR, LC RT and LC MR. Non-parametric repeated-measures Friedman tests were performed on each of these four groups due to the non-normal distribution of the data. These tests were performed across the three interventions to assess whether the task performance was significantly different across the three sessions.

Thereafter, an exponential Gaussian distribution was fit to each participants RT data in each session, again in the latter four blocks. As previously described, this provides the Gaussian mean (μ), Gaussian standard deviation (σ) and exponential long-tail factor (τ). These three measures were split and separated into groups for each intervention. Mauchly's test of sphericity was conducted, due to violations of the sphericity assumption ($p < .05$) non-parametric Friedman tests were employed for the analysis. These tests were performed across the three intervention groups to test whether the task performance recorded during each intervention were significantly different.

The analyses thus far has compared RT and MR data collated across the duration of the latter four blocks. However, cortical excitability induced by anodal tDCS may be dependent on the duration of the stimulation [271]. To that end, MRs and RTs were collated block-

wise, enabling the testing of the effects of the stimulation over time. Since each session began with a sham block, task performance in subsequent blocks was calculated relative to this initial sham block to account for inter-session variability. The change in MR was calculated as the difference between each block's MR and the initial sham block's MR. For RT, the difference was calculated between each block's RT and the median RT of the initial sham block. In the case of block-wise RT performance, the median RT was taken as opposed to fitting an exponential Gaussian. This was due to the low number of RT samples recorded in a single block resulting a poorly fitting ex-Gaussian. Non-parametric, repeated-measures Friedman tests were performed as data violates both Mauchly's test for sphericity ($p < .05$) and Shapiro-Wilk test for normality ($p < .05$). These tests compared task performance in each block across the three interventions.

Participant-Specific Predictors of Task Performance

As previously discussed, resting-state EEG measures for eyes-open alpha, eyes-closed alpha and eyes-open theta:beta ratios were recorded at the beginning of each session. In addition, participants filled out the ADHD ASRS questionnaire, and their scores in the first nine questions pertaining to inattentiveness were aggregated into a score. The age of participants was also recorded. Henceforth, these measures are collectively referred to as participant-specific predictors.

Initially, these measures were compared to the MR for LC stimuli and ex-Gaussian parameters (Gaussian mean (μ), Gaussian standard deviation (σ) and long tail factor (τ)) for HC stimuli over the duration of the sham session. Bonferroni-corrected Spearman's rho correlations were calculated for each combination of participant-specific predictors and the task performance measures.

To further elucidate the change in performance over the duration of the task a comparison between the median RT to HC stimuli in the first block compared to the fifth and final block was performed. Bonferroni-corrected Spearman's rho tests were again applied to all combinations of these measures and task performance measures.

Participant-Specific Predictors of Stimulation Efficacy

To evaluate predictors of stimulation efficacy, participant-specific factors (age, ADHD ASRS inattention scores, and resting-state EEG measures) and the predicted peak E-field magnitudes were compared to changes in task performance during stimulation.

Participant-specific predictors were tested against the change in performance between the sham session and stimulation sessions across the final four blocks. This included the natural logarithm of the change in LC MRs, and the change in the three RT parameters to HC stimuli obtained from the ex-Gaussian models (Gaussian mean (μ), Gaussian standard deviation (σ) and long tail factor (τ)). Spearman's rho tests were performed on each combination with Bonferroni-correction applied to account for multiple comparisons.

Participant-specific predictors were also compared to the change in task performance during stimulation. To that end, the change in the median RT to HC stimuli between the first (sham) block and the final (active stimulation) block during 1mA and 2mA of stimulation was performed. As before, Bonferroni-corrected Spearman's rho tests were performed.

Finally, for the analysis of the impact of the predicted E-field independent of age, gender and head circumference partial correlations were conducted. Specifically, Bonferroni-corrected Spearman's rank order partial correlations between the predicted peak E-field magnitude and the change in task performance (HC RT parameters and LC MR) between sham and active stimulation sessions controlling for age, gender and head circumference.

6.2.7 Comparative E-field Analysis of tDCS Montages

The E-field generated in this work was compared to the E-field produced by the montage used by Brosnan et al. [33]. While both studies utilised the same electrode positions (anode: F4, cathode: Cz), the Brosnan et al. montage employed rectangular electrodes measuring 5×7 cm. In contrast, this work used circular electrodes with a 28 mm radius.

E-field simulations were performed on the New York head reference model [272] using ROAST version 3.0 [15]. Default conductivity values for the following tissues: white matter 0.126 S/m, grey matter 0.276 S/m, bone 0.01 S/m, skin 0.465 S/m, air 2.5e-14 S/m, gel 0.3 S/m and electrodes 5.9e7 S/m. The conductivity value of 0.85 S/m was used for CSF to account for the meninges [18]. In the resultant E-field, voxels corresponding to the white and grey matter according to the New York head reference model segmentation map were extracted. The average of the 95th percentile of the E-field within the brain was used to determine the peak E-field magnitude. The centroid of the voxels within this 95th percentile region was used to determine the location of the centre of the peak E-field region.

6.3. Results

6.3.1 Effects of Stimulation on Task Performance

The MRs and RTs were extracted for HC and LC stimuli for each intervention (sham, 1mA and 2mA) and each participant, excluding the initial sham block. The median average RTs and mean average MRs were taken across all four blocks. These results were subsequently collated together, resulting in an average MR and RT value for each participant and each session. Bonferroni-corrected repeated-measures Friedman tests with were performed across the three interventions for HC MR ($X^2 = 1.10, p > .05$), HC RT ($X^2 = 1.73, p > .05$), LC MR ($X^2 = 2.16, p > .05$) and LC RT ($X^2 = 1.79, p > .05$). This data is shown in Figure 6.3, neither RTs or MRs were significantly correlated with the stimulation conditions.

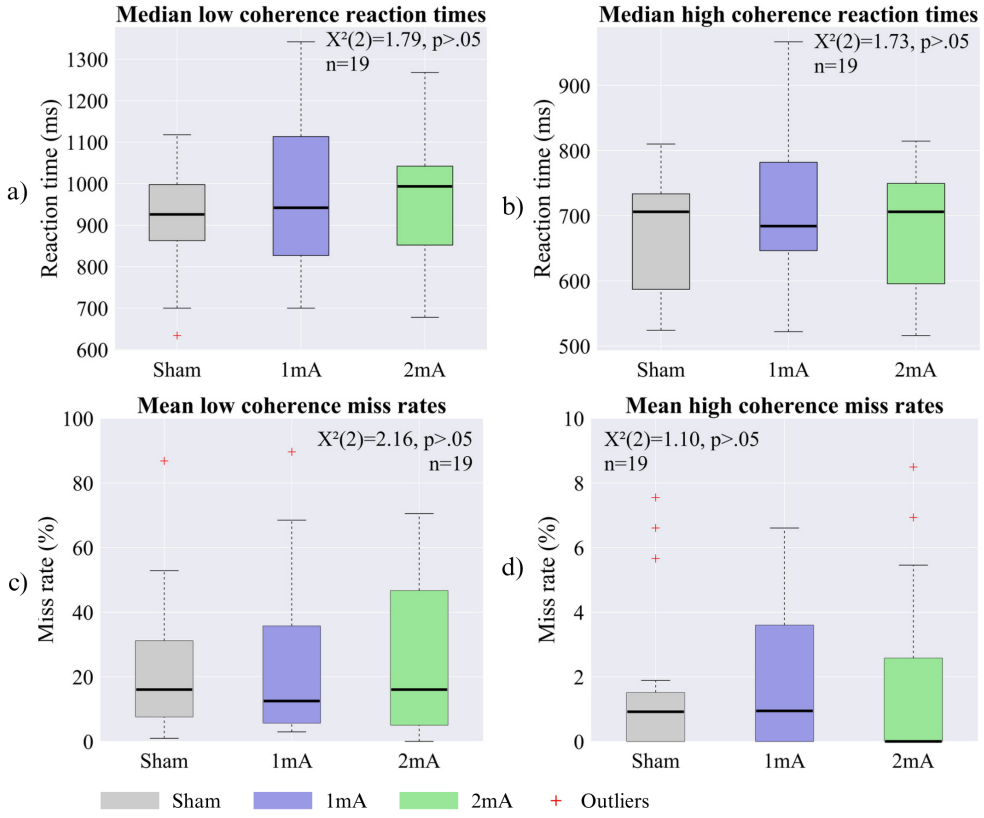

Figure 6.3.: Task performance during sham, 1mA and 2mA of stimulation. a) Median average RTs to LC stimuli. b) Median average RTs to HC stimuli. c) Mean average MRs for LC stimuli. d) Mean average MRs for HC stimuli. Bonerroni-corrected Friedmans tests revealed no significant difference in the distributions across the three interventions and all four outcome measures. In each box plot, whiskers represent extreme values, the top and bottom edges of the boxes represent the 75th and 25th percentiles, respectively, and the horizontal black line represents the median. Outliers are displayed as red crosses. (RT=reaction time, MR=miss rate, HC=high-coherence, LC=low-coherence)

As previously discussed, RTs can be characterised by fitting exponential Gaussians to the RT distribution rather than simply the median RT. Ex-Gaussians fit to all RT data across all participants and sessions are shown in Figure 6.4 a). For the purposes of this analysis, ex-Gaussians were fit to the final four blocks of each session across all interventions and participants. Box plots for the Gaussian mean (μ), Gaussian standard deviation (σ) and long tail factor (τ) are presented in Figure 6.4 b), c) and d) respectively. Bonferroni-corrected repeated-measures Friedman tests did not indicate any significant effects. LC RT ($X^2 = 1.79, p > .05$), HC RT ($X^2 = 1.73, p > .05$), LC MR ($X^2 = 2.16, p > .05$) and HC MR ($X^2 = 1.10, p > .05$).

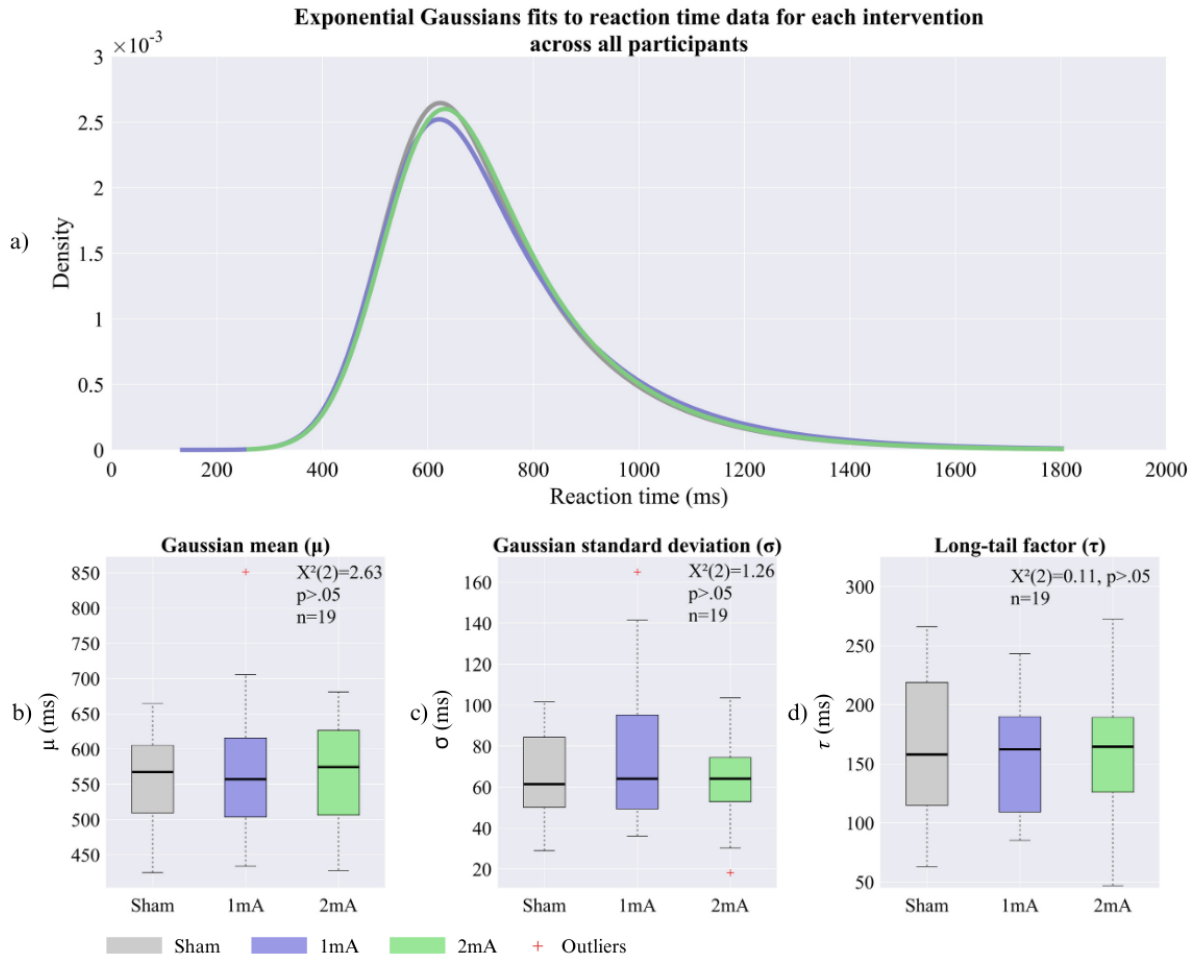

Figure 6.4.: Exponential Gaussian distributions and their parameters of reaction times for sham, 1mA and 2mA interventions across all participants. a) Exponential Gaussian fit across all participants reaction time data. b) Box plots for the distribution of the Gaussian mean (μ). c) Box plots for the distribution of Gaussian standard deviation (σ) d) Box plots for the distribution of the long-tail factor (τ). Repeated-measures Friedman test results are above each plot and indicate no significant differences. In each box plot, whiskers represent extreme values, the top and bottom edges of the boxes represent the 75th and 25th percentiles, respectively, and the horizontal black line represents the median. Outliers are displayed as red crosses.

Thus far, analyses has been conducted across the four latter blocks of each session, without considering the initial sham block or block-wise changes in task performance. In Figure 6.5 below, the change in the MR and RT, compared to the median of the initial sham block, is shown. Bonferroni-corrected repeated-measures Friedman tests did not indicate significant changes ($p > .05$) in RT or MR across the three interventions for any block of the task.

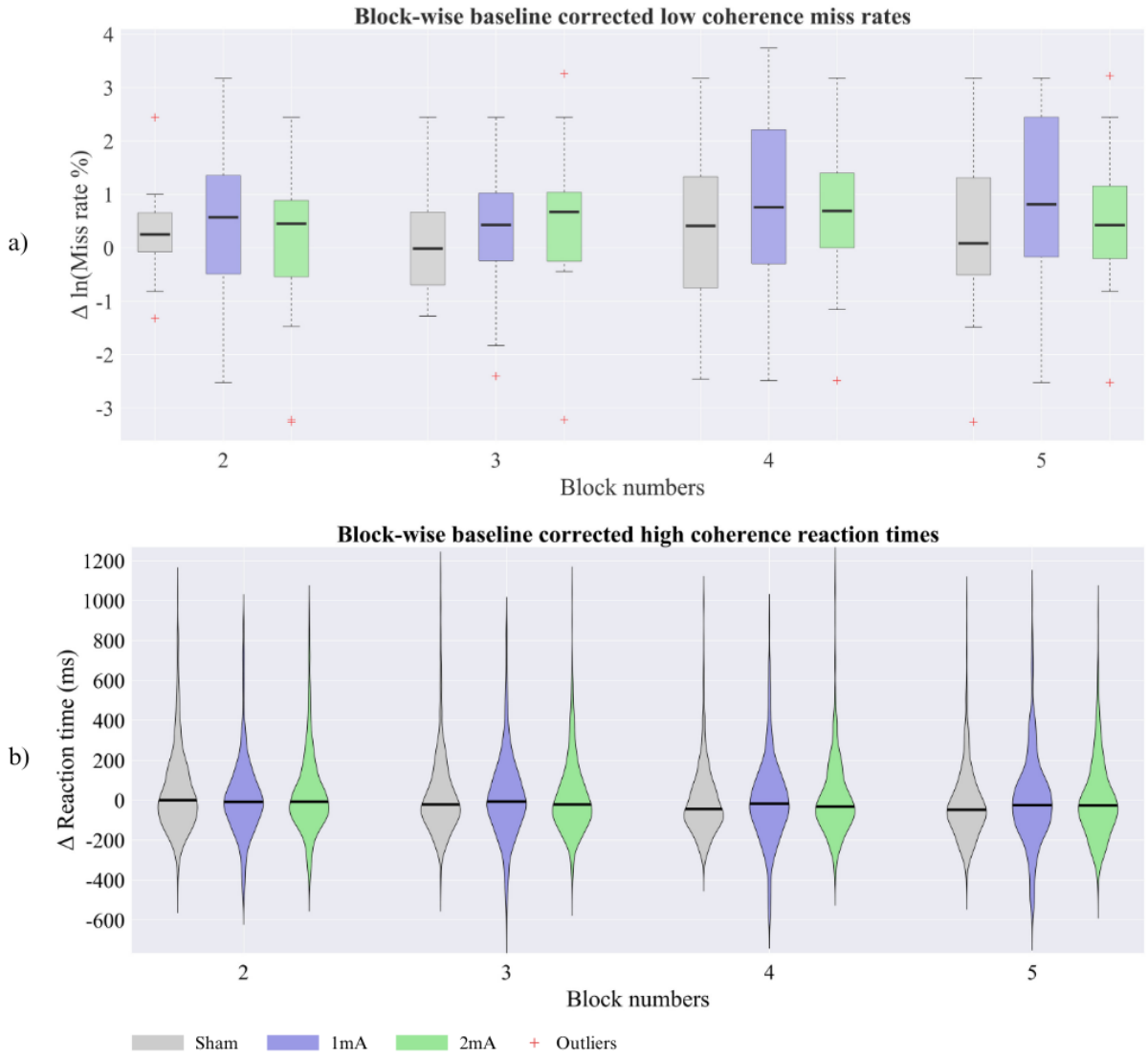

Figure 6.5.: Baseline corrected, block-wise task performance. a) The log of the change is the miss rate between the sham block at the beginning of each session and the block displayed on the x-axis. b) The change in reaction time between the sham block and reaction times in each block. In each box plot, whiskers represent extreme values, the top and bottom edges of the boxes represent the 75th and 25th percentiles, respectively, and the horizontal black line represents the median. Outliers are displayed as red crosses.

6.3.2 Associations Between Participant-Specific Predictors and Task Performance

Age and ADHD ASRS inattention scores were recorded for each participant, along with resting-state parietal alpha band and frontal theta:beta ratio EEG data. In order to test whether these measures and the average task performance in the sham sessions were correlated Spearman's rho correlations were performed with Bonferroni correction applied to account for multiple comparisons. No significant correlations ($p > .05$). were observed across both ex-Gaussian parameters fit to RT data for HC stimuli (Figure 6.6) and MRs for LC stimuli (Figure 6.7).

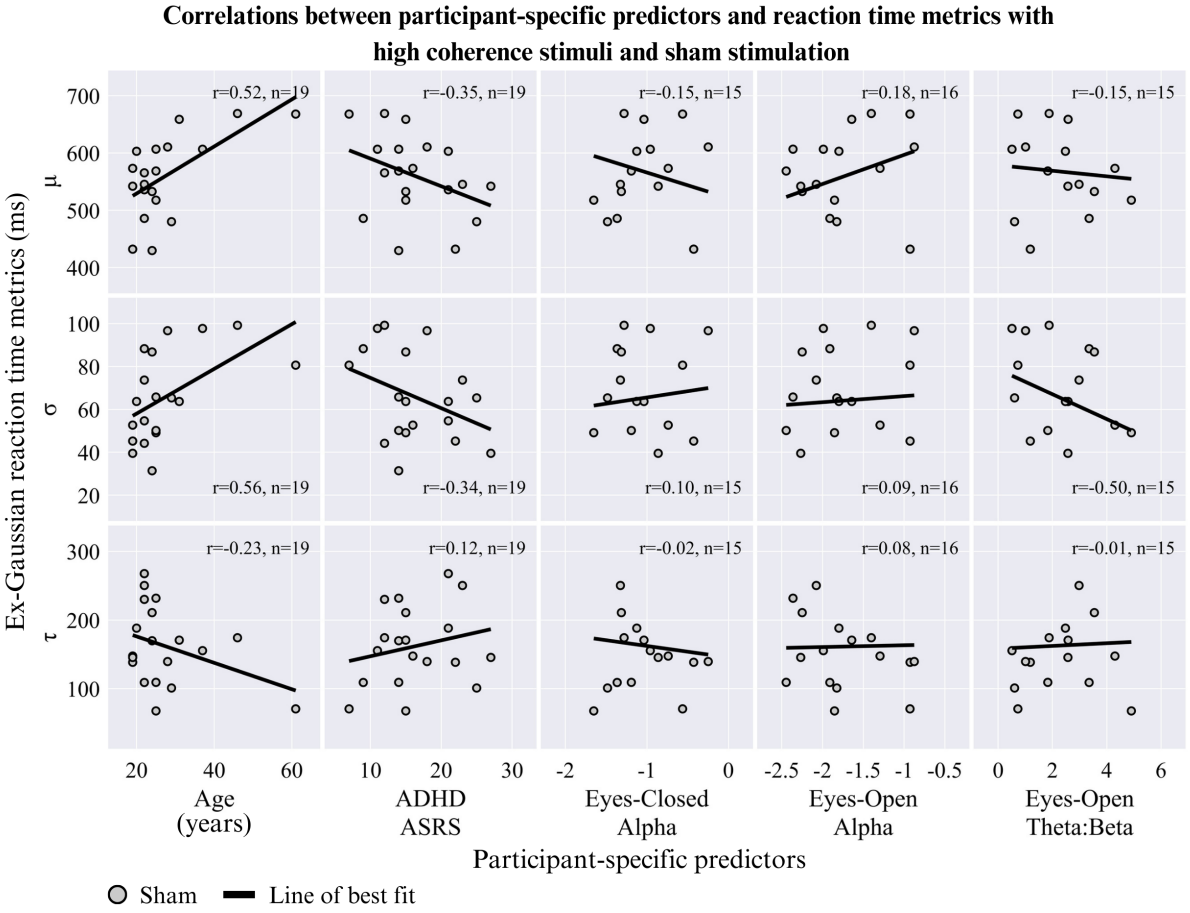

Figure 6.6.: Correlates of task performance during sham stimulation. Scatter plots, with the line of best fit between reaction time metrics and participant-specific predictors during the sham stimulation session. μ=Gaussian mean, σ=Gaussian standard deviation and τ=long tail factor. ADHD ASRS=ADHD adult-self-report scale inattention results. Eyes-closed alpha, eyes-open alpha and eyes-open theta:beta refers to resting-state EEG frequency measures.

In addition to the comparison between participant-specific predictors and ex-Gaussian RT metrics, these predictors were also compared to MRs. As before, none of the Bonferroni-corrected Spearman's rho correlations found significant effects ($p > .05$).

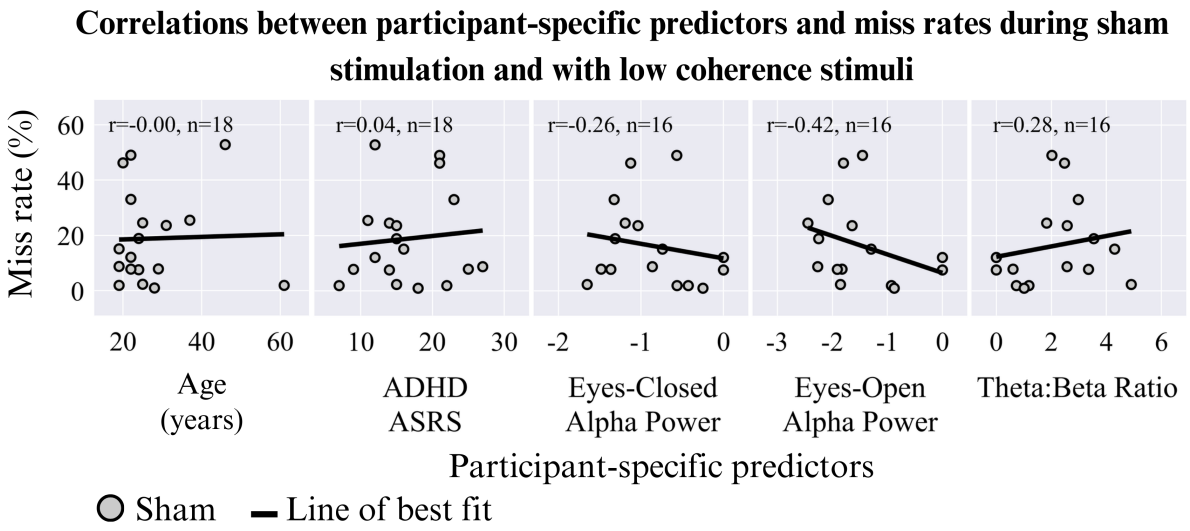

Figure 6.7.: The relationships between the miss rate (%) for low coherence stimuli in the sham session and participant-specific predictors. (Grey dots=sham, and the black line=line of best fit)

To determine whether changes in RTs during the sham session were related to participant-specific predictors, the difference in RTs between the first and final blocks was compared to these predictors for the sham session with HC stimuli. Spearman's rho analyses revealed no significant correlation between the predictors and the change in RTs over the session ($p > .05$).

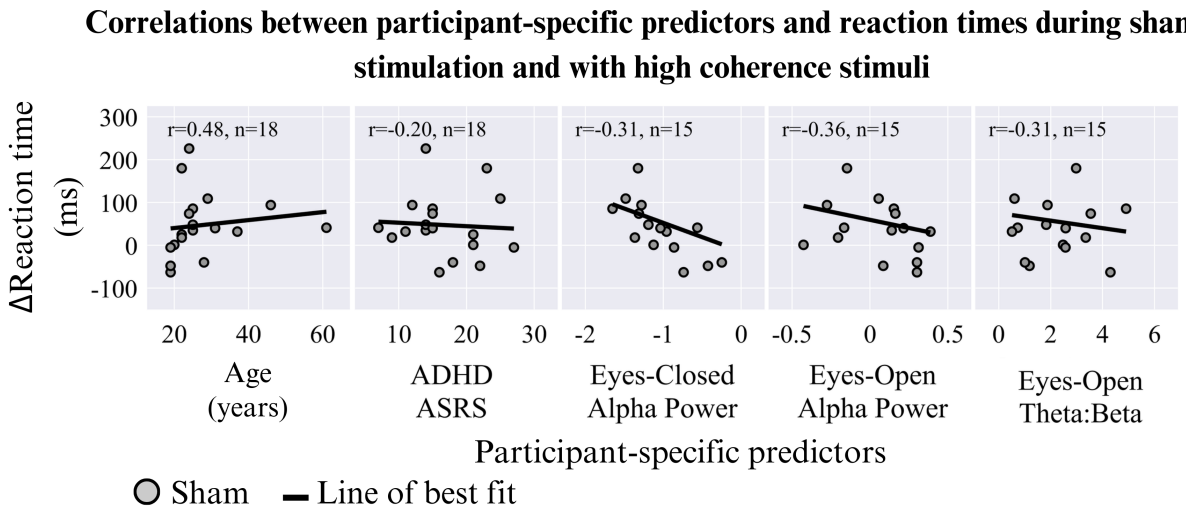

Figure 6.8.: The relationships between reaction time (ms) between the first block and the final block in the sham session for high coherence stimuli.(Grey dots=sham, black line=line of best fit).

6.3.3 Associations Between Participant-Specific Predictors and Stimulation Efficacy

Further analyses were conducted to examine whether the changes in task performance between the sham sessions and the stimulation sessions were significantly correlated with participant-specific predictors, including the estimated peak E-field magnitude. Bonferroni-corrected Spearman's rho correlational analyses comparing participant-specific predictors with changes in ex-Gaussian RT parameters to HC stimuli showed no significant effects ($p > .05$). As illustrated in Figure 6.10.

Bonferroni-corrected Spearman's rho correlational analyses also did not demonstrate a significant correlation between participant-specific predictors and the natural logarithm of the change in MRs to LC stimuli between the sham session and the stimulation sessions ($p > .05$). Thee results are illustrated in Figure 6.9.

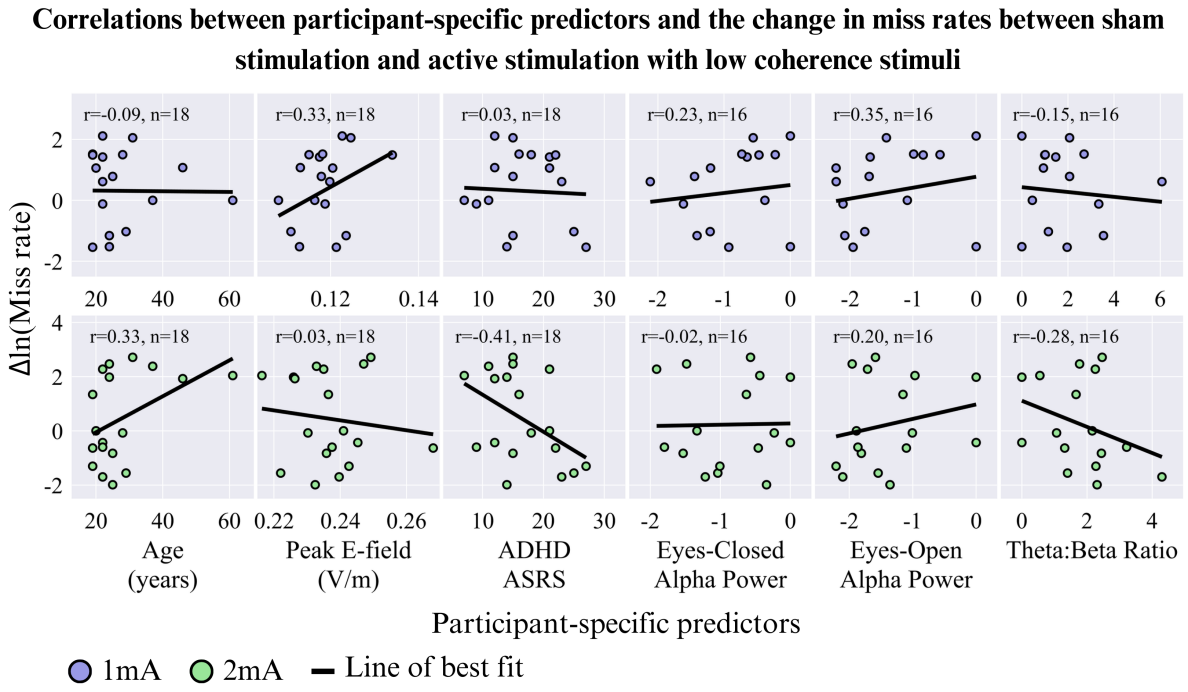

Figure 6.9.: The relationships between the natural log of the change in miss rates with low coherence stimuli between the sham session and the stimulation sessions and participant-specific predictors. Bonferroni-corrected Spearman's rho correlational analyses were performed, no significant results were observed. (Blue dots=1mA, green dots=2mA and the black line=line of best fit).

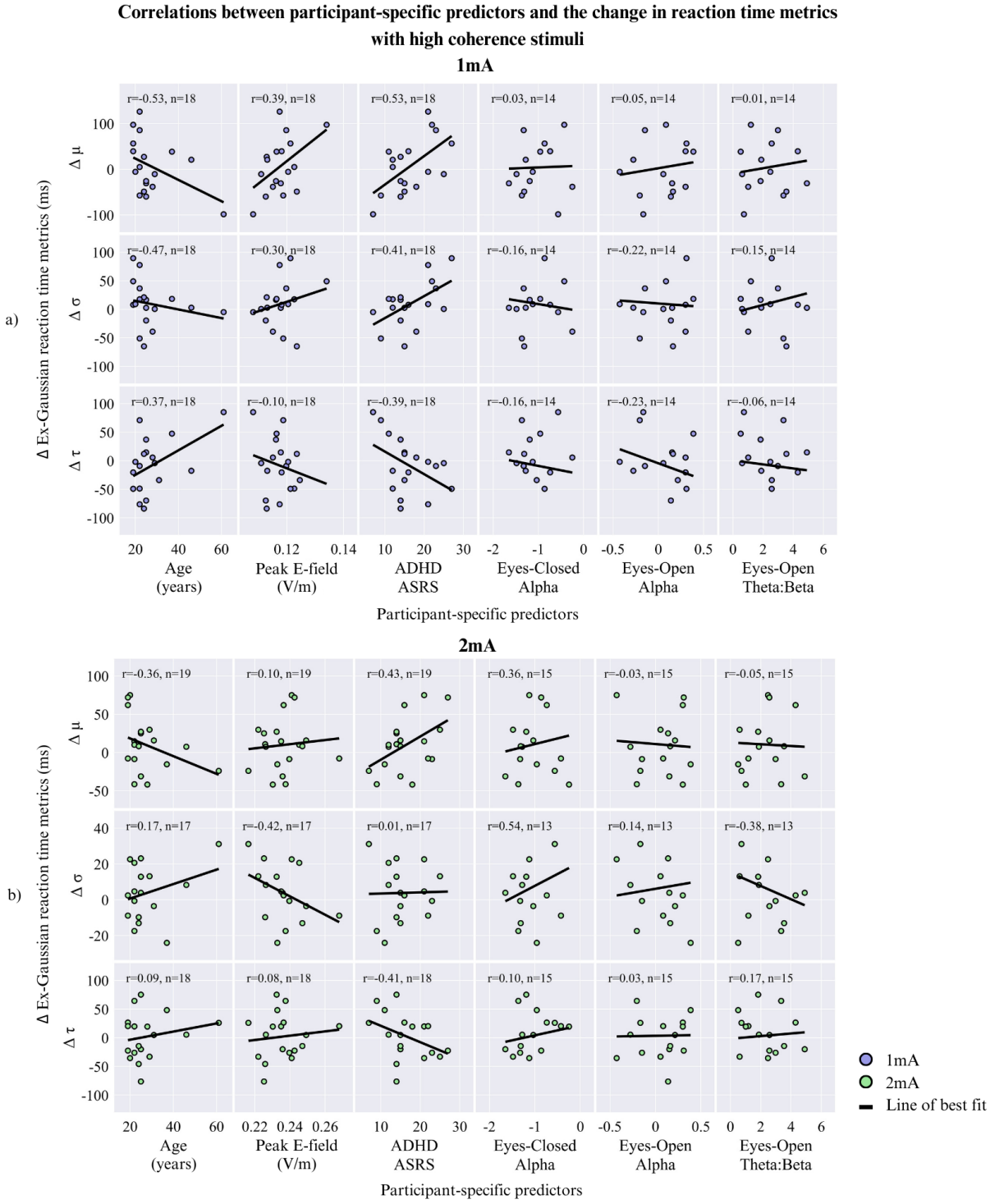

Figure 6.10.: a) Changes in task performance metrics during 1mA of stimulation compared to the sham stimulation block. b) Changes in task performance metrics during 2mA of stimulation compared to the sham stimulation block. $\Delta\mu$=change in Gaussian mean, $\Delta\sigma$=change in Gaussian standard deviation and $\Delta\tau$=change in the long tail factor. ADHD ASRS=ADHD adult-self-report scale inattention results. Eyes-closed alpha, eyes-open alpha and eyes-open theta:beta refers to resting-state EEG frequency measures. Lines of best fit are also present in all plots.

Furthermore, participant-specific predictors did not significantly correlate with changes in RTs to HC stimuli within the stimulation sessions. Within-session changes in RT were calculated as the difference between the median RT in block one compared to the final block five. Bonferroni-corrected Spearman's rho correlational analyses did not demonstrate any significant effects ($p > .05$).

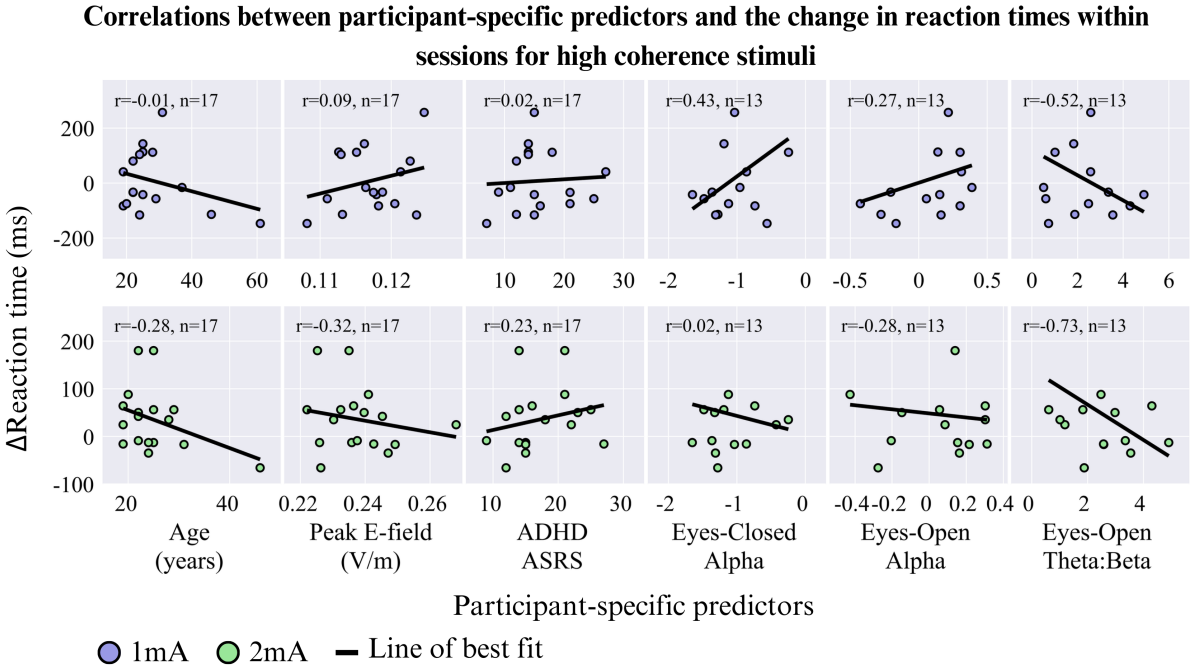

Figure 6.11.: The relationships between reaction time (ms) between the first block and the final block in the 1mA and 2mA sessions for high coherence stimuli. (Blue dots=1mA, green dots=2mA, black line=line of best fit)

Finally, peak E-field magnitudes were compared to changes in task performance during stimulation while controlling for age, gender and head circumference. No significant results with 1mA or 2mA of stimulation.

Stimulation magnitude	Δ Ex-Gaussian reaction time metrics						Δ Miss-rates	
	τ		μ		σ			
	r	p-value	r	p-value	r	p-value	r	p-value
1mA	-0.224	$p > .05$	0.175	$p > .05$	-0.343	$p > .05$	-0.415	$p > .05$
2mA	-0.371	$p > .05$	0.138	$p > .05$	-0.010	$p > .05$	-0.222	$p > .05$

Table 6.1.: Spearman's partial correlations between the predicted electric field and changes task performance during stimulation, controlling for age, gender and head circumference. Task performance outcomes include changes (Δ in ex-Gaussian reaction time metrics (τ, μ and σ for miss rates (Δ MR) across two stimulation magnitudes (1mA and 2mA). Bonferroni corrections were applied to account for multiple comparisons.

6.3.4 Electric Field Simulations

Visualisations of the magnitudes of the E-field generated in both electrode cases are shown in Figure 6.12. The peak regions in both E-fields occupy similar regions. The centroid of the 95th percentile of the E-field generated by the rectangular electrodes was located 1.11 mm left medial, 1.63 mm posterior, and 1.15 mm dorsal relative to the centroid generated by circular electrodes. The magnitude of the 95th percentile of the E-field generated by circular electrodes (0.155 V/m) is 12% higher than the 95th percentile E-field strength generated with rectangular electrodes (0.138 V/m).

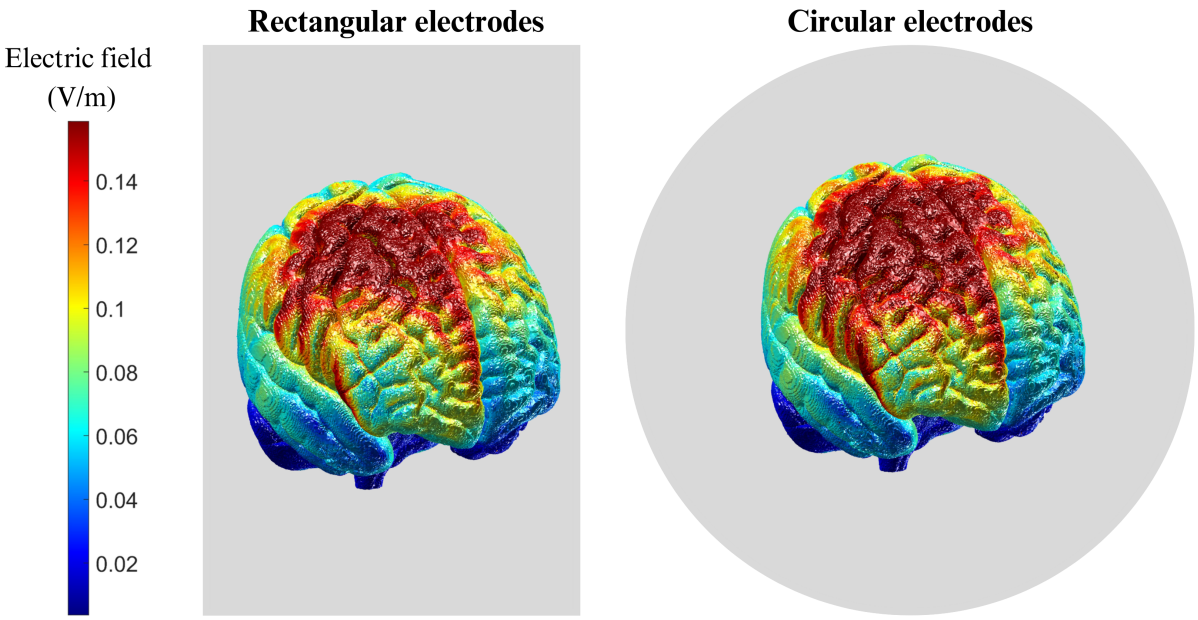

Figure 6.12.: Visualisation of the simulated electric field magnitudes across the brain surface for rectangular electrodes, displayed on the left, and circular electrodes, displayed on the right.

6.4. Discussion

In this chapter, a within-participant sham-controlled EEG/tDCS experiment was conducted on twenty-nine healthy participants. tDCS was applied to the rDLPFC across sham, 1mA, and 2mA sessions. It was hypothesised that RTs and MRs would increase over the duration of each session as participants engaged in a random-dot motion task. However, no significant decrements in performance were observed.

There are a range of plausible explanations for this, including experimental design. In this work, the random-dot motion task took place over five blocks lasting 6 minutes and 20 seconds. However, in previous works, such as that by O'Connell et al. [225], participants took part in seven to ten blocks, each of a similar length. This work's shorter total session duration likely contributed to fewer instances of a decline in VA.

In addition, nine of the twenty-seven participants with complete behavioural data were rejected due to having high MRs to high coherence stimuli (33%). Such a high rejection rate may indicate a lack of task comprehension. In previous work by Brosnan et al., participants were screened before being accepted to take part in the task, ensuring they scored 23 or higher on the Montreal Cognitive Assessment and were all right-handed [33]. Neither such screening steps were undertaken for this experiment. In addition to screening steps, future work could include a more rigorous training procedure to reduce the incidence of poor task comprehension. This could include a longer testing period where participants only progress to the main task if they achieve specific performance metrics. It may also include training at the beginning of every session to reinforce participants' understanding of the task.

Potential distractors during the task may have caused participants to lose focus at times when their attention would otherwise be expected to remain steady, such as at the beginning of a session. A lapse in attention to the task may have also acted as an unintended break, potentially reducing the likelihood of a vigilance decrement. These distractors may have included the neoprene head cap used to secure the electrodes, which was often tightened to ensure good electrode contact. However, the cap may have caused minor, yet distracting, discomfort for participants. Additionally, noise levels were not controlled during this experiment. Environmental noise from the surrounding area may have further contributed as a source of distraction.

Resting-state frontal theta:beta power was trending, but was not significantly inversely correlated with task performance. Gaussian mean and Gaussian standard deviation of RTs to HC stimuli were reduced with greater theta:beta ratios ($r = -0.15, r = -0.50$) while the long tail factor was largely flat ($r = -0.01$). MRs were also not significantly positively correlated with theta:beta ratios ($r = 0.28$). In addition, the changes in RT between the first and final block in the final session were negatively correlated with the theta:beta ratios. Although these results are not statistically significant and should be interpreted cautiously, they suggest a possible relationship between theta:beta ratios and task performance. Specifically, higher theta:beta ratios appear to be associated with poorer performance which is consistent with the literature on this topic [191].

Furthermore, it was hypothesised that stimulation at 1mA would enhance task performance. On the contrary, this work demonstrated no significant differences in task performance between the sham, 1mA and 2mA conditions. The null results found in this chapter may reflect a genuine lack of efficacy. However, there are a plethora of other reasons why a null result could have been found. Notably, as previously mentioned, measures taken did not correlate with task performance in the sham session, indicating the experimental paradigm itself may have been flawed.

The stimulation itself may not have been properly blinded as the blinding procedure was not systematically checked to ensure that all three stimulation parameters caused similar sensations. Any effects generated by the E-field induced in the brain may have been masked by the effects of the sensation of stimulation.

Another potential contributory factor to the null results observed in this work is the intermittent nature of the stimulation protocol used. As previously described, stimulation was active during the duration of task blocks (6 minutes 20 seconds) and off during the rest period (30 seconds). Vestring et al. evaluated the impact of different tDCS protocols, including variations in block length and repetition patterns, on synaptic plasticity. Their findings suggest that longer-duration single-block protocols may be more efficacious at inducing lasting plasticity effects compared to repeated shorter blocks of stimulation [273]. However, Fricke et al. evaluated motor cortex excitability with different stimulation protocols by measuring transcranial magnetic stimulation induced motor evoked potentials (MEPs) post tDCS. MEPs were not significantly different immediately after stimulation ceased regardless of a 0 minute, 3 minute or 30 minute break between 5 minute stimulation blocks [274]. The effects of the block design used in this experiment are unclear and may have contributed to the null findings.

The predicted peak E-field magnitude was also hypothesised to correlate with task per-

formance improvements, but no significant relationship was observed. Additionally, it was hypothesised that individual factors, including age and ADHD-ASRS inattentive scores, would inversely correlate with the magnitude of performance changes. However, these variables did not show significant correlations with task performance.

Regarding the predicted peak E-field for each participant, age, gender and head circumference were included in the predictions. These three values were significantly correlated with simulated peak E-fields in a partial correlational analysis from Chapter 3 (see Figure 3.4). Cephalic index and body-mass index were not significantly correlated with peak E-field magnitudes, the most pertinent factors to the model's performance were included in the peak E-field estimation. Notably, however, the model used accounts for 34.5% of the variance over the simulated population. A full table of these results can be found in Appendix A.3. A participant-specific, MRI scan informed E-field simulation would have been preferable.

The E-field analysis performed resulted in similar E-fields to those estimated to be generated during previous work [33]. Consequently, it is unlikely that the E-field induced during this work was sufficiently novel to cause different behavioural effects.

Another contributing factor for the lack of significant findings in this work is the small sample size which reduces statistical power and the ability to detect subtle effects. Additionally, the analysis involved multiple comparisons, and the use of the strict Bonferroni adjustment method further increased the likelihood of type II errors. These factors may have collectively obscured potential effects.

Ultimately, while the null results found in this work may be representative of the genuine lack of effects from stimulation, they may also have been driven by methodological shortcomings. In future work, these shortcomings, including task duration, noise, participant comfort and proper blinding, must be taken into consideration and rigorously tested for.

Furthermore, future works should analyse simultaneously collected EEG data and behavioural data during stimulation for VA to further improve our understanding of how rDLPFC modulated VA frontal P300 [225], centro-parietal positivity [228] and various frequency domain features [250] should be analysed.

6.5. Conclusions

This chapter investigated the impact of tDCS on VA by applying sham, 1mA and 2mA tDCS to the rDLPFC in a within-participant, sham-controlled experiment. Contrary to the initial hypotheses, no significant effects of stimulation were observed on RTs or MRs. Additionally, participant-specific predictors, such as age, ADHD ASRS inattention scores, and resting-state EEG measures and the predicted peak E-field magnitudes did not correlate with task performance or stimulation efficacy.

These null findings are likely attributed to several methodological factors. High rejection rates due to poor task performance, external distractors like the neoprene head cap and environmental noise, and short session durations may have limited the ability to observe significant effects. These factors underscore the need for rigorous participant screening and training, along with more controlled experimental environments in future research.

The intermittent nature of the stimulation protocol (6 minutes and 20 seconds on, 30 seconds off) may have limited the change in cortical excitability. Additionally, the absence of systematic blinding verification and the small sample size may have further obscured potential effects. Future studies should address these limitations to provide more definitive evidence for the effects of tDCS on vigilant attention.

7

Market Intelligence and Readiness Assessment for Transcranial Electrical Stimulation Dose Standardisation

7.1. Introduction

Chapter 3 presented the development of an accessible approach to transcranial electrical stimulation dose standardisation. A key motivator for this work was the stated need for an accessible and scalable approach to tES dosing. To evaluate the potential impact and adoption of this software both in academia and industry, it is crucial to understand the size and readiness of the market. To that end, in this chapter, I evaluated the current state of the market surrounding this work. This chapter discusses the current state of tES research, both in academia and in industry. It also provides an overview of the qualitative results derived from interviews with various tES product manufacturers.

7.2. Trends in Non-Invasive Brain Stimulation Publications

To evaluate the market size, I first assessed the number of academic publications on different NIBS modalities and how the number of publications changes over time.

To achieve this, I performed a systematic search of the PubMed and Scopus databases. This was intended to extract the number of published works that reference NIBS in any form as an approximate measure of the popularity of each modality. The search terms mentioned below were entered into both databases, and comma-separated values (CSV) files generated by the respective databases were downloaded. Using MATLAB 2023a, all CSV were concatenated into one large table, including the Digital Object Identifier (DOI) of each publication and the year of publication. After this, duplicate DOIs were removed from the table. All searches were performed on the 4th of July, 2024. Papers identified through this process were not manually inspected. As a result, there are likely some irrelevant papers in this sample and potentially some relevant papers that were omitted. However, this approach provides an approximation of the literature landscape for analysis.

The search terms used for each modality are listed below:
Transcranial electrical stimulation:
Search 1: *brain* OR *neuromodulation* AND *"temporal interference"* AND *"electrical"*
Search 2:*brain* OR *neuromodulation* AND *"transcranial electrical stimulation"*
Search 3: *brain* OR *neuromodulation* AND *"transcranial direct current stimulation"*
Search 4: *brain* OR *neuromodulation* AND *"transcranial alternating current stimulation"*
Search 5: *brain* OR *neuromodulation* AND *"transcranial random noise stimulation"*

Transcranial ultrasound stimulation:

Search 1: *brain* OR *neuromodulation* AND *"transcranial ultrasound stimulation"*

Search 2: *brain* OR *neuromodulation* AND *"focused ultrasound stimulation"*

Search 4: *brain* OR *neuromodulation* AND *"focused ultrasound"* AND *noninvasive* NOT *implanted* NOT *implantable*

Search 5: *brain* OR *neuromodulation* AND *"low intensity"* AND *noninvasive* NOT *implanted* NOT *implantable*

Transcranial magnetic stimulation:

Search 1: *brain* OR *neuromodulation* AND *"transcranial magnetic stimulation"*

Search 2: *brain* OR *neuromodulation* AND *"repetitive magnetic temporal interference"*

Photobiomodulation:

Search 1: *brain* OR *neuromodulation* AND *photobiomodulation*

Search 3: *brain* OR *neuromodulation* AND *"low-level light therapy"*

Search 4: *brain* OR *neuromodulation* AND *"low-level laser therapy"*

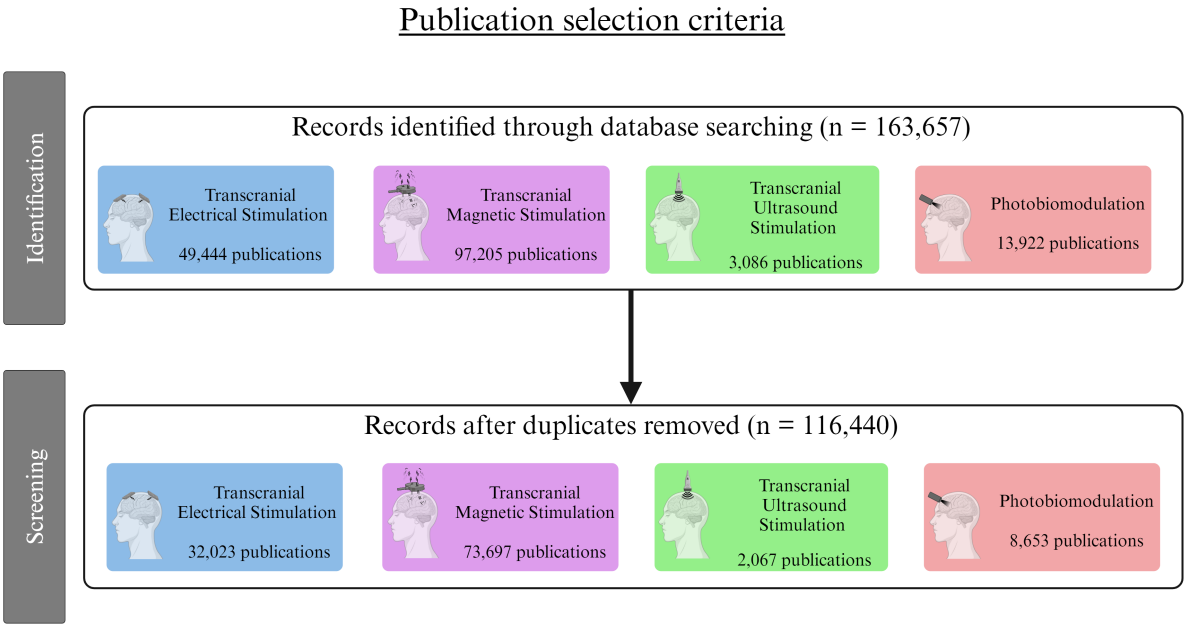

Sources: PubMed and Scopus up to July 2024.

Figure 7.1.: Publication selection flowchart for the four NIBS modalities across PubMed and Scopus databases. This includes the number of identified search results and remaining publications after removing duplicates. Created with BioRender.com.

After the removal of duplicates, 116,440 publications were included in subsequent analyses. Firstly, the cumulative number of publications per year was plotted by modality as shown in Figure 7.2. This clearly shows that TMS is the modality with the greatest number of total publications (73,697), followed by tES (32,023), tPBM (8,653) and finally TUS (2,067). Regarding the number of publications, currently, tES represents a substantial share of academic publications (28%).

Figure 7.2.: Stacked area plot for the cumulative number of publications by modality. Created with BioRender.com.

The cumulative number of publications indicates past trends, but caution should be exercised when extrapolating these to predict future developments, particularly in this emerging and dynamic research area. To better understand the future potential of tES in terms of the number of academic publications, the annual percentage change is shown in Figure 7.3. Years with less than 20 identified publications were excluded from this plot. In years with very few publications, small absolute changes can result in extreme percentage increases (for example, an increase from 1 to 2 publications would show as 100% growth) or even infinite growth rates. Additionally, years with more than 20 publications preceded and succeeded by years with greater than 20 publications were excluded. These exclusions help maintain a more meaningful representation of growth trends.

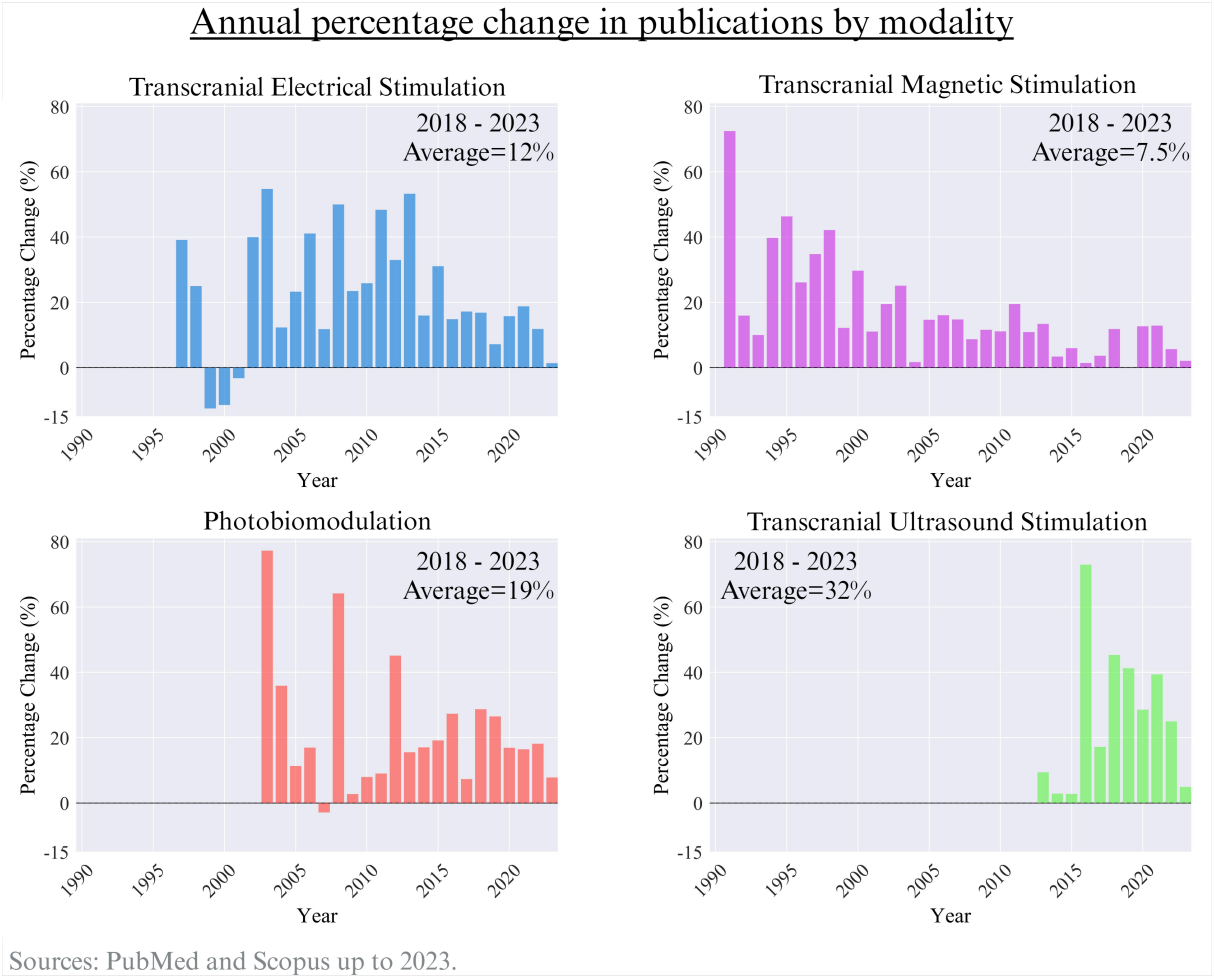

Figure 7.3.: Year over year percentage change in the number of publications for each modality. Years with less than 20 publications were removed for clarity.

In the last 5 full years (2018-2023), the number of tES publications grew at an average annual rate of 12%. While a growing number of publications is a positive signal for the future of the academic tES market, this growth rate is less than the average of 28% in the 5 preceding years (2012-2017). However, a proportion of this apparent decline is likely due to the COVID-19 pandemic, the number of publications in TMS and TUS also show a reduction when comparing these time periods.

TUS and tPBM show a larger annual growth rate than tES from 2018-2023 at 32% and 19%, respectively. Overall, tES represents a mature and growing academic market compared to other NIBS modalities. This provides a positive indication of the potential for products and services that target tES research.

7.3. Trends in Commercial Usage of Transcranial Electrical Stimulation

To assess the current commercial utilization of tES, a list of tES companies has been collated below, as well as a list of potential competitors to the participant-specific MRI-free dose control system developed in Chapter 3. These companies were found by performing a comprehensive search on Google, LinkedIn and GlobalData.

Name	Description
Flow Neuroscience	Manufactures a tDCS device and accompanying software for the treatment of depression.
Soterix Medical	Manufactures tES hardware and software for researchers and the treatment of depression and pain.
Sooma	Manufacture a tDCS based device for the treatment of depression and pain.
Neuroelectrics	tES device manufacturer for researchers. In clinical trials for depression and epilepsy.
Ghoonuts	tES startup initially focused on treating aphasia.
Pulvinar Neuro	Manufacture tES devices for research and product development.
Neuro Device Group (Nurostym tES)	Manufacture tES devices for research applications.
Nexalin	Manufacturer of a tACS device for the treatment of anxiety and insomnia.
Newronika	tDCS device manufacturer for research and clinical usage.
neuroConn GmbH (Neurocare group)	tES device manufacturer for therapy and research.
Samphire Neuroscience	tES device manufacturer for menstrual health including pain perception and emotional regulation.
Somnee	Manufacturer of a tACS device for sleep enhancement.
PlatoScience	Manufacturer of a tDCS headset intended for researchers and healthcare professionals.

Table 7.1.: A list of companies that use transcranial electrical stimulation in their product(s) accompanied by a brief description. Companies were collated from Google search, LinkedIn and GlobalData.

While the companies in table 7.1 do not represent an exhaustive list, they do provide insights into the state of the market. The 12 companies presented supply for multiple markets; 7 supply researchers, 7 supply clinicians, and 3 market their product(s) directly to consumers. Companies were collated from Google search, LinkedIn and GlobalData.

A full financial breakdown is not available for many of these companies, but some have publicly announced funding rounds or grants in recent years. This includes a seed round by Flow Neuroscience, raising $9 million in 2019 [275], followed by recent collaborations by the National Health Service in the United Kingdom [276]. Additionally, Neuroelectrics raised $17.5 million in a series A round in 2021 [277] and Samphire Neuroscience raised $2.3 million in a pre-seed round in the same year [278].

There is insufficient information to make definitive statements about macro trends in the tES market other than concluding funding rounds are continuing in several companies. Many companies serve the academic market, and there has not yet been broad international adoption of any tES device for any application. That is, the future of commercial opportunities is nascent and unclear.

Name	MRI required?	Open-source?
SimNIBS	Yes	Yes
Soterix Medical (HD-Explore)	Yes	No
Neuroelectrics (StimWeaver)	Yes	No
Neurophet	Yes	No
ROAST	Yes	Yes
COMSOL	Yes	No
Antonenko et al. [146]	No	Yes

Table 7.2.: Companies, software solutions and publications that present potential competition for the MRI-free dose control software.

7.4. Clinical Trials Trends for Transcranial Electrical Stimulation

Previous sections describe the growth of tES publications compared to other NIBS modalities and the companies that work with tES. However, the conditions being targeted have not been discussed thus far. To address this, a systematic search of the ClinicalTrials.gov database was completed. The following search terms were performed separately.

Search 1: *"Transcranial Electrical Stimulation"*
Search 2: *"Transcranial Alternating Current Stimulation"*
Search 3: *"Transcranial Direct Current Stimulation"*
Search 4: *"Transcranial Random Noise Stimulation"*

CSV files containing the search results were downloaded and processed with MATLAB 2023a. Trials registered on ClinicalTrials.gov are assigned a unique "NCT number" identifier. After concatenating the CSV files generated from each of the the aforementioned search terms, duplicate entries, based on their NCT numbers, were removed. This resulted in a reduction in the number of trials from the original 2,531 down to 2,012. 3,019 total instances of conditions were identified across those trials, as many trials listed multiple conditions.

The number of trials found for each search term are displayed in Figure 7.4. Of these stimulation types, transcranial direct current stimulation produced the most results (n=1,665), followed by transcranial alternating current (n=180) and, finally, transcranial random noise stimulation (n=51). The catch-all term transcranial electrical stimulation produced 635 clinical trials. Dose control is relevant for all three types of transcranial electrical stimulation.

To generate Figure 7.5, the conditions present in each clinical trial are distinguished. This was achieved using the "Conditions" column generated by ClinicalTrials.gov CSV files. Many

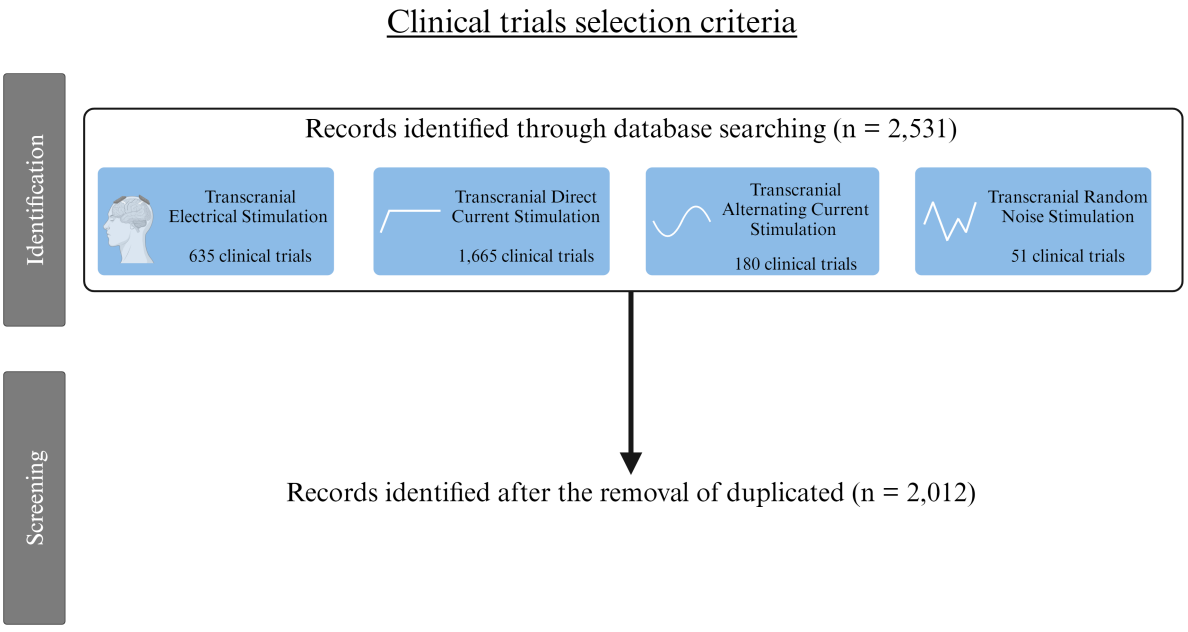

Sources: ClinicalTrials.gov up to July 2024.

Figure 7.4.: Transcranial electrical stimulation clinical trials selection criteria. Searchers were performed in the ClinicalTrials.gov database on the 7th of July 2024.

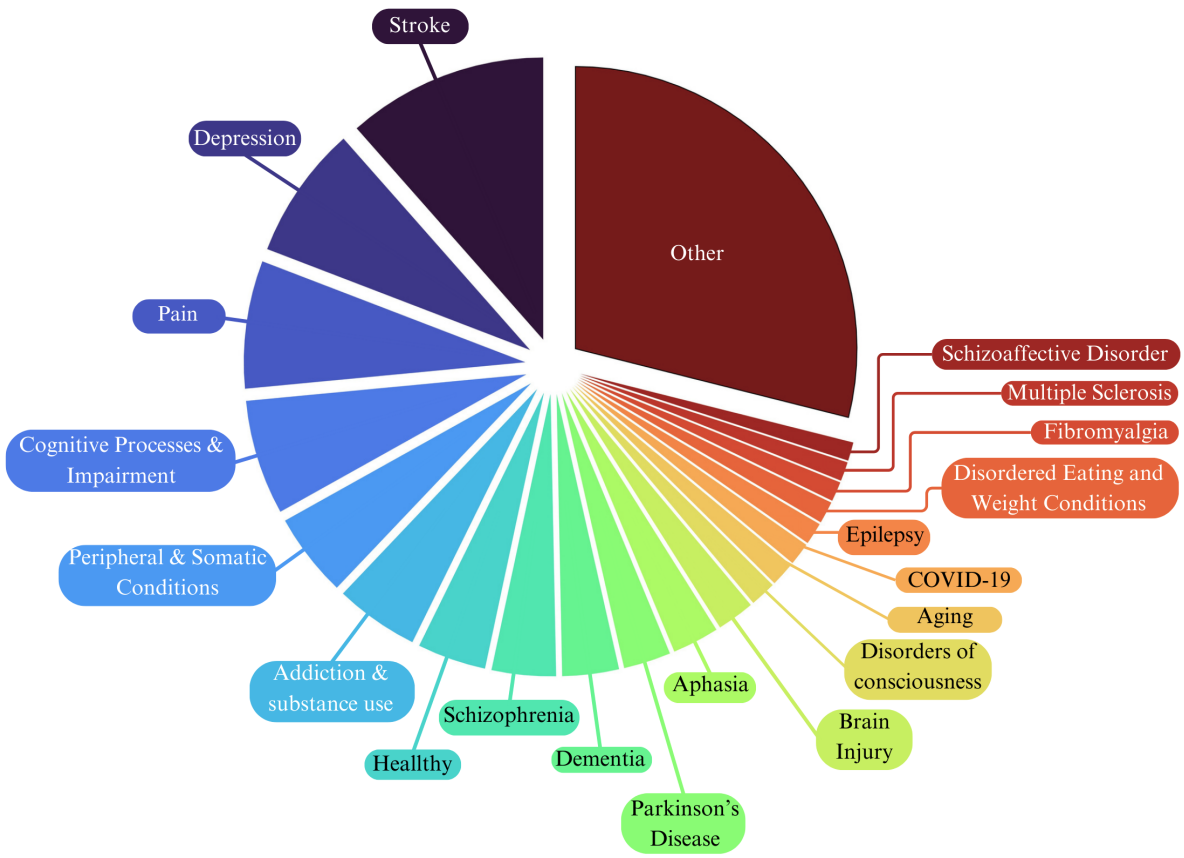

Figure 7.5.: Conditions listed in clinical trials with transcranial electrical stimulation. 3,019 total condition instances across all 2,012 clinical trials.

trials have multiple relevant conditions, all of which were extracted for the purposes of this analysis. For example, if a trial was using tES to treat depression in stroke patients, this study would be present in both the stroke and depression categories. Alternative spellings and sub-types of conditions were combined to produce a representative dataset. For example, 'stroke', 'Stroke' and "Ischemic stroke" are all combined into the "Stroke" category.

Stroke (n=348) is the most common condition listed in clinical trials, followed by depression (n=231) and pain (n=221). The number of conditions mentioned varied, with the 'Other' category including autism (n=30) and tinnitus (n=28) among others. Ultimately, a large variety of conditions have been studied in clinical trials, but most have yet to be translated into clinical treatments.

7.5. Demand for MRI-Free Dose Control

The market trends discussed previously confirm that both the number of academic studies and clinical trials using tES are growing year on year, and that tES is the leading form of NIBS in academia. However, they do not confirm whether there is currently demand for an MRI-free approach to tES dose estimation. To determine if there is currently a commercial need for this work, I contacted five companies and held meetings with four of them as one did not respond to attempts to contact them. These conversations provide anecdotal evidence of demand but do not constitute an exhaustive exploration of the market.

To respect the privacy of the individuals involved, all companies and individuals will be kept anonymous. However, it should be noted that these companies were chosen for their size and the advanced stage of the application of their product(s) or potential product(s).

Overall, these conversations signalled three key points. First, the market is small and may not be sufficient in size to justify a spinout company. Rather a license agreement may be more appropriate. Second, companies at an advanced stage regarding their technology readiness level (TRL) are interested in the concept. However, to justify the investment, they must be convinced that using this software will improve outcomes for patients/users. Third, the value to potential customers is likely in the form of a bespoke database and software framework that can be used for commercial applications that are also proven to enhance efficacy. Finally, it is not clear if the revenue generated from selling this software as a stand-alone product for research purposes would generate sufficient revenue to justify the cost of its development. Indeed, tES is a relatively inexpensive approach to brain stimulation. Many academics that use tES in their research may be price-sensitive. However, a more thorough analysis is required to understand the price sensitivity of academics and its implications.

7.6. Intellectual Property

The software, as described in Chapter 3, is not suitable for commercial use due to licensing restrictions. In this section, the specific licenses used and strategies to mitigate potential conflicts with commercialisation are discussed.

Firstly, the CamCAN dataset that was used states that the data is to be used for "scientific investigation, teaching or the planning of clinical research studies only". For uses outside of these terms, the administrators of the dataset must be contacted to discuss approval. In the absence of the license holder's approval, an alternative solution could be the collection of a

proprietary dataset. Doing so would provide the benefit of collecting a dataset that fits the needs of this work. This would include physical measurements of the cephalic index and head circumference, taking into account posture in the MRI scanner [178] and performing T1 scans with fat suppression for more accurate multi-layer skull segmentation [176]. Additionally, a proprietary dataset would allow for a multi-arm study directly comparing MRI-informed dose control and dose controlled by this work.

After obtaining the dataset, E-fields were simulated using the ROAST library, which is covered by a GPL-3.0 license [279]. This license does allow for commercial use. However, it does so with copyleft terms attached. This would also require our derivative work to use a GPL-3.0 license. This would allow others to freely use, modify, and redistribute this work, including for commercial purposes, as long as they also distribute their modifications under the same GPL-3.0 terms[1]. As a result, an alternative solution should be sought for E-field simulation. ROAST performs several functions that would have to be replicated with alternative software. First, segmentation of the MRI scans into the subsequent tissue types can be achieved with open-source alternatives such as ForkNet [280], which is covered by a BSD-3 license [281]. COMSOL Multiphysics with a commercial license could then be used for E-field modelling[1].

After simulating the E-fields FSL was used to transform them to MNI-152 space. FSL has bespoke software licensing terms, which require approvals from the license holder to be sought by licensees [282][1]. While commercial use may still be plausible with FSL, an alternative solution with an existing commercial-friendly license would be preferable. The 6th generation MNI-152 reference brain has a bespoke license that allows for commercial use on the condition that the copyright of the license holder is provided in all copies created [283][1].

Next, MATLAB was used extensively throughout this work, including E-field simulations, E-field transformations and regression. A commercial license costing £800 per year [284] would be required to use this for commercial purposes[1]. MATLAB was used to simulate E-fields, some of the steps of transformation and regression. An alternative solution could be translating this code to an alternative programming language suitable for commercial use, such as Python.

[1]The license terms described reflect the information available as of July 8th, 2024, and are subject to change. This description may not encompass all aspects of the licenses and should not be considered a comprehensive representation of the full terms and conditions.

7.7. Conclusions

In Chapter 3, an approach to personalize tES dosing without participant-specific MRI scans was introduced. In this chapter, the tES market was explored. Ultimately, this work is best suited for academic publication. This conclusion was reached for several reasons. Firstly, conversations with companies that use tES indicate that proof of the impact on outcomes is required. Additionally, significant work and capital are required to re-develop the software for commercial usage. To provide a return on this investment, a clear revenue stream must be identified.

There are two potential revenue streams for this work: academic and commercial uses. Academics working with tES often do so in part due to its low cost. A thorough price analysis would be required to make definitive statements; however, after discussions with businesses that serve the academic market, it appears unlikely that academia would provide a sufficient source of revenue to justify further investment. Commercial uses could potentially provide a large enough revenue stream, particularly in the form of a license agreement. However, without proof of improvements in outcomes, none of the companies contacted were willing to continue discussions on their use of this work.

The tES market covers a diverse array of conditions, and as the field progresses, the commercial opportunities are likely to grow. Unfortunately, at this time, it is unlikely that this work could raise enough revenue to justify the investment required to bring it to market. Future versions of accessible dose control methodologies serving a more mature market, particularly when paired with evidence of improved outcomes, may have the potential for commercial success. Ultimately, researchers, businesses, and patients will be best served by releasing this work as an academic publication.

8

Conclusions and Future Research Directions

8.1. Key Achievements

Through its research outcomes, this thesis has contributed new and important knowledge to the field of non-invasive brain stimulation.

- This thesis provided a comprehensive critical analysis of the challenges facing NIBS research and made recommendations for future work. This included various NIBS modalities, sources of variability, inclusive research practices, multi-site and multimodal stimulation.
- This thesis demonstrated a novel and accessible approach to personalised tES dosing without the need for MRI scans. This was achieved through the development of interpretable algorithms that utilize readily available morphological and demographic data to determine participant-specific tES doses.
- Electrophysiological and behavioural correlates of vigilant attention in two datasets with and without tDCS were investigated in this thesis. I explored EEG-based correlates of VA and discussed the methodological implications of the null findings in a within-participant sham-controlled EEG and tDCS experiment.

8.2. General Discussion

8.2.1 Challenges Facing Non-Invasive Brain Stimulation

To address the thesis' aim of advancing strategies for personalised, accessible and effective cognitive enhancement, a broad critical analysis of NIBS was performed in Chapter 2, in which several key challenges were identified.

Inter-individual variations in head and brain morphology, including age and gender related changes in skull thickness and brain structure, can lead to substantial variations in the intensity of electric fields generated by identical tES parameters. This variability can result in unintended stimulation of off-target regions and dosing heterogeneity across the population. Additionally, the complex and insufficiently characterised relationship between the dose received and the response produced was also discussed.

Furthermore, the functional state of the brain during stimulation was identified as a crucial factor influencing NIBS efficacy. Ongoing neural activity and neurotransmitter concentrations modulate the response to stimulation, highlighting the need for brain-state dependent, closed-loop stimulation.

In this chapter, the challenges posed by variations in neuron type and orientation were also discussed, as well as the potential for stimulation itself to change structural components of the brain. Finally, the limitations of single-site stimulation when addressing complex behaviours and disorders involving distributed brain activity were highlighted. By comprehensively examining these challenges, Chapter 2 laid the groundwork for developing more effective and personalised NIBS.

8.2.2 Accessible and personalised Transcranial Electrical Stimulation Dosing

To satisfy the first objective of this thesis, I developed an accessible approach to tES dose standardisation without requiring participant-specific MRI scans. This work significantly reduced peak E-field strength variability without a participant-specific MRI scan, as discussed in Chapter 3. In order to train the regression algorithms used in this thesis, the largest tES-induced electric field simulation of its kind was performed on 418 participants and 10 montages.

Spearman's partial correlations analysis demonstrated that age is the strongest predictor of E-field variability, followed by head circumference. To demonstrate the capability of this approach, robust multiple linear regression models were developed for both conventional and HD montages. Montage-specific models trained on conventional montages accounted for 43% of E-field variability, while those trained on HD montages accounted for 21% of E-field variability in unseen individuals.

In addition to the montage-specific models, montage-agnostic models were also trained for use on novel montages. These models, which considered the inter-electrode distance, accounted for 36% and 13% of peak E-field strength variability in conventional and HD montages, respectively, in unseen individuals and montages. Due to the non-linear relationship between inter-electrode distance and E-field strength, both linear and non-linear models were used. This chapter, therefore, was successful in developing an accessible approach to tES dose standardisation.

8.2.3 Electrophysiological and Behavioural Correlates of Vigilant Attention

The second objective of this thesis was to investigate electrophysiological and behavioural correlates with tDCS efficacy in vigilant attention. To successfully address this objective, two studies were conducted.

Chapter 5 presented the use of a continuous random-dot motion task to identify frequency domain EEG features associated with VA. Wilcoxon rank-sum tests revealed significant differences in the frequency domain data collected from two EEG channels. For HC stimuli, significant differences were observed in frequency bands associated with arousal levels and off-task thought. EEG markers during LC stimuli were associated with arousal levels and active visuospatial suppression.

In Chapter 6, a comprehensive within-participant, sham-controlled study investigating the effects of tDCS on VA was performed. This included EEG measures, ADHD ASRS questionnaire results and estimated peak E-field strengths. All participants received sham, 1mA and 2mA of stimulation. While no statistically significant results were found, this work provided methodological insights for future research.

These chapters provide insights into the electrophysiological correlates of vigilant attention and highlight important considerations for future tDCS studies in this domain.

8.2.4 Future Research Directions

The findings presented in this thesis point to several promising directions for advancing the fields of personalised tES dosing and vigilant attention enhancement.

An Accessible Approach to Transcranial Electrical Stimulation Dose Standardisation

- The performance of non-linear montage-agnostic models proposed in this thesis may be further improved by incorporating a wider range of montages. This would enhance the models' generalizability and potentially improve their accuracy across diverse stimulation configurations.
- The underlying electric field simulations could be enhanced by incorporating more detailed tissue models, including fat distribution and variations in skull density. In doing so, future work may better represent the electric field distributions across a diverse population.
- Testing the impacts of this dose standardisation approach on the efficacy of stimulation in humans is an important next step for this area of research. Ideally, this would involve comparing outcomes of stimulation using accessible dose standardisation against traditional fixed-dose approaches and MRI-informed personalised dosing across a range of applications.
- Accessible, dose standardisation could also be improved beyond the scope of the demographic and morphological measures discussed in this work. For instance, incorporating a smartphone-based 3D head scan or tissue conductivity estimation using electrical impedance tomography.
- Future research should focus on demonstrating the clinical efficacy of personalised tES dosing using the dose standardisation approach developed in this thesis. Conducting rigorous clinical trials to provide evidence of improved outcomes across various tES applications would be crucial for both academic advancement and potential commercial adoption.

Validating Accessible Dose Standardisation

Chapter 3 demonstrated an accessible approach to tDCS dose standardisation. However, the effect of this standardisation method on patient outcomes remains unproven. This section describes an experimental design to assess the impact of the proposed dosage standardisation procedure on outcomes in human participants. There are many potential applications for tDCS as described in Chapter 4. Given the primary aim of validating the dose standardisation procedure, an application with robust evidence of tDCS efficacy is required.

tDCS enhances motor-evoked potentials (MEPs) induced by TMS, with the amplitude and polarity of the tDCS stimulation affecting the size and duration of MEPs [6]. However, recent work by Laasko et al. found that personalised tDCS dosing through E-field modelling did not enhance MEPs [267]. As a result, the use of tDCS for MEP enhancement may not be the ideal target for the proposed dose standardisation study. Working memory (WM) is another potential target, with initial evidence suggesting that E-field characteristics, including its magnitude, might partly explain the effects of prefrontal tDCS [285, 286]. However, as described in Chapter 4, a review of the effects of tDCS on WM found no effect from single sessions, and a moderate effect for multi-session studies for WM training [194]. The ideal target to validate the dose standardisation approach requires an established application with robust evidence of efficacy.

There is accumulating evidence through several clinical trials that pre-frontal tDCS for major depressive disorder (MDD) is efficacious compared to placebo [287, 288] and is non-inferior to escitalopram [136]. These trials include the use of tDCS over several sessions, for instance in the ELECT-tDCS study 2mA of tDCS was applied for 30 minutes for 15-consecutive weekdays followed by 7 weekly treatments. A retrospective analysis of this study indicated that E-field magnitudes may have been associated with different outcomes [141]. In addition, recent work by Albizu et al. was able to achieve 91.25% classification accuracy between responders and non-responders in the ELEC-TDCS trial using MRI-informed E-field simulations and a support vector machine model. Notably, in this work current density magnitudes outperformed current density vectors and density directions [289].

The ELECT-TDCS trial was a single-centre trial where patients attended the clinic. Subsequent work with tDCS used at home did not find significant results [290]. However, Woodham et al. performed a successful at home randomised controlled trial with significant improvements on the Hamilton Depression Rating Scale (HDRS) compared to sham [288], the authors explain how the previous null results may have been due to small sample sizes and short trial durations. A notable area of improvement for the Woodham et al. study is blinding

as the patients were able to distinguish between sham and active stimulation. The proposed study would act as both a replication study for confirming that tDCS reduces symptoms of MDD through the reduction in HDRS scores, as well as testing the hypothesis that personalised dosing improves efficacy.

Patients will be recruited on the basis that they are currently clinically diagnosed with MDD and are not currently taking any medication for their condition. Patients will also be required to score at least 16 in the 17-item HDRS [291] as in previous work [288]. They will also be chosen based on their availability to visit the clinic/laboratory and their suitability for stimulation. For example, patients that are pregnant, have a history of epilepsy or have abrasions to the skin around the stimulation site will be excluded. To ensure the dose standardisation model is trained on a representative sample patients will be included based on demographic inclusion criteria such as an even distribution of ages and genders. Four patient groups will be recruited. Each of these groups will aim to include 90 patients resulting in a total sample size of 360. The target sample size was chosen to ensure comparability with previous studies that demonstrated statistically significant results [136, 288].

T1w and T2w MRI scans will be collected for patients across all groups. The combination of T1w and T2w scans enhances segmentation accuracy compared to T1w scans alone [166]. Patients will also use a vertical MRI scanner to replicate the upright position they will be in when they receive stimulation, as posture can impact E-field magnitudes induced by tDCS [178]. Demographic data, including age, gender, BMI, and race, will be collected to inform the dose standardisation model training procedure. In addition, a 3D head scan will be taken with a smartphone at the beginning of each session for precise head measurements, and to potentially localise the tDCS electrodes in future work. Smartphone based EEG electrode localisation has been demonstrated previously [123]. Head circumference will also be measured manually with a tape measure for comparison with head circumferences attained from the 3D scans and MRI scans. In Chapter 3, a montage with the anode at F3 and cathode at F4 montage was simulated and used to train a dose standardisation model. In this model, age, head circumference and gender but not BMI and cephalic index were significantly correlated with the peak E-field. This model was able to explain 30% of the variability in the peak E-field magnitude.

The proposed experiment will be conducted in three stages, the first replicates previous work on the use of tDCS for the treatment of MDD. It will also includes the collection of data for the training of the dose standardisation models used to inform the second and third stages. The second stage will evaluate the efficacy of MRI-informed dose personalisation. The third and final stage will test the effectiveness of the accessible dose standardisation

approach in improving tDCS treatment outcomes.

All patients will receive stimulation to the left dorsolateral prefrontal cortex with the anode placed over F3 and the cathode over F4. Fixed-dose patients will receive 2mA of stimulation in line with previous work [292]. The ideal sham protocol is not well understood, however ramping stimulation up at the beginning and end of the session may be superior to simply ramping up and down at the beginning [293]. However, ramping up to 1mA over 30 seconds and down over 15 seconds at the beginning and end of each session did not successfully blind patients in previous work [288]. As a result, the blinding procedure in this work will ramp up to 2mA to induce greater sensations. Stimulation will only commence once impedance is measured as being below 10kΩ, and single-use saline soaked sponges will be used as opposed to rubber electrodes with conductive paste to reduce the risk of burns [294].

It should be noted that assessors may not be adequately blinded due to redness on the skin caused by 2mA of stimulation [295]. As a result, for full blinding, evaluation of the data will be completed by individuals that did not attend the data collection stage. These individuals will be instructed not to discuss the experiment with others until the experiment and data analysis is concluded.

In stage one of this study two groups will take part in the experiment over a period of ten weeks to maximise effect size [296]. Patients will attend the clinic/laboratory in person and receive 30 minutes of stimulation per day, 5 days per week. At the end of the study, all of the patients will be asked whether they believe they received active or sham stimulation. Group 1 will receive sham stimulation (N=90). Group 2 (N=90) will have an identical procedure, with the addition of 2mA as opposed to sham stimulation. Patients will be randomly allocated to each group. Due to potential logistical constraints with enrolling 180 participants concurrently, stage one may be divided into four 10-week phases, resulting in a total duration of 40 weeks.

After data collection, the data from stage 1 will be processed to evaluate the efficacy of tDCS. The T1w and T2w MRI scans will then be used to simulate the E-field across all 180 patients using the same approach described in Chapter 3 Section 3.2.3. This includes the use of ROAST for simulating the E-field [15], and a multiple linear regression model for predicting the peak E-field. The simulated E-field will be examined to determine correlates with the peak E-field magnitudes and the reduction in the HDRS score. This may be solely the peak E-field (average of the 95th percentile) as in Chapter 3 or it may also include the peak E-field across a series of relevant brain regions including the left and right superior frontal gyrus and the right supplementary motor area [289]. The optimal independent variables to include in the model (such as age, head circumference, gender, cephalic index, race and BMI) and

the optimal E-field parameters (such as peak E-field, average E-field in specific regions and E-field direction) will be tested to maximise model performance in predicting MDD symptom reduction.

Stage two will involve the testing of MRI-informed dose standardisation compared to fixed-dosing and sham stimulation. Once again 90 patients will be enrolled in an identical design to stage one aside from the magnitude of stimulation that patients will receive. Patient specific MRI scans will be used to inform patient specific dosing that aligns with results from stage one. The results from stage two will be compared to the stimulation applied in stage one and sham stimulation to evaluate whether fixed-dose stimulation is inferior to MRI-informed dose controlled stimulation.

If MRI-informed dose personalisation achieves significant improvements in the HDRS score, the third and final stage of the experiment will commence. This requires the training of the dose standardisation model, which will be trained on data from all of the patients that have gone through the experiment thus far (n=270). 5-fold cross validation will be used to evaluate the variability in the peak E-field (or other E-field parameters) explained by the dose standardisation model. As in Chapter 3 model performance will be defined in terms of the normalised root-mean-squared error and adjusted R^2.

The proposed study investigates whether personalised tDCS dosing, with and without patient-specific MRI scans improves treatment outcomes for MDD compared to fixed-dose and sham stimulation. Building on prior research demonstrating tDCS efficacy for MDD and the potential relationship between E-field magnitudes and clinical outcomes, the study proposes a three-stage design involving 360 participants. Stage one replicates existing tDCS protocols for MDD while collecting data for dose standardisation model training. Stage two tests the effects of MRI-informed personalised dosing on outcomes, and stage three tests an accessible, MRI-free dose standardisation approach based on demographic and anatomical data. This study aims to demonstrate that personalised tDCS dosing, particularly through an accessible approach, enhances the efficacy of tDCS for MDD.

Transcranial Electrical Stimulation for Vigilant Attention

- In addition to the resting-state EEG that was analysed before stimulation in this work. Future work could incorporate ERP analysis to elucidate the relationships between real-time EEG measures and participants' responses to stimulation. These ERPs include frontal P3 ERP, the lateralised readiness potential and the centro-partietal positivity.
- Methodological improvements could be made to future work to minimise confounding factors. These include longer task duration, the minimisation of distractors such as noise and head cap discomfort and robust blinding procedures.
- Vigilant attention is a complex cognitive process associated with distributed brain activity. As such, future work could investigate the use of multi-site stimulation. Such as the cathodal simulation of the posterior parietal cortex during high attentional load, and anodal stimulation to the right dorsolateral prefrontal cortex for top-down attentional regulation of early sensory processing.

8.3. Conclusions

This thesis has explored the use of tES for cognitive enhancement, with a specific focus on VA. A broad overview of the obstacles and opportunities facing NIBS research has been provided, and the development of a novel, accessible approach to standardised tES dosing without the need for participant specific MRI scans has been presented. This thesis also examined the electrophysiological and behavioural correlates of VA, discussing the methodological implications of an EEG and tDCS experiment.

Future research directions include validating the efficacy of the proposed tES dose standardisation approach. Additionally, further investigation of the electrophysiological and behavioural correlates of VA could involve a more detailed examination of various ERP components and their relationship to tDCS stimulation. Methodological improvements in future VA tDCS studies, such as longer task durations, the minimisation of distractors, and robust blinding procedures are also considered.

References

[1] Marom Bikson, Pnina Grossman, Chris Thomas et al. 'Safety of transcranial direct current stimulation: evidence based update 2016'. In: *Brain stimulation* 9.5 (2016), pp. 641–661 (cit. on pp. 2, 10).

[2] Paolo Cassano, Richard Norton, Marco Antonio Caldieraro et al. 'Tolerability and safety of transcranial photobiomodulation for mood and anxiety disorders'. In: *Photonics*. Vol. 9. MDPI. 2022, p. 507 (cit. on pp. 2, 10).

[3] Umer Najib and Jared Cooney Horvath. 'Transcranial magnetic stimulation (TMS) safety considerations and recommendations'. In: *Transcranial magnetic stimulation* (2014), pp. 15–30 (cit. on pp. 2, 10).

[4] Penny Ping Qin, Minxia Jin, Adam Weili Xia et al. 'The effectiveness and safety of low-intensity transcranial ultrasound stimulation: A systematic review of human and animal studies'. In: *Neuroscience & Biobehavioral Reviews* (2023), p. 105501 (cit. on pp. 2, 10).

[5] Cyril Atkinson-Clement, Andrea Junor and Marcus Kaiser. 'A large-scale online survey of patients and the general public: Preferring safe and noninvasive neuromodulation for mental health'. In: *medRxiv* (2024), pp. 2024–01 (cit. on pp. 2, 10).

[6] Michael A Nitsche and Walter Paulus. 'Excitability changes induced in the human motor cortex by weak transcranial direct current stimulation'. In: *The Journal of physiology* 527.Pt 3 (2000), p. 633 (cit. on pp. 2, 120).

[7] Ulrich Palm, Alkomiet Hasan, Wolfgang Strube and Frank Padberg. 'tDCS for the treatment of depression: a comprehensive review'. In: *European Archives of Psychiatry and Clinical Neuroscience* 266.8 (Dec. 2016), pp. 681–694 (cit. on p. 2).

[8] Nigel I. Kennedy, Won Hee Lee and Sophia Frangou. 'Efficacy of non-invasive brain stimulation on the symptom dimensions of schizophrenia: A meta-analysis of randomized controlled trials'. In: *European Psychiatry* 49 (Mar. 2018), pp. 69–77 (cit. on p. 2).

[9] Stephen Vanhaerents, Bernard S. Chang, Alexander Rotenberg, Alvaro Pascual-Leone and Mouhsin M. Shafi. 'Noninvasive Brain Stimulation in Epilepsy'. In: *Journal of Clinical Neurophysiology* 37.2 (2020), pp. 118–130 (cit. on p. 2).

[10] Alkomiet Hasan, Kristina Misewitsch, Michael A Nitsche et al. 'Impaired motor cortex responses in non-psychotic first-degree relatives of schizophrenia patients: a cathodal tDCS pilot study'. In: *Brain stimulation* 6.5 (2013), pp. 821–829 (cit. on pp. 2, 17).

[11] Hannah McCann and Leandro Beltrachini. 'Does participant's age impact on tDCS induced fields? Insights from computational simulations'. In: *Biomedical Physics & Engineering Express* 7.4 (2021), p. 045018 (cit. on pp. 2, 22).

[12] Sagarika Bhattacharjee, Rajan Kashyap, Alicia M Goodwill et al. 'Sex difference in tDCS current mediated by changes in cortical anatomy: A study across young, middle and older adults'. In: *Brain stimulation* 15.1 (2022), pp. 125–140 (cit. on pp. 2, 22).

[13] Carys Evans, Ainslie Johnstone, Catharina Zich et al. 'The impact of brain lesions on tDCS-induced electric fields'. In: *Scientific Reports* 13.1 (2023), p. 19430 (cit. on p. 2).

[14] Carys Evans, Clarissa Bachmann, Jenny S.A. Lee et al. 'Dose-controlled tDCS reduces electric field intensity variability at a cortical target site'. In: *Brain Stimulation* 13.1 (Jan. 2020), pp. 125–136 (cit. on pp. 2, 13, 15, 22, 81).

[15] Yu Huang, Abhishek Datta, Marom Bikson and Lucas C Parra. 'Realistic volumetric-approach to simulate transcranial electric stimulation—ROAST—a fully automated open-source pipeline'. In: *Journal of Neural Engineering* 16.5 (July 2019), p. 056006 (cit. on pp. 2, 25, 61, 89, 122).

[16] Guilherme B Saturnino, Oula Puonti, Jesper D Nielsen et al. 'SimNIBS 2.1: a comprehensive pipeline for individualized electric field modelling for transcranial brain stimulation'. In: *Brain and human body modeling* (2019), pp. 3–25 (cit. on p. 2).

[17] Yu Huang, Anli A. Liu, Belen Lafon et al. 'Measurements and models of electric fields in the in vivo human brain during transcranial electric stimulation'. In: *eLife* 6 (Feb. 2017) (cit. on pp. 2, 22, 62).

[18] Jimmy Jiang, Dennis Q Truong, Zeinab Esmaeilpour et al. 'Enhanced tES and tDCS computational models by meninges emulation'. In: *Journal of neural engineering* 17.1 (2020), p. 016027 (cit. on pp. 2, 26, 62, 89).

[19] Asif Jamil, Giorgi Batsikadze, Hsiao-I. Kuo et al. 'Current intensity- and polarity-specific online and aftereffects of transcranial direct current stimulation: An fMRI study'. In: *Human Brain Mapping* 41.6 (Apr. 2020), pp. 1644–1666 (cit. on pp. 2, 22, 62).

[20] JSA Lee, S Bestmann and C Evans. 'A Future of Current Flow Modelling for Transcranial Electrical Stimulation?' In: *Current Behavioral Neuroscience Reports* (2021), pp. 1–10 (cit. on pp. 2, 16, 17, 22, 54, 80).

[21] Alessandra Vergallito, Sarah Feroldi, Alberto Pisoni and Leonor J Romero Lauro. 'Inter-individual variability in tDCS effects: A narrative review on the contribution of stable, variable, and contextual factors'. In: *Brain Sciences* 12.5 (2022), p. 522 (cit. on pp. 2, 17, 19).

[22] Mohd Faizal Mohd Zulkifly, Ornela Merkohitaj, Jürgen Brockmöller and Walter Paulus. 'Confounding effects of caffeine on neuroplasticity induced by transcranial alternating current stimulation and paired associative stimulation'. In: *Clinical Neurophysiology* 132.6 (2021), pp. 1367–1379 (cit. on pp. 2, 17).

[23] Claire Bradley, Abbey S Nydam, Paul E Dux and Jason B Mattingley. 'State-dependent effects of neural stimulation on brain function and cognition'. In: *Nature Reviews Neuroscience* 23.8 (2022), pp. 459–475 (cit. on pp. 2, 16).

[24] Hannah L Filmer, Shane E Ehrhardt, Saskia Bollmann, Jason B Mattingley and Paul E Dux. 'Accounting for individual differences in the response to tDCS with baseline levels of neurochemical excitability'. In: *Cortex* 115 (2019), pp. 324–334 (cit. on pp. 2, 16).

[25] Nicholas Ketz, Aaron P Jones, Natalie B Bryant, Vincent P Clark and Praveen K Pilly. 'Closed-loop slow-wave tACS improves sleep-dependent long-term memory generalization by modulating endogenous oscillations'. In: *Journal of Neuroscience* 38.33 (2018), pp. 7314–7326 (cit. on pp. 2, 18, 59, 66).

[26] Amir Homayoun Javadi, Paul Cheng and Vincent Walsh. 'Short duration transcranial direct current stimulation (tDCS) modulates verbal memory'. In: *Brain stimulation* 5.4 (2012), pp. 468–474 (cit. on pp. 2, 59).

[27] Emma Caravati, Federica Barbeni, Giovanni Chiarion, Matteo Raggi and Luca Mesin. 'Closed-Loop Transcranial Electrical Neurostimulation for Sustained Attention Enhancement: A Pilot Study towards Personalized Intervention Strategies'. In: *Bioengineering* 11.5 (2024), p. 467 (cit. on pp. 2, 57, 81).

[28] Ian H. Robertson, Tom Manly, Jackie Andrade, Bart T. Baddeley and Jenny Yiend. ''Oops!': Performance correlates of everyday attentional failures in traumatic brain injured and normal subjects'. In: *Neuropsychologia* 35.6 (May 1997), pp. 747–758 (cit. on pp. 2, 45, 66, 80).

[29] Nash Unsworth. 'Consistency of attentional control as an important cognitive trait: A latent variable analysis'. In: *Intelligence* 49 (Mar. 2015), pp. 110–128 (cit. on pp. 2, 45, 64, 66, 80).

[30] Francesca C. Fortenbaugh, Joseph DeGutis, Laura Germine et al. 'Sustained attention across the lifespan in a sample of 10,000: Dissociating ability and strategy'. In: *Psychological science* 26.9 (Sept. 2015), p. 1497 (cit. on pp. 3, 66).

[31] Aisling M. O'Halloran, Nils Pénard, Alessandra Galli et al. 'Falls and falls efficacy: The role of sustained attention in older adults'. In: *BMC Geriatrics* 11.1 (Dec. 2011), p. 85 (cit. on pp. 3, 45, 64, 66, 80).

[32] Heather E.K. Walker and Lana M. Trick. 'Mind-wandering while driving: The impact of fatigue, task length, and sustained attention abilities'. In: *Transportation Research Part F: Traffic Psychology and Behaviour* 59 (Nov. 2018), pp. 81–97 (cit. on pp. 3, 45, 54, 64, 66).

[33] Méadhbh B Brosnan, Mahnaz Arvaneh, Siobhán Harty et al. 'Prefrontal modulation of visual processing and sustained attention in aging, a tDCS–EEG coregistration approach'. In: *Journal of cognitive neuroscience* 30.11 (2018), pp. 1630–1645 (cit. on pp. 3, 10, 25, 43, 54, 55, 80, 89, 99, 101).

[34] Lucia M Li, Kazumasa Uehara and Takashi Hanakawa. 'The contribution of interindividual factors to variability of response in transcranial direct current stimulation studies'. In: *Frontiers in cellular neuroscience* 9 (2015), p. 181 (cit. on p. 3).

[35] Jake Toth, Danielle Lauren Kurtin, Méadhbh Brosnan and Mahnaz Arvaneh. 'Opportunities and obstacles in non-invasive brain stimulation'. In: *Frontiers in Human Neuroscience* 18 (2024), p. 1385427 (cit. on p. 10).

[36] Suzana Herculano-Houzel. 'The human brain in numbers: a linearly scaled-up primate brain'. In: *Frontiers in human neuroscience* (2009), p. 31 (cit. on p. 10).

[37] Louis Sokoloff. 'The metabolism of the central nervous system in vivo'. In: *Handbook of physiology, section I, neurophysiology* 3 (1960), pp. 1843–1864 (cit. on p. 10).

[38] Grace Katja. *AI Impacts - Brain performance in TEPS*. https://aiimpacts.org/brain-performance-in-teps/. 2015 (cit. on p. 10).

[39] Rafael Polanía, Michael A Nitsche and Christian C Ruff. 'Studying and modifying brain function with non-invasive brain stimulation'. In: *Nature neuroscience* 21.2 (2018), pp. 174–187 (cit. on p. 10).

[40] Maria Sperens, Katarina Hamberg, Gun-Marie Hariz et al. 'Are patients ready for "EARLYSTIM"? Attitudes towards deep brain stimulation among female and male patients with moderately advanced Parkinson's disease'. In: *Parkinson's Disease* 2017 (2017) (cit. on p. 10).

[41] Peter Tarr. *FDA clears saint rapid-acting brain stimulation approach for those suffering from resistant major depression*. https://bbrfoundation.org/content/fda-clears-saint-rapid-acting-brain-stimulation-approach-those-suffering-resistant-major. [Accessed 17-01-2023]. 2023 (cit. on p. 10).

[42] Eleanor J Cole, Angela L Phillips, Brandon S Bentzley et al. 'Stanford neuromodulation therapy (SNT): a double-blind randomized controlled trial'. In: *American Journal of Psychiatry* 179.2 (2022), pp. 132–141 (cit. on p. 10).

[43] Medtech innovation briefing. *Flow transcranial direct current stimulation for treating depression [NICE 2023]*. https://www.nice.org.uk/advice/mib324/. 2023 (cit. on p. 10).

[44] James J Mahoney, Daisy GY Thompson-Lake, Manish Ranjan et al. 'Low-Intensity Focused Ultrasound Targeting the Bilateral Nucleus Accumbens as a Potential Treatment for Substance Use Disorder: A First-in-Human Report'. In: *Biological Psychiatry* (2023) (cit. on p. 10).

[45] Xianwei Che, Robin FH Cash, Xi Luo et al. 'High-frequency rTMS over the dorsolateral prefrontal cortex on chronic and provoked pain: A systematic review and meta-analysis'. In: *Brain Stimulation* 14.5 (2021), pp. 1135–1146 (cit. on p. 10).

[46] Shrey Grover, Wen Wen, Vighnesh Viswanathan, Christopher T Gill and Robert MG Reinhart. 'Long-lasting, dissociable improvements in working memory and long-term memory in older adults with repetitive neuromodulation'. In: *Nature neuroscience* 25.9 (2022), pp. 1237–1246 (cit. on p. 11).

[47] Hayley Thair, Amy L Holloway, Roger Newport and Alastair D Smith. 'Transcranial direct current stimulation (tDCS): a beginner's guide for design and implementation'. In: *Frontiers in neuroscience* 11 (2017), p. 641 (cit. on p. 11).

[48] Abhishek Datta, Varun Bansal, Julian Diaz et al. 'Gyri-precise head model of transcranial direct current stimulation: improved spatial focality using a ring electrode versus conventional rectangular pad'. In: *Brain stimulation* 2.4 (Oct. 2009), pp. 201–207 (cit. on p. 11).

[49] Marom Bikson, Masashi Inoue, Hiroki Akiyama et al. 'Effects of uniform extracellular DC electric fields on excitability in rat hippocampal slices in vitro'. In: *The Journal of physiology* 557.1 (2004), pp. 175–190 (cit. on p. 11).

[50] Charlotte J Stagg, Velicia Bachtiar and Heidi Johansen-Berg. 'The role of GABA in human motor learning'. In: *Current biology* 21.6 (2011), pp. 480–484 (cit. on p. 11).

[51] Michael A Hunter, Brian A Coffman, Charles Gasparovic et al. 'Baseline effects of transcranial direct current stimulation on glutamatergic neurotransmission and large-scale network connectivity'. In: *Brain research* 1594 (2015), pp. 92–107 (cit. on p. 11).

[52] Sankaraleengam Alagapan, Stephen L Schmidt, Jérémie Lefebvre et al. 'Modulation of cortical oscillations by low-frequency direct cortical stimulation is state-dependent'. In: *PLoS biology* 14.3 (2016), e1002424 (cit. on p. 11).

[53] Michael Nitsche, K Fricke, U Henschke et al. 'Pharmacological modulation of cortical excitability shifts induced by transcranial direct current stimulation in humans'. In: *The Journal of physiology* 553.1 (2003), pp. 293–301 (cit. on p. 11).

[54] Thomas Reed and Roi Cohen Kadosh. 'Transcranial electrical stimulation (tES) mechanisms and its effects on cortical excitability and connectivity'. In: *Journal of inherited metabolic disease* 41 (2018), pp. 1123–1130 (cit. on p. 11).

[55] Ryota Kanai, Leila Chaieb, Andrea Antal, Vincent Walsh and Walter Paulus. 'Frequency-dependent electrical stimulation of the visual cortex'. In: *Current Biology* 18.23 (2008), pp. 1839–1843 (cit. on p. 11).

[56] Andrea Antal, Klára Boros, Csaba Poreisz et al. 'Comparatively weak after-effects of transcranial alternating current stimulation (tACS) on cortical excitability in humans'. In: *Brain stimulation* 1.2 (2008), pp. 97–105 (cit. on p. 11).

[57] Daniella Terney, Leila Chaieb, Vera Moliadze, Andrea Antal and Walter Paulus. 'Increasing human brain excitability by transcranial high-frequency random noise stimulation'. In: *Journal of Neuroscience* 28.52 (2008), pp. 14147–14155 (cit. on p. 11).

[58] William C Stacey and Dominique M Durand. 'Stochastic resonance improves signal detection in hippocampal CA1 neurons'. In: *Journal of Neurophysiology* 83.3 (2000), pp. 1394–1402 (cit. on p. 11).

[59] Leila Chaieb, Andrea Antal and Walter Paulus. 'Transcranial random noise stimulation-induced plasticity is NMDA-receptor independent but sodium-channel blocker and benzodiazepines sensitive'. In: *Frontiers in neuroscience* 9 (2015), p. 125 (cit. on p. 11).

[60] Bruce Hutcheon and Yosef Yarom. 'Resonance, oscillation and the intrinsic frequency preferences of neurons'. In: *Trends in neurosciences* 23.5 (2000), pp. 216–222 (cit. on p. 13).

[61] Nir Grossman, David Bono, Nina Dedic et al. 'Noninvasive deep brain stimulation via temporally interfering electric fields'. In: *cell* 169.6 (2017), pp. 1029–1041 (cit. on p. 13).

[62] Ines R Violante, Ketevan Alania, Antonino M Cassarà et al. 'Non-invasive temporal interference electrical stimulation of the human hippocampus'. In: *Nature neuroscience* (2023), pp. 1–11 (cit. on pp. 13, 43).

[63] Janine D Bijsterbosch, Anthony T Barker, Kwang-Hyuk Lee and Peter WR Woodruff. 'Where does transcranial magnetic stimulation (TMS) stimulate? Modelling of induced field maps for some common cortical and cerebellar targets'. In: *Medical & biological engineering & computing* 50 (2012), pp. 671–681 (cit. on p. 13).

[64] Wanalee Klomjai, Rose Katz and Alexandra Lackmy-Vallée. 'Basic principles of transcranial magnetic stimulation (TMS) and repetitive TMS (rTMS)'. In: *Annals of physical and rehabilitation medicine* 58.4 (2015), pp. 208–213 (cit. on p. 13).

[65] Samuel Frazer Cooke and Timothy VP Bliss. 'Plasticity in the human central nervous system'. In: *Brain* 129.7 (2006), pp. 1659–1673 (cit. on p. 13).

[66] Alexander V Chervyakov, Andrey Yu Chernyavsky, Dmitry O Sinitsyn and Michael A Piradov. 'Possible mechanisms underlying the therapeutic effects of transcranial magnetic stimulation'. In: *Frontiers in human neuroscience* 9 (2015), p. 303 (cit. on p. 13).

[67] Kilian Prei, Carolina Kanig, Mirja Osnabruegge et al. 'Limited evidence for reliability of low and high frequency rTMS over the motor cortex'. In: *Brain Research* 1820 (2023), p. 148534 (cit. on p. 13).

[68] Sung Wook Chung, Kate E Hoy and Paul B Fitzgerald. 'Theta-burst stimulation: A new form of TMS treatment for depression?' In: *Depression and anxiety* 32.3 (2015), pp. 182–192 (cit. on p. 13).

[69] Anthony T Barker, Reza Jalinous and Ian L Freeston. 'Non-invasive magnetic stimulation of human motor cortex'. In: *The Lancet* 325.8437 (1985), pp. 1106–1107 (cit. on p. 13).

[70] Jessica Moretti and Jennifer Rodger. 'A little goes a long way: Neurobiological effects of low intensity rTMS and implications for mechanisms of rTMS'. In: *Current Research in Neurobiology* 3 (2022), p. 100033 (cit. on p. 13).

[71] Abraham Zangen, Yiftach Roth, Bernhard Voller and Mark Hallett. 'Transcranial magnetic stimulation of deep brain regions: evidence for efficacy of the H-coil'. In: *Clinical neurophysiology* 116.4 (2005), pp. 775–779 (cit. on p. 13).

[72] Adam Khalifa, Seyed Mahdi Abrishami, Mohsen Zaeimbashi et al. 'Magnetic temporal interference for noninvasive and focal brain stimulation'. In: *Journal of Neural Engineering* 20.1 (2023), p. 016002 (cit. on p. 13).

[73] Lari M Koponen, Jaakko O Nieminen and Risto J Ilmoniemi. 'Multi-locus transcranial magnetic stimulation—theory and implementation'. In: *Brain Stimulation* 11.4 (2018), pp. 849–855 (cit. on p. 13).

[74] Farzad Salehpour, Javad Mahmoudi, Farzin Kamari et al. 'Brain photobiomodulation therapy: a narrative review'. In: *Molecular neurobiology* 55 (2018), pp. 6601–6636 (cit. on pp. 13, 14).

[75] Marco A Caldieraro and Paolo Cassano. 'Transcranial and systemic photobiomodulation for major depressive disorder: A systematic review of efficacy, tolerability and biological mechanisms'. In: *Journal of affective disorders* 243 (2019), pp. 262–273 (cit. on pp. 13, 14).

[76] Paolo Cassano, Samuel R Petrie, Michael R Hamblin, Theodore A Henderson and Dan V Iosifescu. 'Review of transcranial photobiomodulation for major depressive disorder: targeting brain metabolism, inflammation, oxidative stress, and neurogenesis'. In: *Neurophotonics* 3 (2016), pp. 031404–031404 (cit. on p. 14).

[77] Paula Askalsky and Dan V Iosifescu. 'Transcranial photobiomodulation for the management of depression: current perspectives'. In: *Neuropsychiatric disease and treatment* (2019), pp. 3255–3272 (cit. on p. 14).

[78] Luyao Tang, Hui Jiang, Miao Sun and Muqing Liu. 'Pulsed transcranial photobiomodulation generates distinct beneficial neurocognitive effects compared with continuous wave transcranial light'. In: *Lasers in Medical Science* 38.1 (2023), p. 203 (cit. on p. 14).

[79] Willians Fernando Vieira, Maia Gersten, Marco Antonio Knob Caldieraro and Paolo Cassano. 'Photobiomodulation for major depressive disorder: Linking transcranial infrared light, biophotons and oxidative stress'. In: *Harvard Review of Psychiatry* 31.3 (2023), pp. 124–141 (cit. on p. 14).

[80] Farzad Salehpour, Mahsa Khademi and Michael R Hamblin. 'Photobiomodulation therapy for dementia: A systematic review of pre-clinical and clinical studies'. In: *Journal of Alzheimer's disease* 83.4 (2021), pp. 1431–1452 (cit. on p. 14).

[81] Marjorie Dole, Vincent Auboiroux, Lilia Langar and John Mitrofanis. 'A systematic review of the effects of transcranial photobiomodulation on brain activity in humans'. In: *Reviews in the Neurosciences* 0 (2023) (cit. on p. 14).

[82] Xiaoqing Li, Vamsidhara Vemireddy, Qi Cai et al. 'Reversibly modulating the blood–brain barrier by laser stimulation of molecular-targeted nanoparticles'. In: *Nano Letters* 21.22 (2021), pp. 9805–9815 (cit. on p. 14).

[83] Qi Cai, Xiaoqing Li, Hejian Xiong et al. 'Optical blood-brain-tumor barrier modulation expands therapeutic options for glioblastoma treatment'. In: *Nature communications* 14.1 (2023), p. 4934 (cit. on p. 14).

[84] Willem A Velema, Wiktor Szymanski and Ben L Feringa. 'Photopharmacology: beyond proof of principle'. In: *Journal of the American Chemical Society* 136.6 (2014), pp. 2178–2191 (cit. on p. 14).

[85] Kullervo Hynynen, Nathan McDannold, Natalia Vykhodtseva and Ferenc A Jolesz. 'Noninvasive MR imaging–guided focal opening of the blood-brain barrier in rabbits'. In: *Radiology* 220.3 (2001), pp. 640–646 (cit. on p. 14).

[86] Ernst Martin, Daniel Jeanmonod, Anne Morel, Eyal Zadicario and Beat Werner. 'High-intensity focused ultrasound for noninvasive functional neurosurgery'. In: *Annals of Neurology: Official Journal of the American Neurological Association and the Child Neurology Society* 66.6 (2009), pp. 858–861 (cit. on p. 14).

[87] Bashar W Badran, Kevin A Caulfield, Sasha Stomberg-Firestein et al. 'Sonication of the anterior thalamus with MRI-Guided transcranial focused ultrasound (tFUS) alters pain thresholds in healthy adults: A double-blind, sham-controlled study'. In: *Brain stimulation* 13.6 (2020), pp. 1805–1812 (cit. on p. 14).

[88] Wynn Legon, Tomokazu F Sato, Alexander Opitz et al. 'Transcranial focused ultrasound modulates the activity of primary somatosensory cortex in humans'. In: *Nature neuroscience* 17.2 (2014), pp. 322–329 (cit. on p. 14).

[89] Pejman Ghanouni, Kim Butts Pauly, W Jeff Elias et al. 'Transcranial MR-guided focused ultrasound: a review of the technology and neuro applications'. In: *AJR. American journal of roentgenology* 205.1 (2015), p. 150 (cit. on p. 14).

[90] Anton Fomenko, Clemens Neudorfer, Robert F Dallapiazza, Suneil K Kalia and Andres M Lozano. 'Low-intensity ultrasound neuromodulation: an overview of mechanisms and emerging human applications'. In: *Brain stimulation* 11.6 (2018), pp. 1209–1217 (cit. on p. 14).

[91] Roland Beisteiner, Eva Matt, Christina Fan et al. 'Transcranial pulse stimulation with ultrasound in Alzheimer's disease—a new navigated focal brain therapy'. In: *Advanced Science* 7.3 (2020), p. 1902583 (cit. on p. 14).

[92] Federico E Turkheimer, Fernando E Rosas, Ottavia Dipasquale et al. 'A complex systems perspective on neuroimaging studies of behavior and its disorders'. In: *The Neuroscientist* 28.4 (2022), pp. 382–399 (cit. on p. 15).

[93] Elizabeth M Lillie, Jillian E Urban, Sarah K Lynch, Ashley A Weaver and Joel D Stitzel. 'Evaluation of Skull Cortical Thickness Changes With Age and Sex From Computed Tomography Scans'. In: *Journal of Bone and Mineral Research* 31.2 (Feb. 2016), pp. 299–307 (cit. on pp. 15, 61–63).

[94] Herve Lemaitre, Aaron L Goldman, Fabio Sambataro et al. 'Normal age-related brain morphometric changes: nonuniformity across cortical thickness, surface area and gray matter volume?' In: *Neurobiology of aging* 33.3 (Mar. 2012), 617–e1 (cit. on pp. 15, 63).

[95] Richard AI Bethlehem, Jakob Seidlitz, Simon R White et al. 'Brain charts for the human lifespan'. In: *Nature* 604.7906 (2022), pp. 525–533 (cit. on pp. 15, 63).

[96] Ghazaleh Soleimani, Rayus Kuplicki, Jazmin Camchong et al. *Are we really targeting and stimulating DLPFC by placing transcranial electrical stimulation (tES) electrodes over F3/F4?* Tech. rep. Wiley Online Library, 2023 (cit. on p. 15).

[97] Muyue Yang, Zhen Yang, Pu Wang and Zhihui Sun. 'Current application and future directions of photobiomodulation in central nervous diseases'. In: *Neural Regeneration Research* 16.6 (2021), p. 1177 (cit. on p. 15).

[98] Morteza Mohammadjavadi, Ryan T Ash, Ningrui Li et al. 'Transcranial ultrasound neuromodulation of the thalamic visual pathway in a large animal model and the dose-response relationship with MR-ARFI'. In: *Scientific Reports* 12.1 (2022), p. 19588 (cit. on p. 15).

[99] Zeinab Esmaeilpour, Paola Marangolo, Benjamin M. Hampstead et al. 'Incomplete evidence that increasing current intensity of tDCS boosts outcomes'. In: *Brain Stimulation* 11.2 (Mar. 2018), pp. 310–321 (cit. on pp. 15, 58, 81).

[100] Pai-Feng Yang, M Anthony Phipps, Sumeeth Jonathan et al. 'Bidirectional and state-dependent modulation of brain activity by transcranial focused ultrasound in non-human primates'. In: *Brain stimulation* 14.2 (2021), pp. 261–272 (cit. on p. 16).

[101] Aino E Tervo, Jaakko O Nieminen, Pantelis Lioumis et al. 'Closed-loop optimization of transcranial magnetic stimulation with electroencephalography feedback'. In: *Brain Stimulation* 15.2 (2022), pp. 523–531 (cit. on p. 16).

[102] Christoph Zrenner, Debora Desideri, Paolo Belardinelli and Ulf Ziemann. 'Real-time EEG-defined excitability states determine efficacy of TMS-induced plasticity in human motor cortex'. In: *Brain stimulation* 11.2 (2018), pp. 374–389 (cit. on p. 16).

[103] Kai Yu, Xiaodan Niu, Esther Krook-Magnuson and Bin He. 'Intrinsic functional neuron-type selectivity of transcranial focused ultrasound neuromodulation'. In: *Nature communications* 12.1 (2021), p. 2519 (cit. on p. 17).

[104] Hyeyeon Chung, Cheolki Im, Hyeon Seo and Sung Chan Jun. 'Key factors in the cortical response to transcranial electrical Stimulations—A multi-scale modeling study'. In: *Computers in Biology and Medicine* 144 (2022), p. 105328 (cit. on p. 17).

[105] Alexander D Tang, William Bennett, Aidan D Bindoff et al. 'Subthreshold repetitive transcranial magnetic stimulation drives structural synaptic plasticity in the young and aged motor cortex'. In: *Brain Stimulation* 14.6 (2021), pp. 1498–1507 (cit. on p. 17).

[106] JL Beros, ES King, D Clarke, J Rodger and AD Tang. 'Static magnetic stimulation induces structural plasticity at the axon initial segment of inhibitory cortical neurons'. In: *bioRxiv* (2022), pp. 2022–01 (cit. on p. 17).

[107] Fei-Fei Zhang, Wei Peng, John A Sweeney, Zhi-Yun Jia and Qi-Yong Gong. 'Brain structure alterations in depression: Psychoradiological evidence'. In: *CNS neuroscience & therapeutics* 24.11 (2018), pp. 994–1003 (cit. on p. 17).

[108] Juliana Corlier, Andrew Wilson, Reza Tadayonnejad et al. 'Multi-target repetitive transcranial magnetic stimulation (rTMS) protocol for the treatment of comorbid depression and chronic pain'. In: *Brain Stimulation: Basic, Translational, and Clinical Research in Neuromodulation* 14.6 (2021), pp. 1729–1730 (cit. on p. 17).

[109] David B Fischer, Peter J Fried, Giulio Ruffini et al. 'Multifocal tDCS targeting the resting state motor network increases cortical excitability beyond traditional tDCS targeting unilateral motor cortex'. In: *Neuroimage* 157 (2017), pp. 34–44 (cit. on p. 17).

[110] Nina M Rzechorzek, Michael J Thrippleton, Francesca M Chappell et al. 'A daily temperature rhythm in the human brain predicts survival after brain injury'. In: *Brain* 145.6 (2022), pp. 2031–2048 (cit. on p. 17).

[111] Nancy Doyle. 'Neurodiversity at work: a biopsychosocial model and the impact on working adults'. In: *British Medical Bulletin* 135.1 (2020), p. 108 (cit. on p. 17).

[112] Susan Young, Nicoletta Adamo, Bryndís Björk Ásgeirsdóttir et al. 'Females with ADHD: An expert consensus statement taking a lifespan approach providing guidance for the identification and treatment of attention-deficit/hyperactivity disorder in girls and women'. In: *BMC psychiatry* 20.1 (2020), pp. 1–27 (cit. on p. 17).

[113] Weiming Sun, JingJing Song, Xiangli Dong et al. 'Bibliometric and visual analysis of transcranial direct current stimulation in the web of science database from 2000 to 2022 via CiteSpace'. In: *Frontiers in Human Neuroscience* 16 (2022), p. 1049572 (cit. on p. 18).

[114] Taiwei Wang, Xuemiao Huang, Lijing Zhao et al. 'A bibliometric analysis of global publication trends on rTMS and aphasia'. In: *Medicine* 102.20 (2023) (cit. on p. 18).

[115] Wesley Medeiros, Tayná Barros and Fabio V Caixeta. 'Bibliometric mapping of non-invasive brain stimulation techniques (NIBS) for fluent speech production'. In: *Frontiers in Human Neuroscience* 17 (2023), p. 1164890 (cit. on p. 18).

[116] Til O Bergmann. 'Brain state-dependent brain stimulation'. In: *Frontiers in psychology* 9 (2018), p. 2108 (cit. on p. 18).

[117] Egidio D'Angelo and Viktor Jirsa. 'The quest for multiscale brain modeling'. In: *Trends in neurosciences* (2022) (cit. on p. 18).

[118] Ernesto E Vidal-Rosas, Hubin Zhao, Reuben W Nixon-Hill et al. 'Evaluating a new generation of wearable high-density diffuse optical tomography technology via retinotopic mapping of the adult visual cortex'. In: *Neurophotonics* 8.2 (2021), pp. 025002–025002 (cit. on p. 18).

[119] Matthew J Brookes, James Leggett, Molly Rea et al. 'Magnetoencephalography with optically pumped magnetometers (OPM-MEG): the next generation of functional neuroimaging'. In: *Trends in Neurosciences* (2022) (cit. on p. 18).

[120] Seyed Yahya Shirazi and Helen J Huang. 'More reliable EEG electrode digitizing methods can reduce source estimation uncertainty, but current methods already accurately identify brodmann areas'. In: *Frontiers in neuroscience* 13 (2019), p. 1159 (cit. on p. 18).

[121] Kevin A Caulfield, Holly H Fleischmann, Claire E Cox et al. 'Neuronavigation maximizes accuracy and precision in TMS positioning: Evidence from 11,230 distance, angle, and electric field modeling measurements'. In: *Brain stimulation* 15.5 (2022), pp. 1192–1205 (cit. on p. 18).

[122] Petru-Daniel Tudosiu, Walter Hugo Lopez Pinaya, Mark S Graham et al. 'Morphology-Preserving Autoregressive 3D Generative Modelling of the Brain'. In: *International Workshop on Simulation and Synthesis in Medical Imaging*. Springer. 2022, pp. 66–78 (cit. on p. 18).

[123] Alicia Everitt, Haley Richards, Yinchen Song et al. 'EEG electrode localization with 3D iPhone scanning using point-cloud electrode selection (PC-ES)'. In: *Journal of Neural Engineering* 20.6 (2023), p. 066033 (cit. on pp. 18, 121).

[124] Mariano Fernández-Corazza, Sergei Turovets, Phan Luu et al. 'Skull modeling effects in conductivity estimates using parametric electrical impedance tomography'. In: *IEEE Transactions on Biomedical Engineering* 65.8 (2017), pp. 1785–1797 (cit. on p. 19).

[125] Churan He, Yun Jing and Aiguo Han. 'Human skull profile and speed of sound estimation using pulse-echo ultrasound signals with deep learning'. In: *The Journal of the Acoustical Society of America* 150.4 (2021), A33–A33 (cit. on p. 19).

[126] Alfredo Lucas, Thomas Campbell Arnold, Serhat V Okar et al. 'Multi-contrast high-field quality image synthesis for portable low-field MRI using generative adversarial networks and paired data'. In: *medRxiv* (2023), pp. 2023–12 (cit. on p. 19).

[127] Courtney C Louis, Christopher T Webster, Lilianne M Gloe and Jason S Moser. 'Hair me out: Highlighting systematic exclusion in psychophysiological methods and recommendations to increase inclusion'. In: *Frontiers in Human Neuroscience* 16 (2022), p. 1058953 (cit. on p. 19).

[128] Jasmine Kwasa, Hannah M Peterson, Kavon Karrobi et al. 'Demographic reporting and phenotypic exclusion in fNIRS'. In: *Frontiers in Neuroscience* 17 (2023), p. 1086208 (cit. on p. 19).

[129] Le Xing and Alexander J Casson. '3D-printed, directly conductive and flexible electrodes for personalized electroencephalography'. In: *Sensors and Actuators A: Physical* 349 (2023), p. 114062 (cit. on p. 19).

[130] Roanne Hurley and Liana Machado. 'Using tDCS priming to improve brain function: Can metaplasticity provide the key to boosting outcomes?' In: *Neuroscience & Biobehavioral Reviews* 83 (2017), pp. 155–159 (cit. on p. 19).

[131] Parikshat Sirpal, Ali Kassab, Philippe Pouliot, Dang Khoa Nguyen and Frédéric Lesage. 'fNIRS improves seizure detection in multimodal EEG-fNIRS recordings'. In: *Journal of Biomedical Optics* 24.5 (2019), pp. 051408–051408 (cit. on p. 19).

[132] Antonios N Pouliopoulos, Maria F Murillo, Rebecca Lynn Noel et al. 'Non-invasive optogenetics with ultrasound-mediated gene delivery and red-light excitation'. In: *Brain stimulation* 15.4 (2022), pp. 927–941 (cit. on p. 19).

[133] Sayantanava Mitra, Urvakhsh Meherwan Mehta, Bhaskarapillai Binukumar, Ganesan Venkatasubramanian and Jagadisha Thirthalli. 'Statistical power estimation in non-invasive brain stimulation studies and its clinical implications: An exploratory study of the meta-analyses'. In: *Asian journal of psychiatry* 44 (Aug. 2019), pp. 29–34 (cit. on p. 20).

[134] Nicholas J Schork. 'Personalized medicine: time for one-person trials'. In: *Nature* 520.7549 (2015), pp. 609–611 (cit. on p. 20).

[135] Adam J Woods, Andrea Antal, Marom Bikson et al. 'A technical guide to tDCS, and related non-invasive brain stimulation tools'. In: *Clinical neurophysiology* 127.2 (Feb. 2016), pp. 1031–1048 (cit. on p. 22).

[136] André Russowsky Brunoni, Bernardo Sampaio-Junior, Adriano Henrique Moffa et al. 'The Escitalopram versus Electric Current Therapy for Treating Depression Clinical Study (ELECT-TDCS): rationale and study design of a non-inferiority, triple-arm, placebo-controlled clinical trial'. In: *São Paulo Medical Journal* 133 (2015), pp. 252–263 (cit. on pp. 22, 120, 121).

[137] Suellen Marinho Andrade, Maria Cecília de Araújo Silvestre, Eduardo Ériko Tenório de França et al. 'Efficacy and safety of HD-tDCS and respiratory rehabilitation for critically ill patients with COVID-19 The HD-RECOVERY randomized clinical trial'. In: *Brain Stimulation* 15.3 (2022), pp. 780–788 (cit. on p. 22).

[138] Jiheon Kim, Hansol Kim, Hyewon Jeong, Daeyoung Roh and Do Hoon Kim. 'tACS as a promising therapeutic option for improving cognitive function in mild cognitive impairment: a direct comparison between tACS and tDCS'. In: *Journal of Psychiatric Research* 141 (2021), pp. 248–256 (cit. on p. 22).

[139] Kym Wansbrough, Jane Tan, Ann-Maree Vallence and Hakuei Fujiyama. 'Recent advancements in optimising transcranial electrical stimulation: reducing response variability through individualised stimulation'. In: *Current Opinion in Behavioral Sciences* 56 (2024), p. 101360 (cit. on p. 22).

[140] Ilkka Laakso, Satoshi Tanaka, Soichiro Koyama, Valerio De Santis and Akimasa Hirata. 'Inter-subject variability in electric fields of motor cortical tDCS'. In: *Brain Stimulation* 8.5 (Sept. 2015), pp. 906–913 (cit. on pp. 22, 58, 60, 64).

[141] Paulo JC Suen, Sarah Doll, Marcelo C Batistuzzo et al. 'Association between tDCS computational modeling and clinical outcomes in depression: data from the ELECT-TDCS trial'. In: *European archives of psychiatry and clinical neuroscience* 271 (2021), pp. 101–110 (cit. on pp. 22, 120).

[142] Alejandro Albizu, Ruogu Fang, Aprinda Indahlastari et al. 'Machine learning and individual variability in electric field characteristics predict tDCS treatment response'. In: *Brain Stimulation* 13.6 (Nov. 2020), pp. 1753–1764 (cit. on p. 22).

[143] Alexander Opitz, Walter Paulus, Susanne Will, Andre Antunes and Axel Thielscher. 'Determinants of the electric field during transcranial direct current stimulation'. In: *Neuroimage* 109 (Apr. 2015), pp. 140–150 (cit. on p. 22).

[144] Daria Antonenko, Axel Thielscher, Guilherme Bicalho Saturnino et al. 'Towards precise brain stimulation: Is electric field simulation related to neuromodulation?' In: *Brain stimulation* 12.5 (2019), pp. 1159–1168 (cit. on p. 22).

[145] Michael Russell, Theodore Goodman, Qiang Wang, Bennett Groshong and Bruce G. Lyeth. 'Gender Differences in Current Received during Transcranial Electrical Stimulation'. In: *Frontiers in Psychiatry* 0.AUG (2014), p. 104 (cit. on pp. 22, 35, 63, 64).

[146] Daria Antonenko, Ulrike Grittner, Oula Puonti, Agnes Flöel and Axel Thielscher. 'Estimation of individually induced e-field strength during transcranial electric stimulation using the head circumference'. In: *Brain Stimulation* 14.5 (2021), pp. 1055–1058 (cit. on pp. 22, 27, 35, 63, 64, 109).

[147] Sriharsha Ramaraju, Mohammed A Roula and Peter W McCarthy. 'Modelling the effect of electrode displacement on transcranial direct current stimulation (tDCS)'. In: *Journal of Neural Engineering* 15.1 (2018), p. 016019 (cit. on p. 22).

[148] Jason R Taylor, Nitin Williams, Rhodri Cusack et al. 'The Cambridge Centre for Ageing and Neuroscience (Cam-CAN) data repository: Structural and functional MRI, MEG, and cognitive data from a cross-sectional adult lifespan sample'. In: *neuroimage* 144 (2017), pp. 262–269 (cit. on p. 25).

[149] Meredith A Shafto, Lorraine K Tyler, Marie Dixon et al. 'The Cambridge Centre for Ageing and Neuroscience (Cam-CAN) study protocol: a cross-sectional, lifespan, multidisciplinary examination of healthy cognitive ageing'. In: *BMC neurology* 14 (2014), pp. 1–25 (cit. on p. 25).

[150] Jesper LR Andersson, Mark Jenkinson and Stephen Smith. 'High resolution nonlinear registration with simultaneous modelling of intensities'. In: *BioRxiv* (2019), p. 646802 (cit. on p. 25).

[151] Jesper LR Andersson, Mark Jenkinson, Stephen Smith et al. 'Non-linear registration, aka Spatial normalisation FMRIB technical report TR07JA2'. In: *FMRIB Analysis Group of the University of Oxford* 2.1 (2007), e21 (cit. on pp. 25, 26).

[152] Nela V Ili, Emilija Dubljanin-Raspopovi, Una Nedeljkovi et al. 'Effects of anodal tDCS and occupational therapy on fine motor skill deficits in patients with chronic stroke'. In: *Restorative neurology and neuroscience* 34.6 (2016), pp. 935–945 (cit. on p. 25).

[153] AR Brunoni, R Ferrucci, M Bortolomasi et al. 'Transcranial direct current stimulation (tDCS) in unipolar vs. bipolar depressive disorder'. In: *Progress in Neuro-Psychopharmacology and Biological Psychiatry* 35.1 (2011), pp. 96–101 (cit. on p. 25).

[154] Andre R Brunoni, Leandro Valiengo, Alessandra Baccaro et al. 'The sertraline vs electrical current therapy for treating depression clinical study: results from a factorial, randomized, controlled trial'. In: *JAMA psychiatry* 70.4 (2013), pp. 383–391 (cit. on p. 25).

[155] Daria Antonenko, Ulrike Grittner, Guilherme Saturnino et al. 'Inter-individual and age-dependent variability in simulated electric fields induced by conventional transcranial electrical stimulation'. In: *NeuroImage* 224 (Jan. 2021), p. 117413 (cit. on pp. 25, 63, 64).

[156] Graziella Orrù, Ciro Conversano, Paul Kenneth Hitchcott and Angelo Gemignani. 'Motor stroke recovery after tDCS: a systematic review'. In: *Reviews in the Neurosciences* 31.2 (2020), pp. 201–218 (cit. on p. 25).

[157] Toralf Neuling, Sven Wagner, Carsten H Wolters, Tino Zaehle and Christoph S Herrmann. 'Finite-element model predicts current density distribution for clinical applications of tDCS and tACS'. In: *Frontiers in psychiatry* 3 (2012), p. 25619 (cit. on p. 25).

[158] Jiajing Zhao, Wenyu Li and Lin Yao. 'HD-tDCS Applied on DLPFC Cortex for Sustained Attention Enhancement: A Preliminary EEG Study'. In: *International Conference on Intelligent Robotics and Applications*. Springer. 2022, pp. 656–665 (cit. on p. 25).

[159] Mauricio F Villamar, Pakorn Wivatvongvana, Jayanton Patumanond et al. 'Focal modulation of the primary motor cortex in fibromyalgia using 4× 1-ring high-definition transcranial direct current stimulation (HD-tDCS): immediate and delayed analgesic effects of cathodal and anodal stimulation'. In: *The Journal of Pain* 14.4 (2013), pp. 371–383 (cit. on p. 25).

[160] Andrea Phillipou, Melissa Kirkovski, David J Castle et al. 'High-definition transcranial direct current stimulation in anorexia nervosa: A pilot study'. In: *International Journal of Eating Disorders* 52.11 (2019), pp. 1274–1280 (cit. on p. 25).

[161] Brooke Sasia and Laura Cacciamani. 'High-definition transcranial direct current stimulation of the lateral occipital cortex influences figure-ground perception'. In: *Neuropsychologia* 155 (2021), p. 107792 (cit. on p. 25).

[162] John Ashburner, Gareth Barnes, Chun-Chuan Chen et al. 'SPM12 manual'. In: *Wellcome Trust Centre for Neuroimaging, London, UK* 2464.4 (2014) (cit. on p. 25).

[163] Qianqian Fang and David A Boas. 'Tetrahedral mesh generation from volumetric binary and grayscale images'. In: *2009 IEEE international symposium on biomedical imaging: from nano to macro*. Ieee. 2009, pp. 1142–1145 (cit. on p. 26).

[164] Patrick Dular, Christophe Geuzaine, François Henrotte and Willy Legros. 'A general environment for the treatment of discrete problems and its application to the finite element method'. In: *IEEE transactions on magnetics* 34.5 (1998), pp. 3395–3398 (cit. on p. 26).

[165] David J Griffiths. *Introduction to electrodynamics*. Cambridge University Press, 2023 (cit. on p. 26).

[166] Sybren Van Hoornweder, Raf Meesen and Kevin A Caulfield. 'On the importance of using both T1-weighted and T2-weighted structural magnetic resonance imaging scans to model electric fields induced by non-invasive brain stimulation in SimNIBS'. In: *Brain Stimulation: Basic, Translational, and Clinical Research in Neuromodulation* 15.3 (2022), pp. 641–644 (cit. on pp. 26, 121).

[167] Günther Grabner, Andrew L Janke, Marc M Budge et al. 'Symmetric atlasing and model based segmentation: an application to the hippocampus in older adults'. In: *Medical Image Computing and Computer-Assisted Intervention–MICCAI 2006: 9th International Conference, Copenhagen, Denmark, October 1-6, 2006. Proceedings, Part II 9*. Springer. 2006, pp. 58–66 (cit. on p. 26).

[168] Mark W Woolrich, Saad Jbabdi, Brian Patenaude et al. 'Bayesian analysis of neuroimaging data in FSL'. In: *Neuroimage* 45.1 (2009), S173–S186 (cit. on p. 26).

[169] Douglas N Greve and Bruce Fischl. 'Accurate and robust brain image alignment using boundary-based registration'. In: *Neuroimage* 48.1 (2009), pp. 63–72 (cit. on p. 26).

[170] KM Bushby, T Cole, JN Matthews and JA Goodship. 'Centiles for adult head circumference.' In: *Archives of disease in childhood* 67.10 (1992), pp. 1286–1287 (cit. on p. 27).

[171] Kevin A Caulfield and Mark S George. 'Optimized APPS-tDCS electrode position, size, and distance doubles the on-target stimulation magnitude in 3000 electric field models'. In: *Scientific Reports* 12.1 (2022), p. 20116 (cit. on pp. 30, 36, 63).

[172] Chris Thomas, Iman Ghodratitoostani, Alexandre CB Delbem, Afaq Ali and Abhishek Datta. 'Influence of gender-related differences in transcranial direct current stimulation: A Computational Study'. In: *2019 41st Annual International Conference of the IEEE Engineering in Medicine and Biology Society (EMBC)*. IEEE. 2019, pp. 5196–5199 (cit. on p. 35).

[173] Dennis Q Truong, Greta Magerowski, George L Blackburn, Marom Bikson and Miguel Alonso-Alonso. 'Computational modeling of transcranial direct current stimulation (tDCS) in obesity: impact of head fat and dose guidelines'. In: *NeuroImage: Clinical* 2 (2013), pp. 759–766 (cit. on pp. 35, 36, 63).

[174] Marko Mikkonen, Ilkka Laakso, Satoshi Tanaka and Akimasa Hirata. 'Cost of focality in TDCS: Interindividual variability in electric fields'. In: *Brain Stimulation* 13.1 (Jan. 2020), pp. 117–124 (cit. on p. 35).

[175] Oula Puonti, Guilherme B Saturnino, Kristoffer H Madsen and Axel Thielscher. 'Value and limitations of intracranial recordings for validating electric field modeling for transcranial brain stimulation'. In: *Neuroimage* 208 (2020), p. 116431 (cit. on p. 36).

[176] Weiqian Sun, Heng Wang, Jianxu Zhang, Tianyi Yan and Guangying Pei. 'Multi-layer skull modeling and importance for tDCS simulation'. In: *Proceedings of the 2021 International Conference on Bioinformatics and Intelligent Computing*. 2021, pp. 250–256 (cit. on pp. 36, 113).

[177] Syed Salman Shahid, Marom Bikson, Humaira Salman, Peng Wen and Tony Ahfock. 'The value and cost of complexity in predictive modelling: role of tissue anisotropic conductivity and fibre tracts in neuromodulation'. In: *Journal of neural engineering* 11.3 (2014), p. 036002 (cit. on p. 36).

[178] Marko Mikkonen and Ilkka Laakso. 'Effects of posture on electric fields of non-invasive brain stimulation'. In: *Physics in Medicine & Biology* 64.6 (2019), p. 065019 (cit. on pp. 36, 113, 121).

[179] Sara Beroiz Bilbao. 'Realistic head modeling based system for the estimation of tissue conductivities for brain stimulation from accurate electrical impedance tomography measurements'. B.S. thesis. Universitat Politècnica de Catalunya, 2019 (cit. on p. 36).

[180] Dirk Hagemann, Johannes Hewig, Christof Walter and Ewald Naumann. 'Skull thickness and magnitude of EEG alpha activity'. In: *Clinical Neurophysiology* 119.6 (2008), pp. 1271–1280 (cit. on p. 36).

[181] Walter HL Pinaya, Mark S Graham, Eric Kerfoot et al. 'Generative ai for medical imaging: extending the monai framework'. In: *arXiv preprint arXiv:2307.15208* (2023) (cit. on p. 36).

[182] Emiliano Santarnecchi, Anna-Katharine Brem, Erica Levenbaum et al. 'Enhancing cognition using transcranial electrical stimulation'. In: *Current Opinion in Behavioral Sciences* 4 (2015), pp. 171–178 (cit. on p. 40).

[183] Philip D Harvey. 'Domains of cognition and their assessment'. In: *Dialogues in clinical neuroscience* 21.3 (2019), pp. 227–237 (cit. on pp. 40, 43).

[184] Gabriel Damon Lavezzi, Sofia Sanz Galan, Hallie Andersen, Daniel Tomer and Laura Cacciamani. 'The effects of tDCS on object perception: A systematic review and meta-analysis'. In: *Behavioural Brain Research* 430 (2022), p. 113927 (cit. on p. 42).

[185] Francisco Gurdiel-Álvarez, Yeray González-Zamorano, Sergio Lerma-Lara et al. 'Transcranial direct current stimulation (tDCS) effects on quantitative sensory testing (QST) and nociceptive processing in healthy subjects: a systematic review and Meta-analysis'. In: *Brain Sciences* 14.1 (2023), p. 9 (cit. on p. 42).

[186] Ronak Patel, James Ashcroft, Ashish Patel et al. 'The impact of transcranial direct current stimulation on upper-limb motor performance in healthy adults: a systematic review and meta-analysis'. In: *Frontiers in Neuroscience* 13 (2019), p. 1213 (cit. on p. 42).

[187] Nyeonju Kang, Jeffery J Summers and James H Cauraugh. 'Transcranial direct current stimulation facilitates motor learning post-stroke: a systematic review and meta-analysis'. In: *Journal of Neurology, Neurosurgery & Psychiatry* 87.4 (2016), pp. 345–355 (cit. on p. 42).

[188] Kun Hu, Ruihan Wan, Ying Liu et al. 'Effects of transcranial alternating current stimulation on motor performance and motor learning for healthy individuals: A systematic review and meta-analysis'. In: *Frontiers in Physiology* 13 (2022), p. 1064584 (cit. on p. 42).

[189] Pierre Vassiliadis, Elena Beanato, Traian Popa et al. 'Non-invasive stimulation of the human striatum disrupts reinforcement learning of motor skills'. In: *Nature Human Behaviour* (2024), pp. 1–18 (cit. on p. 42).

[190] Michal Weiss and Michal Lavidor. 'When less is more: Evidence for a facilitative cathodal tDCS effect in attentional abilities'. In: *Journal of Cognitive Neuroscience* 24.9 (Sept. 2012), pp. 1826–1833 (cit. on pp. 43, 56).

[191] Siobhán Harty and Roi Cohen Kadosh. 'Suboptimal Engagement of High-Level Cortical Regions Predicts Random-Noise-Related Gains in Sustained Attention'. In: *Psychological Science* 30.9 (Sept. 2019), pp. 1318–1332 (cit. on pp. 43, 51, 56, 80, 81, 85, 100).

[192] Julien Ouellet, Alexander McGirr, Frederique Van den Eynde et al. 'Enhancing decision-making and cognitive impulse control with transcranial direct current stimulation (tDCS) applied over the orbitofrontal cortex (OFC): A randomized and sham-controlled exploratory study'. In: *Journal of Psychiatric Research* 69 (Oct. 2015), pp. 27–34 (cit. on pp. 43, 53, 56, 80).

[193] Marieke J Begemann, Bodyl A Brand, Branislava uri-Blake, André Aleman and Iris E Sommer. 'Efficacy of non-invasive brain stimulation on cognitive functioning in brain disorders: a meta-analysis'. In: *Psychological medicine* 50.15 (2020), pp. 2465–2486 (cit. on pp. 43, 44).

[194] Daniel Senkowski, Rabea Sobirey, David Haslacher and Surjo R Soekadar. 'Boosting working memory: uncovering the differential effects of tDCS and tACS'. In: *Cerebral Cortex Communications* 3.2 (2022), tgac018 (cit. on pp. 43, 120).

[195] Dario Müller, Ute Habel, Edward S Brodkin and Carmen Weidler. 'High-definition transcranial direct current stimulation (HD-tDCS) for the enhancement of working memory–A systematic review and meta-analysis of healthy adults'. In: *Brain stimulation* 15.6 (2022), pp. 1475–1485 (cit. on p. 43).

[196] Nina S de Boer, Renée S Schluter, Joost G Daams et al. 'The effect of non-invasive brain stimulation on executive functioning in healthy controls: a systematic review and meta-analysis'. In: *Neuroscience & Biobehavioral Reviews* 125 (2021), pp. 122–147 (cit. on p. 44).

[197] Hongliang Lu, Yajuan Zhang, Huake Qiu et al. 'A new perspective for evaluating the efficacy of tACS and tDCS in improving executive functions: A combined tES and fNIRS study'. In: *Human Brain Mapping* 45.1 (2024), e26559 (cit. on p. 44).

[198] Samuel J Westwood, Joaquim Radua and Katya Rubia. 'Noninvasive brain stimulation in children and adults with attention-deficit/hyperactivity disorder: a systematic review and meta-analysis'. In: *Journal of Psychiatry and Neuroscience* 46.1 (2021), E14–E33 (cit. on p. 44).

[199] Amy R Price, Harrison McAdams, Murray Grossman and Roy H Hamilton. 'A meta-analysis of transcranial direct current stimulation studies examining the reliability of effects on language measures'. In: *Brain stimulation* 8.6 (2015), pp. 1093–1100 (cit. on p. 44).

[200] Alessia Monti, Roberta Ferrucci, Manuela Fumagalli et al. 'Transcranial direct current stimulation (tDCS) and language'. In: *Journal of Neurology, Neurosurgery & Psychiatry* 84.8 (2013), pp. 832–842 (cit. on p. 44).

[201] Norman Mackworth. 'The breakdown of vigilance durning prolonged visual search'. In: *Quarterly Journal of Experimental Psychology* 1.1 (1948), pp. 6–21 (cit. on pp. 45, 52).

[202] Nash Unsworth and Matthew K Robison. 'A locus coeruleus-norepinephrine account of individual differences in working memory capacity and attention control'. In: *Psychonomic bulletin & review* 24 (2017), pp. 1282–1311 (cit. on pp. 46, 47, 80).

[203] Robert Kurzban, Angela Duckworth, Joseph W Kable and Justus Myers. 'An opportunity cost model of subjective effort and task performance'. In: *Behavioral and brain sciences* 36.6 (2013), pp. 661–679 (cit. on pp. 46, 47).

[204] Jennifer C McVay and Michael J Kane. 'Does mind wandering reflect executive function or executive failure? Comment on Smallwood and Schooler (2006) and Watkins (2008).' In: (2010) (cit. on pp. 46, 47, 49).

[205] Jennifer C McVay and Michael J Kane. 'Why does working memory capacity predict variation in reading comprehension? On the influence of mind wandering and executive attention.' In: *Journal of experimental psychology: general* 141.2 (2012), p. 302 (cit. on pp. 46, 47).

[206] Jonathan Smallwood and Jonathan W Schooler. 'The restless mind.' In: *Psychological bulletin* 132.6 (2006), p. 946 (cit. on pp. 46, 47, 49).

[207] Jonathan W Schooler. 'Re-representing consciousness: Dissociations between experience and meta-consciousness'. In: *Trends in cognitive sciences* 6.8 (2002), pp. 339–344 (cit. on p. 46).

[208] David Rothlein, Joseph DeGutis and Michael Esterman. 'Attentional fluctuations influence the neural fidelity and connectivity of stimulus representations'. In: *Journal of cognitive neuroscience* 30.9 (2018), pp. 1209–1228 (cit. on pp. 46, 47).

[209] Yi-Sheng Wong, Adrian R Willoughby and Liana Machado. 'Reconceptualizing mind wandering from a switching perspective'. In: *Psychological Research* 87.2 (2023), pp. 357–372 (cit. on pp. 46, 48).

[210] Michael Esterman and David Rothlein. 'Models of sustained attention'. In: *Current opinion in psychology* 29 (2019), pp. 174–180 (cit. on pp. 47–49, 54, 58, 66).

[211] Jonathan Smallwood, Kevin S Brown, Christine Tipper et al. 'Pupillometric evidence for the decoupling of attention from perceptual input during offline thought'. In: *PloS one* 6.3 (2011), e18298 (cit. on p. 47).

[212] Jonathan Smallwood, Emily Beach, Jonathan W Schooler and Todd C Handy. 'Going AWOL in the brain: Mind wandering reduces cortical analysis of external events'. In: *Journal of cognitive neuroscience* 20.3 (2008), pp. 458–469 (cit. on p. 47).

[213] Francesca C Fortenbaugh, David Rothlein, Regina McGlinchey, Joseph DeGutis and Michael Esterman. 'Tracking behavioral and neural fluctuations during sustained attention: A robust replication and extension'. In: *Neuroimage* 171 (2018), pp. 148–164 (cit. on p. 48).

[214] Jonathan Smallwood. 'Distinguishing how from why the mind wanders: a process–occurrence framework for self-generated mental activity.' In: *Psychological bulletin* 139.3 (2013), p. 519 (cit. on pp. 48, 49).

[215] Niels A Taatgen, Marieke K van Vugt, Jeroen Daamen et al. 'The resource-availability model of distraction and mind-wandering'. In: *Cognitive Systems Research* 68 (2021), pp. 84–104 (cit. on pp. 48, 49).

[216] David R Thomson, Derek Besner and Daniel Smilek. 'A resource-control account of sustained attention: Evidence from mind-wandering and vigilance paradigms'. In: *Perspectives on psychological science* 10.1 (2015), pp. 82–96 (cit. on p. 48).

[217] Robert Langner and Simon B Eickhoff. 'Sustaining attention to simple tasks: a meta-analytic review of the neural mechanisms of vigilant attention.' In: *Psychological bulletin* 139.4 (2013), p. 870 (cit. on pp. 50, 64, 80).

[218] Monica D. Rosenberg, Emily S. Finn, Dustin Scheinost et al. 'A neuromarker of sustained attention from whole-brain functional connectivity'. In: *Nature Neuroscience* 19.1 (Dec. 2015), pp. 165–171 (cit. on p. 50).

[219] Andrea Biasiucci, Benedetta Franceschiello and Micah M Murray. 'Electroencephalography'. In: *Current Biology* 29.3 (2019), R80–R85 (cit. on p. 50).

[220] Robert J Barry, Adam R Clarke, Stuart J Johnstone, Christopher A Magee and Jacqueline A Rushby. 'EEG differences between eyes-closed and eyes-open resting conditions'. In: *Clinical neurophysiology* 118.12 (2007), pp. 2765–2773 (cit. on pp. 51, 80, 86).

[221] Michal Teplan et al. 'Fundamentals of EEG measurement'. In: *Measurement science review* 2.2 (2002), pp. 1–11 (cit. on p. 51).

[222] Martijn Arns, C Keith Conners and Helena C Kraemer. 'A Decade of EEG Theta/Beta Ratio Research in ADHD: A Meta-Analysis'. In: *Journal of Attention Disorders* 17.5 (2013), pp. 374–383 (cit. on p. 51).

[223] Adam R Clarke, Robert J Barry, Diana Karamacoska and Stuart J Johnstone. 'The EEG theta/beta ratio: a marker of arousal or cognitive processing capacity?' In: *Applied psychophysiology and biofeedback* 44.2 (2019), pp. 123–129 (cit. on pp. 51, 80).

[224] Angelos Angelidis, Willem van der Does, Lemmy Schakel and Peter Putman. 'Frontal EEG theta/beta ratio as an electrophysiological marker for attentional control and its test-retest reliability'. In: *Biological psychology* 121 (2016), pp. 49–52 (cit. on pp. 51, 80).

[225] Redmond G O'Connell, Paul M Dockree, Ian H Robertson et al. 'Uncovering the neural signature of lapsing attention: electrophysiological signals predict errors up to 20s before they occur'. In: *Journal of Neuroscience* 29.26 (2009), pp. 8604–8611 (cit. on pp. 51, 66, 74, 76, 77, 99, 101).

[226] Adrien Martel, Sven Dahne and Benjamin Blankertz. 'EEG predictors of covert vigilant attention'. In: *Journal of Neural Engineering* 11.3 (May 2014), p. 035009 (cit. on pp. 51–53, 66, 78).

[227] Robert J Barry, Adam R Clarke, Stuart J Johnstone et al. 'Caffeine effects on resting-state arousal in children'. In: *International Journal of Psychophysiology* 73.3 (2009), pp. 355–361 (cit. on pp. 51, 66, 74, 77, 78).

[228] Simon P Kelly, Edmund C Lalor, Richard B Reilly and John J Foxe. 'Increases in alpha oscillatory power reflect an active retinotopic mechanism for distracter suppression during sustained visuospatial attention'. In: *Journal of neurophysiology* 95.6 (2006), pp. 3844–3851 (cit. on pp. 51, 52, 67, 74, 77, 78, 101).

[229] David Friedman, Yael M Cycowicz and Helen Gaeta. 'The novelty P3: an event-related brain potential (ERP) sign of the brain's evaluation of novelty'. In: *Neuroscience & Biobehavioral Reviews* 25.4 (2001), pp. 355–373 (cit. on pp. 51, 66).

[230] Nya M. Boayue, Gábor Csifcsák, Isabel V. Kreis et al. 'The interplay between executive control, behavioural variability and mind wandering: Insights from a high-definition transcranial direct-current stimulation study'. In: *European Journal of Neuroscience* 53.5 (Mar. 2021), pp. 1498–1516 (cit. on pp. 52, 57).

[231] Lindsey K McIntire, R Andy McKinley, Chuck Goodyear and Justin Nelson. 'A comparison of the effects of transcranial direct current stimulation and caffeine on vigilance and cognitive performance during extended wakefulness'. In: *Brain stimulation* 7.4 (July 2014), pp. 499–507 (cit. on pp. 53, 57).

[232] Simon P Kelly and Redmond G O'connell. 'Behavioral/Cognitive Internal and External Influences on the Rate of Sensory Evidence Accumulation in the Human Brain'. In: (2013) (cit. on pp. 53, 66).

[233] Murray W Johns. 'A new method for measuring daytime sleepiness: the Epworth sleepiness scale'. In: *sleep* 14.6 (1991), pp. 540–545 (cit. on p. 54).

[234] Michael J Silverstein, Samuel Alperin, Stephen V Faraone, Ronald C Kessler and Lenard A Adler. 'Test–retest reliability of the adult ADHD Self-Report Scale (ASRS) v1. 1 Screener in non-ADHD controls from a primary care physician practice'. In: *Family practice* 35.3 (2018), pp. 336–341 (cit. on pp. 54, 80).

[235] Suman Das, Peter Holland, Maarten A. Frens and Opher Donchin. 'Impact of Transcranial Direct Current Stimulation (tDCS) on Neuronal Functions'. In: *Frontiers in Neuroscience* 10.11 (Nov. 2016), p. 550 (cit. on pp. 54, 60, 80).

[236] André Nieoullon. *Dopamine and the regulation of cognition and attention*. May 2002 (cit. on p. 54).

[237] Clara Fonteneau, Jérome Redoute, Frédéric Haesebaert et al. 'Frontal Transcranial Direct Current Stimulation Induces Dopamine Release in the Ventral Striatum in Human'. In: *Cerebral Cortex* 28.7 (July 2018), pp. 2636–2646 (cit. on pp. 54, 55).

[238] Lisa Marshall, Matthias Mölle, Manfred Hallschmid and Jan Born. 'Transcranial direct current stimulation during sleep improves declarative memory'. In: *Journal of Neuroscience* 24.44 (2004), pp. 9985–9992 (cit. on p. 55).

[239] Nora D Volkow, Gene-Jack Wang, Joanna S Fowler and Yu-Shin Ding. 'Imaging the effects of methylphenidate on brain dopamine: new model on its therapeutic actions for attention-deficit/hyperactivity disorder'. In: *Biological psychiatry* 57.11 (2005), pp. 1410–1415 (cit. on p. 55).

[240] Mina Fukai, Tomoyasu Bunai, Tetsu Hirosawa et al. 'Endogenous dopamine release under transcranial direct-current stimulation governs enhanced attention: a study with positron emission tomography'. In: *Translational psychiatry* 9.1 (Dec. 2019), p. 115 (cit. on p. 55).

[241] Fernando G. Luna, Rafael Román-Caballero, Pablo Barttfeld, Juan Lupiáñez and Elisa Martín-Arévalo. 'A High-Definition tDCS and EEG study on attention and vigilance: Brain stimulation mitigates the executive but not the arousal vigilance decrement'. In: *Neuropsychologia* 142 (May 2020), p. 107447 (cit. on pp. 56, 80, 81).

[242] Vadim Axelrod, Xingxing Zhu and Jiang Qiu. 'Transcranial stimulation of the frontal lobes increases propensity of mind-wandering without changing meta-awareness'. In: *Scientific reports* 8.1 (2018), pp. 1–14 (cit. on p. 57).

[243] Daniel M. Wolpert, R. Chris Miall and Mitsuo Kawato. *Internal models in the cerebellum*. Sept. 1998 (cit. on p. 57).

[244] Peter L Strick, Richard P Dum and Julie A Fiez. 'Cerebellum and Nonmotor Function M1: primary motor cortex'. In: (2009) (cit. on p. 57).

[245] Daniela Mannarelli, Caterina Pauletti, Antonio Currà et al. 'The Cerebellum Modulates Attention Network Functioning: Evidence from a Cerebellar Transcranial Direct Current Stimulation and Attention Network Test Study'. In: *Cerebellum* 18.3 (June 2019), pp. 457–468 (cit. on p. 57).

[246] Iñaki Iturrate, Michael Pereira and José del R Millán. 'Closed-loop electrical neurostimulation: challenges and opportunities'. In: *Current Opinion in Biomedical Engineering* 8 (2018), pp. 28–37 (cit. on pp. 58, 59).

[247] Marco Esposito, Clarissa Ferrari, Claudia Fracassi, Carlo Miniussi and Debora Brignani. 'Arousal levels explain inter-subject variability of neuromodulation effects'. In: *bioRxiv* (May 2020), p. 2020.05.08.083717 (cit. on pp. 58, 59, 81).

[248] Michael J Imburgio and Joseph M Orr. 'Effects of prefrontal tDCS on executive function: Methodological considerations revealed by meta-analysis'. In: *Neuropsychologia* 117 (2018), pp. 156–166 (cit. on p. 58).

[249] Niranjan Khadka, Helen Borges, Bhaskar Paneri et al. 'Adaptive current tDCS up to 4mA'. In: *Brain Stimulation* 13.1 (Jan. 2020), pp. 69–79 (cit. on p. 58).

[250] Shan Zhang, Zihan Yan, Shardul Sapkota, Shengdong Zhao and Wei Tsang Ooi. 'Moment-to-Moment Continuous Attention Fluctuation Monitoring through Consumer-Grade EEG Device'. In: *Sensors* 21.10 (2021), p. 3419 (cit. on pp. 60, 101).

[251] Adrien Martel, Mahnaz Arvaneh, Ian Robertson and Paul Dockree. 'Predicting intentional and unintentional task unrelated thought with EEG'. In: *bioRxiv* (2019), p. 764803 (cit. on pp. 60, 67, 74, 75, 77).

[252] Paulo J. C. Suen, Sarah Doll, Marcelo C. Batistuzzo et al. 'Association between tDCS computational modeling and clinical outcomes in depression: data from the ELECT-TDCS trial'. In: *European Archives of Psychiatry and Clinical Neuroscience 2020 271:1* 271.1 (Apr. 2020), pp. 101–110 (cit. on pp. 60, 64).

[253] Kevin A Caulfield, Bashar W Badran, William H DeVries et al. 'Transcranial electrical stimulation motor threshold can estimate individualized tDCS dosage from reverse-calculation electric-field modeling'. In: *Brain stimulation* 13.4 (2020), pp. 961–969 (cit. on p. 60).

[254] Yu Huang, Jacek P Dmochowski, Yuzhuo Su et al. 'Automated MRI segmentation for individualized modeling of current flow in the human head'. In: *Journal of Neural Engineering* 10.6 (Oct. 2013), p. 066004 (cit. on p. 61).

[255] Letizia Palumbo., Paolo. Bosco, Maria Evelina Fantacci et al. 'Evaluation of the intra- and inter-method agreement of brain MRI segmentation software packages: A comparison between SPM12 and FreeSurfer v6.0'. In: *Physica Medica* 64 (Aug. 2019), pp. 261–272 (cit. on p. 61).

[256] Gaurav V. Bhalerao, Vanteemar S. Sreeraj, Anushree Bose, Janardhanan C. Narayanaswamy and Ganesan Venkatasubramanian. 'Comparison of electric field modeling pipelines for transcranial direct current stimulation'. In: *Neurophysiologie Clinique* (May 2021) (cit. on p. 61).

[257] Massoud Akhtari, HC Bryant, AN Mamelak et al. 'Conductivities of three-layer live human skull'. In: *Brain topography* 14.3 (2002), pp. 151–167 (cit. on p. 62).

[258] Sumientra M Rampersad, Dick F Stegeman and Thom F Oostendorp. 'Single-layer skull approximations perform well in transcranial direct current stimulation modeling'. In: *IEEE Transactions on Neural Systems and Rehabilitation Engineering* 21.3 (2012), pp. 346–353 (cit. on p. 62).

[259] Yu Huang, Anli A Liu, Belen Lafon et al. 'Correction: Measurements and models of electric fields in the in vivo human brain during transcranial electric stimulation'. In: *elife* 7 (2018), e35178 (cit. on p. 62).

[260] Ruben C Gur, Bruce I Turetsky, Mie Matsui et al. 'Sex differences in brain gray and white matter in healthy young adults: correlations with cognitive performance'. In: *Journal of Neuroscience* 19.10 (1999), pp. 4065–4072 (cit. on p. 63).

[261] Mahtab Alam, Dennis Q Truong, Niranjan Khadka and Marom Bikson. 'Spatial and polarity precision of concentric high-definition transcranial direct current stimulation (HD-tDCS)'. In: *Physics in Medicine & Biology* 61.12 (2016), p. 4506 (cit. on pp. 63, 64).

[262] Michael I Posner and Steven E Petersen. 'The attention system of the human brain'. In: *Annual review of neuroscience* 13.1 (1990), pp. 25–42 (cit. on p. 64).

[263] Jake Toth, Ricken Patel and Mahnaz Arvaneh. 'Electrophysiological correlates of response time in a vigilant attention task'. In: *2022 44th Annual International Conference of the IEEE Engineering in Medicine & Biology Society (EMBC)*. IEEE. 2022, pp. 2340–2343 (cit. on p. 66).

[264] Chin-Teng Lin, Kuan-Chih Huang, Chun-Hsiang Chuang, Li-Wei Ko and Tzyy-Ping Jung. 'Can arousing feedback rectify lapses in driving? Prediction from EEG power spectra'. In: *Journal of neural engineering* 10.5 (2013), p. 056024 (cit. on p. 66).

[265] Standard Electrode Position Nomenclature. 'American electroencephalographic society guidelines for'. In: *Journal of clinical Neurophysiology* 8.2 (1991), pp. 200–202 (cit. on p. 67).

[266] Kai Keng Ang, Zheng Yang Chin, Chuanchu Wang, Cuntai Guan and Haihong Zhang. 'Filter bank common spatial pattern algorithm on BCI competition IV datasets 2a and 2b'. In: *Frontiers in neuroscience* 6 (2012), p. 39 (cit. on p. 77).

[267] Ilkka Laakso, Keisuke Tani, Jose Gomez-Tames, Akimasa Hirata and Satoshi Tanaka. 'Small effects of electric field on motor cortical excitability following anodal tDCS'. In: *Iscience* 27.2 (2024) (cit. on pp. 81, 120).

[268] Annegret Habich, Kristoffer D Fehér, Daria Antonenko et al. 'Stimulating aged brains with transcranial direct current stimulation: opportunities and challenges'. In: *Psychiatry Research: Neuroimaging* 306 (2020), p. 111179 (cit. on p. 81).

[269] Ronald C Kessler, Lenard Adler, Minnie Ames et al. 'The World Health Organization Adult ADHD Self-Report Scale (ASRS): a short screening scale for use in the general population'. In: *Psychological medicine* 35.2 (2005), pp. 245–256 (cit. on p. 85).

[270] Ayumu Yamashita, David Rothlein, Aaron Kucyi et al. 'Variable rather than extreme slow reaction times distinguish brain states during sustained attention'. In: *Scientific reports* 11.1 (2021), p. 14883 (cit. on p. 87).

[271] Philippe Vignaud, Marine Mondino, Emmanuel Poulet, Ulrich Palm and Jérôme Brunelin. 'Duration but not intensity influences transcranial direct current stimulation (tDCS) after-effects on cortical excitability'. In: *Neurophysiologie Clinique* 48.2 (2018), pp. 89–92 (cit. on p. 87).

[272] Yu Huang, Lucas C Parra and Stefan Haufe. 'The New York Head—A precise standardized volume conductor model for EEG source localization and tES targeting'. In: *NeuroImage* 140 (2016), pp. 150–162 (cit. on p. 89).

[273] Stefan Vestring, Elias Wolf, Johanna Dinkelacker et al. 'Lasting effects of transcranial direct current stimulation on the inducibility of synaptic plasticity by paired-associative stimulation in humans'. In: *Journal of NeuroEngineering and Rehabilitation* 21.1 (2024), p. 162 (cit. on p. 100).

[274] Kristina Fricke, Antje A Seeber, Nivethida Thirugnanasambandam et al. 'Time course of the induction of homeostatic plasticity generated by repeated transcranial direct current stimulation of the human motor cortex'. In: *Journal of neurophysiology* 105.3 (2011), pp. 1141–1149 (cit. on p. 100).

[275] Dan Taylor. *Flow Neuroscience raises $9 million, takes depression head on*. https://tech.eu/2021/08/10/flow-neuroscience-raises-9-million-takes-depression-head-on/. [Accessed 13-07-2024]. 2021 (cit. on p. 109).

[276] *NHS Flow Pilot - Flow Neuroscience*. https://www.flowneuroscience.com/nhs/nhs-flow-pilot/. [Accessed 13-07-2024] (cit. on p. 109).

[277] Sean Whooley. *Neuroelectrics raises $17.5M Series A*. https://www.massdevice.com/neuroelectrics-raises-17-5m-series-a/. [Accessed 13-07-2024]. 2021 (cit. on p. 109).

[278] Natasha Lomas. *Samphire Neuroscience is building a brain stimulating wearable for period pain*. https://techcrunch.com/2024/02/21/samphire-neuroscience/. [Accessed 13-07-2024]. 2024 (cit. on p. 109).

[279] *ROAST. A simulator for TES*. https://github.com/andypotatohy/roast?tab=GPL-3.0-1-ov-file. [Accessed 14-07-2024] (cit. on p. 113).

[280] Essam A Rashed, Jose Gomez-Tames and Akimasa Hirata. 'Development of accurate human head models for personalized electromagnetic dosimetry using deep learning'. In: *NeuroImage* 202 (2019), p. 116132 (cit. on p. 113).

[281] *ForkNet is multi-label segmentation CNN designed for human head segmentation.* https://github.com/erashed/ForkNet?tab=BSD-3-Clause-1-ov-file. [Accessed 14-07-2024] (cit. on p. 113).

[282] *FSL License*. https://fsl.fmrib.ox.ac.uk/fsl/docs. [Accessed 14-07-2024] (cit. on p. 113).

[283] *MNI ICBM152 non-linear template*. https://nist.mni.mcgill.ca/mni-icbm152-non-linear-6th-generation-symmetric-average-brain-stereotaxic-registration-model/. [Accessed 14-07-2024] (cit. on p. 113).

[284] *Pricing and Licensing*. https://uk.mathworks.com/pricing-licensing.html?prodcode=ML&intendeduse=comm. [Accessed 14-07-2024] (cit. on p. 113).

[285] Lais B Razza, Stefanie De Smet, Sybren Van Hoornweder et al. 'Investigating the variability of prefrontal tDCS effects on working memory: An individual E-field distribution study'. In: *cortex* 172 (2024), pp. 38–48 (cit. on p. 120).

[286] Alejandro Albizu, Ruogu Fang, Aprinda Indahlastari et al. 'Machine learning and individual variability in electric field characteristics predict tDCS treatment response'. In: *Brain stimulation* 13.6 (2020), pp. 1753–1764 (cit. on p. 120).

[287] Paulo S Boggio, Sergio P Rigonatti, Rafael B Ribeiro et al. 'A randomized, double-blind clinical trial on the efficacy of cortical direct current stimulation for the treatment of major depression'. In: *International Journal of Neuropsychopharmacology* 11.2 (2008), pp. 249–254 (cit. on p. 120).

[288] Rachel D Woodham, Sudhakar Selvaraj, Nahed Lajmi et al. 'Home-based transcranial direct current stimulation treatment for major depressive disorder: a fully remote phase 2 randomized sham-controlled trial'. In: *Nature medicine* (2024), pp. 1–9 (cit. on pp. 120–122).

[289] Alejandro Albizu, Aprinda Indahlastari, Paulo Suen et al. 'Machine learning-optimized non-invasive brain stimulation and treatment response classification for major depression'. In: *Bioelectronic Medicine* 10.1 (2024), p. 25 (cit. on pp. 120, 122).

[290] Ulrike Kumpf, Ulrich Palm, Julia Eder et al. 'TDCS at home for depressive disorders: an updated systematic review and lessons learned from a prematurely terminated randomized controlled pilot study'. In: *European Archives of Psychiatry and Clinical Neuroscience* 273.7 (2023), pp. 1403–1420 (cit. on p. 120).

[291] Max Hamilton. 'A rating scale for depression'. In: *Journal of neurology, neurosurgery, and psychiatry* 23.1 (1960), p. 56 (cit. on p. 121).

[292] Esther Zhiwei Zheng, Nichol ML Wong, Angela SY Yang and Tatia MC Lee. 'Evaluating the effects of tDCS on depressive and anxiety symptoms from a transdiagnostic perspective: a systematic review and meta-analysis of randomized controlled trials'. In: *Translational Psychiatry* 14.1 (2024), p. 295 (cit. on p. 122).

[293] Stefanie De Smet, Stevan Nikolin, Adriano Moffa et al. 'Determinants of sham response in tDCS depression trials: A systematic review and meta-analysis'. In: *Progress in Neuro-Psychopharmacology and Biological Psychiatry* 109 (2021), p. 110261 (cit. on p. 122).

[294] Giuseppina Pilloni, Adam J Woods and Leigh Charvet. 'No risk of skin lesion or burn with transcranial direct current stimulation (tDCS) using standardized protocols'. In: *Brain Stimulation: Basic, Translational, and Clinical Research in Neuromodulation* 14.3 (2021), pp. 511–512 (cit. on p. 122).

[295] Neil E O'connell, John Cossar, Louise Marston et al. 'Rethinking clinical trials of transcranial direct current stimulation: participant and assessor blinding is inadequate at intensities of 2mA'. In: (2012) (cit. on p. 122).

[296] Stevan Nikolin, Adriano Moffa, Lais Razza et al. 'Time-course of the tDCS antidepressant effect: An individual participant data meta-analysis'. In: *Progress in Neuro-Psychopharmacology and Biological Psychiatry* 125 (2023), p. 110752 (cit. on p. 122).

Appendices

A

Appendix A

The Relationship Between Gender and Peak E-field Strength

In addition to Figure 3.4 in the Chapter 3 the relationship between gender and MRI-informed peak E-field strengths when applying 1mA tES, is plotted in Figure A.1.

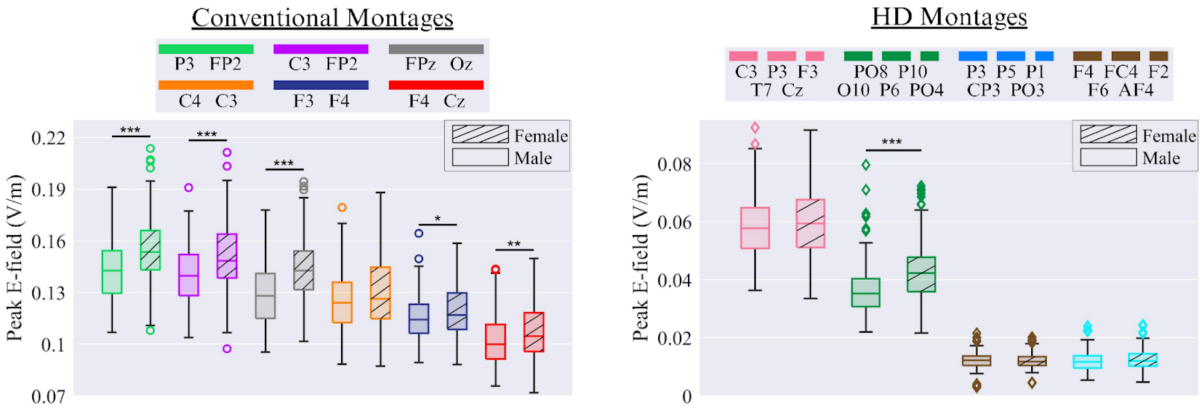

Figure A.1.: Peak E-field strength for each gender across conventional and HD montages. Across all box plots, the whiskers represent the most extreme values, the upper and lower bounds of the box indicate the 75th and 25th percentiles, respectively, and the horizontal line within the boxes displays the median value. Outlier folds are shown as circles for conventional montages and diamonds for HD montages. (*** denotes p<.001, ** denotes p<.01, and * denotes p<.05)

Correlational analysis

In addition to Spearman's rank order partial correlations discussed in Chapter 3, correlational analysis was performed to determine correlations between independent variables and the MRI-obtained peak E-field strength. Normally distributed variables (head circumference and cephalic index) were compared to the 95th percentile of the E-field using Person's correlation. The non-normally distributed body mass index (BMI) and age were compared to the peak E-field using Spearmans Rho tests. Finally, the categorical gender variable was compared using two-sample, two-tailed t-tests. Bonferroni correction was applied to account for multiple comparisons.

Correlational analysis across all independent variables and montages

Montages	Pearson's linear correlation				Spearman's Rho correlation				Two-sample t-test
	Head circumference		Cephalic index		Age		BMI		Gender
	r	p	r	p	r	p	r	p	p
F4, Cz	-0.37	<.001	-0.28	<.001	-0.49	<.001	-0.26	<.001	<.05
C3, FP2	-0.45	<.001	-0.33	<.001	-0.57	<.001	-0.41	<.001	<.001
F3, F4	-0.35	<.001	-0.26	<.001	-0.46	<.001	-0.32	<.001	>0.1
P3, FP2	-0.51	<.001	-0.32	<.001	-0.55	<.001	-0.43	<.001	<.001
C3, C4	-0.33	<.001	-0.23	<.001	-0.48	<.001	-0.35	<.001	>0.1
FPz, Oz	-0.51	<.001	-0.4	<.001	-0.56	<.001	-0.42	<.001	<.001
F4, F2, AF4, F6, FC4	-0.19	<.01	-0.13	>0.1	-0.39	<.001	-0.19	<.05	>0.1
C3, P3, Cz, T7, F3	-0.2	<.01	-0.12	>0.1	-0.42	<.001	-0.33	<.001	>0.1
P3, P1, CP3, P5, PO3	-0.2	<.01	-0.083	>0.1	-0.37	<.001	-0.33	<.001	>0.1
PO8, P6, PO4, P10, O10	-0.4	<.001	-0.24	<.001	-0.5	<.001	-0.36	<.001	<.001

Figure A.2.: Correlational analysis of all the independent variables and the peak E-field strength for each montage. r values indicate the strength, and direction of the correlation and p values indicate statistical significance.

Montage performance results tables

The full results tables for the adjusted R^2 and NRMSE of the models across all folds compared to their respective test sets are presented below. Higher adjusted R^2 and lower NRMSE values indicate a better model fit.

Montage-specific model performance (Conventional montages)

Conventional montages	Adjusted R^2						NRMSE					
	Fold 1	Fold 2	Fold 3	Fold 4	Fold 5	Average	Fold 1	Fold 2	Fold 3	Fold 4	Fold 5	Average
F4, Cz	0.456	0.369	0.275	0.243	0.381	0.345	0.102	0.110	0.119	0.116	0.105	0.110
C3, FP2	0.548	0.581	0.524	0.468	0.396	0.503	0.083	0.080	0.086	0.085	0.091	0.085
F3, F4	0.312	0.248	0.331	0.421	0.184	0.299	0.100	0.106	0.095	0.089	0.107	0.099
P3, FP2	0.627	0.548	0.526	0.448	0.429	0.516	0.074	0.081	0.084	0.085	0.087	0.082
C3, C4	0.141	0.409	0.323	0.356	0.279	0.302	0.133	0.111	0.120	0.112	0.119	0.119
FPz, Oz	0.546	0.616	0.593	0.597	0.574	0.585	0.090	0.083	0.086	0.082	0.084	0.085

Montage-agnostic linear model performance (Conventional montages)

Conventional montages	Adjusted R^2						NRMSE					
	Fold 1	Fold 2	Fold 3	Fold 4	Fold 5	Average	Fold 1	Fold 2	Fold 3	Fold 4	Fold 5	Average
F4, Cz	0.323	0.368	0.245	0.316	0.306	0.312	0.111	0.110	0.124	0.109	0.107	0.112
C3, FP2	0.470	0.487	0.386	0.501	0.417	0.452	0.085	0.092	0.101	0.076	0.082	0.087
F3, F4	0.332	0.256	0.203	0.113	0.257	0.232	0.099	0.104	0.103	0.104	0.102	0.102
P3, FP2	0.436	0.556	0.423	0.470	0.392	0.455	0.087	0.080	0.096	0.086	0.081	0.086
C3, C4	0.357	0.165	0.189	0.259	0.060	0.206	0.111	0.120	0.140	0.121	0.130	0.124
FPz, Oz	0.441	0.540	0.419	0.492	0.381	0.454	0.101	0.091	0.104	0.091	0.083	0.094

Montage-agnostic non-linear model performance (Conventional montages)

Conventional montages	Adjusted R^2						NRMSE					
	Fold 1	Fold 2	Fold 3	Fold 4	Fold 5	Average	Fold 1	Fold 2	Fold 3	Fold 4	Fold 5	Average
F4, Cz	0.350	0.296	0.219	0.277	0.235	0.275	0.109	0.116	0.126	0.112	0.113	0.115
C3, FP2	0.515	0.486	0.406	0.519	0.393	0.464	0.081	0.092	0.099	0.074	0.084	0.086
F3, F4	0.364	0.211	0.219	0.093	0.247	0.227	0.096	0.107	0.102	0.105	0.103	0.103
P3, FP2	0.470	0.577	0.433	0.497	0.390	0.473	0.084	0.078	0.095	0.084	0.081	0.084
C3, C4	0.401	0.095	0.210	0.314	0.039	0.212	0.107	0.125	0.138	0.116	0.132	0.124
FPz, Oz	0.476	0.574	0.444	0.527	0.400	0.484	0.097	0.088	0.102	0.088	0.082	0.091

Figure A.3.: Regression model performance in terms of Adjusted R^2 and NRMSE for conventional montages. 5-fold cross-validation was performed. Performance measures are shown for each fold, as well as an average across all the folds.

Montage-specific model performance (HD montages)

HD montages	Adjusted R^2						NRMSE					
	Fold 1	Fold 2	Fold 3	Fold 4	Fold 5	Average	Fold 1	Fold 2	Fold 3	Fold 4	Fold 5	Average
F4, F2, AF4, F6, FC4	0.090	0.110	0.104	0.005	0.265	0.115	0.210	0.210	0.191	0.201	0.175	0.197
C3, P3, Cz, T7, F3	0.271	0.160	0.180	0.299	0.195	0.221	0.159	0.174	0.162	0.149	0.161	0.161
P3, P1, CP3, P5, PO3	0.184	0.076	0.273	0.194	-0.003	0.145	0.250	0.266	0.222	0.237	0.268	0.249
PO8, P6, PO4, P10, O10	0.245	0.381	0.467	0.330	0.365	0.358	0.208	0.188	0.177	0.205	0.185	0.193

Montage-agnostic linear model performance (HD montages)

HD montages	Adjusted R^2						NRMSE					
	Fold 1	Fold 2	Fold 3	Fold 4	Fold 5	Average	Fold 1	Fold 2	Fold 3	Fold 4	Fold 5	Average
F4, F2, AF4, F6, FC4	0.070	-0.027	-0.083	0.031	0.002	-0.001	0.210	0.225	0.209	0.210	0.180	0.207
C3, P3, Cz, T7, F3	0.156	0.245	0.162	0.176	0.137	0.175	0.143	0.155	0.189	0.172	0.163	0.164
P3, P1, CP3, P5, PO3	0.188	0.077	0.065	0.057	0.105	0.098	0.217	0.254	0.276	0.289	0.247	0.256
PO8, P6, PO4, P10, O10	0.159	0.473	0.202	0.264	0.189	0.257	0.232	0.153	0.232	0.197	0.195	0.202

Montage-agnostic non-linear model performance (HD montages)

HD montages	Adjusted R^2						NRMSE					
	Fold 1	Fold 2	Fold 3	Fold 4	Fold 5	Average	Fold 1	Fold 2	Fold 3	Fold 4	Fold 5	Average
F4, F2, AF4, F6, FC4	0.070	-0.029	-0.084	-0.366	0.002	-0.081	0.210	0.225	0.209	0.249	0.180	0.215
C3, P3, Cz, T7, F3	0.163	0.255	0.169	0.170	0.148	0.181	0.142	0.154	0.188	0.172	0.161	0.164
P3, P1, CP3, P5, PO3	0.178	0.070	0.073	0.059	0.095	0.095	0.219	0.255	0.274	0.289	0.248	0.257
PO8, P6, PO4, P10, O10	0.159	0.469	0.204	0.265	0.185	0.256	0.232	0.154	0.232	0.197	0.196	0.202

Figure A.4.: Regression model performance in terms of Adjusted R^2 and NRMSE for HD montages. 5-fold cross-validation was performed. Performance measures are shown for each fold, as well as an average across all the folds.